The Effect of Microtubule Stabilising Drugs on Immune-Mediated Exocytosis

By

Marcus James Robinson

A thesis submitted to

Victoria University of Wellington

in fulfilment of the requirements for the degree of

Master of Science in Cell and Molecular Biology

Victoria University of Wellington

2009

Abstract

The microtubule network is involved in cellular processes including protein transport and cell division. Microtubule stabilising drugs (MSD) bind to microtubules and alter their dynamic balance in favour of the polymerised state. While primarily known for their anti-mitotic properties, MSD also exert immunomodulatory effects *in vitro* and *in vivo*. It is the aim of this project to investigate the effects of MSD on protein trafficking and secretion to determine how they affect immune-mediated exocytosis.

Previous work in our lab demonstrated that macrophage responses to bacterial lipopolysaccharide, as measured by the production of TNF-α and nitric oxide, are inhibited by both paclitaxel and peloruside. In this thesis we continued this work and saw that inhibition was not affected by temporal IFN-γ priming and found that altered production kinetics were not sufficient to explain the inhibition.

To kill target cells cytotoxic T cells (CTL) reorganise their cytoskeleton so that lytic granules can traffic down microtubules to be delivered to the target. Using an *in vitro* model of CTL killing, we saw that MSD did not inhibit killing by CTL, lytic granule delivery to the cell surface, or antigen-stimulated Interferon-γ (IFN-γ) production by CTL. In contrast to this, in a murine model of antigen-induced killing we saw that a single dose of paclitaxel had a significant inhibitory effect on CTL-mediated cytolysis *in vivo*.

Together these studies suggest that MSD have multiple immunomodulatory effects that are independent of their anti-proliferative effects. The data suggest that patients undergoing taxane therapy may be unable to fight infection long before the anti-mitotic effects of MSD are apparent.

Acknowledgements

First, I thank my supervisor Dr. Anne La Flamme. Her guidance & support have been unequivocally beneficial. I have learned a lot & enjoyed the research project. In kind, thanks to my co-supervisor Prof. Franca Ronchese of the MIMR for advice regarding appropriate assays.

Personal support has been provided in the form of my wonderful girlfriend Rebecca – Thank you for making sure I take a night off from time to time. Mum, as well as proofing, thanks to you & Dad for all your support.

Special note needs to be made of Dr. Mark Yang & Joel Ma at the MIMR for explaining the finer points of assays & mouse physiology, & to Drs. Peter Northcote & John Miller of VUW for providing peloruside. To Dave, you have been awesome. It has been great to bounce ideas off you - All the more since you've been working with MSD. Dr. Jim McIntosh, Ploi & Bhagyashree, thanks for your stats advice.

To Sara, Marie, Bridget, Kirsty, Ariane, Pete, Aashish, Arun, Praneta, Miles, Simon, Ben, Ray & the 601 occassionals – It has been great working with you. Thanks to Kevin, Darren & Bronwyn for help with various methods and processes.

Lastly, kind thanks to the Edith Wheal Scholarship Trust & Lottery Health Research Grants for funding. Cheers guys.

Table of Contents

List of Tables and Figures

Chapter 1:

Chapter 2:

No Figures or Tables

Chapter 3:

Chapter 4:

Chapter 5:

Chapter 6:

No Figures or Tables

List of Abbreviations

Ag - Antigen(s)

Ag^+ - Antigen-treated

Ag^- - Not Exposed to Antigen

ANOVA - Analysis Of Variance

APC - Antigen Presenting Cell(s)

AP - Allophycocyanin

BMDC - Bone Marrow-Derived Dendritic Cell(s)

BMMØ - Bone-Marrow Derived Macrophage(s)

CD - Cluster of Differentiation

CD107a - Lysosomally-Associated Membrane Protein 1 (also called Lamp-1)

CCR7 - Chemokine Receptor type 7

CFSE - 5,6-carboxyfluorescein succinimidyl ester

cIMDM - Complete Iscove's Modified Dulbecco's Medium

cpm - Scintillations (counts) Per Minute

cSMAC - Central Supramolecular Activation Cluster

CTCM - Complete T Cell Medium

CTO - Cell Tracker Orange®

CTL - Cytotoxic T Lymphocyte(s)

Cyc - Cychrome

dPBS - Dulbecco's Phosphate Buffered Saline

DC - Dendritic Cell(s)

DSD - Microtubule Destabilising Drug(s)

ELISA - Enzyme-Linked Immunosorbant Assay

eNOS - Endothelial Nitric Oxide Synthase (also called NOS3)

FasL - Fas Ligand

FCS - Foetal Calf Serum

Fitc	- Fluorescein Isothiocyanate
GM-CSF	- Granulocyte/Macrophage-Colony Stimulating Factor
IMDM	- Iscove's Modified Dulbecco's Medium
iNOS	- Inducible Nitric Oxide Synthase (also called NOS2)
IS	- Immunological Synapse
JAM Assay	- Just Another Method Assay
JNK	- c-Jun N-terminal Kinase
Lamp-1	- CD107a
LCK	- Leukocyte-Specific Protein Tyrosine Kinase
LFA-1	- Lymphocyte Function-Associated Antigen
LPS	- Bacterial Lipopolysaccharide
MAP-K	- Mitogen-Activated Protein Kinase(s)
MDR-1	- Multidrug Resistance Gene
MFI	- Median Fluorescence Intensity
MHC	- Major Histocompatibility Complex
MMP	- Matrix Metalloprotease
MØ	- Macrophage(s)
MSD	- Microtubule Stabilising Drug(s)
MTOC	- Microtubule-Organising Centre
MTT	- (3-(4,5-dimethylthiazoyl-2-yl)-2,5-diphenyltetrazolium bromide)
NF-κβ	- Nuclear Factor-Kappa B
NK	- Natural Killer
NO	- Nitric Oxide
NOS	- Nitric Oxide Synthase
nNOS	- Neuronal Nitric Oxide Synthase (also called NOS1)
OVA	- Ovalbumin Protein
PBMC	- Peripheral Blood Mononuclear Cell(s)

PDL - Poly-$_{D/L}$-Lysine hydrobromide

Peloruside - Peloruside A

PKC-θ - Protein Kinase C-θ

P-gp - P-glycoprotein Efflux Pump

PMØ - Peritoneal Macrophage(s)

pSMAC - Peripheral Supramolecular Activation Cluster

SMAC - Supramolecular Activation Cluster

Taxol - Taxol®

TCR - T Cell Receptor(s)

T_{reg} - Regulatory T Lymphocyte(s)

TLR - Toll-like Receptor(s)

TNF-α - Tumour Necrosis Factor-α

TNF-RI - Tumour Necrosis Factor Receptor-type I

TNF-RII - Tumour Necrosis Factor Receptor-type II

T_{EM} - Effector-Memory T Cell(s)

T_{CM} - Central-Memory T Cell(s)

TC - Target Cell(s)

TLR-$4^{-/-}$ - Toll-Like Receptor-4 Knockout

1. General Introduction

1.1 Microtubules & Microtubule Associated Drugs:

1.1.1 Microtubule Structure and Function

Microtubules are an essential and dynamic component of the cytoskeleton and are involved in many intracellular processes. Microtubules help maintain cellular structure and are involved in cellular transport, exocytosis, polarisation, migration, adhesion and cell division (Bacallao et al., 1989; Dvorak et al., 2002; Ezratty et al., 2005; Hirokawa, 1998; Jordan et al., 1993; Kaverina et al., 1998; Kuncl et al., 2003; Presley et al., 1997; Vasiliev et al., 1970; Yeh et al., 1995; Yisraeli et al., 1990). They consist of α/β-tubulin heterodimers that stack into linear protofilaments, typically thirteen of which associate laterally and fold into 25 nanometer cylindrical tubes (Desai and Mitchison, 1997; Li et al., 2002; Löwe et al., 2001; Nogales et al., 1998). At one end microtubules are bordered by a ring of α-tubulin and at the other by a ring of β-tubulin, known respectively as the minus-end and the plus-end (Nogales et al., 1999). Both α- and β-tubulin possess guanine nucleotide binding sites, but in α-tubulin guanosine triphosphate (GTP) binds this site irreversibly (Nogales et al., 1998). This irreversibile GTP binding, together with associating Mg^{2+} ions, microtubule associated proteins and stabilisation by the microtubule organising centre (MTOC) makes the minus-end a relatively stable structure (Drechsel et al., 1992; Menendez et al., 1998; Piel et al., 2000). Conversely, the β-subunit guanine nucleotide binding site is exchangeable; GTP is hydrolysed to guanosine diphosphate (GDP) as new heterodimers bind to and lengthen the microtubule (Löwe et al., 2001; Nogales et al., 1999; Nogales et al., 1998). Microtubules with GTP-bound β-tubulin exposed at the plus-end favour a straight protofilament conformation which promotes polymerisation, whereas GDP-bound tubulin adopts a curved conformation promoting depolymerisation

(Nogales et al., 1998). As GTP is only hydrolysed on heterodimer addition, the exposed plus-end is stable. However, when GDP-bound tubulin is exposed the conformational change induces depolymerisation (Desai and Mitchison, 1997; Nogales et al., 1999; Walker et al., 1989). Rapid switching between phases of microtubule growth and decay, termed “dynamic instability”, is an important part of cellular microtubule function (Blocker et al., 1998; Desai and Mitchison, 1997; Jordan et al., 1993). As well as processes dependent on dynamicity, MAPs, such as kinesin and dynein, use the microtubule network as a scaffold to move proteins towards the plus-end and minus-end of microtubules, facilitating rapid transport (up to 1.5 µm/s) around the cell (Gibbons, 1981; Presley et al., 1997; Vale et al., 1985). Two classes of compound elicit their effects by altering the microtubule network – Microtubule destabiling drugs (DSD), and microtubule stabilising drugs (MSD). Altering the structure and dynamicity of microtubules has wide-reaching physiological effects and it was the aim of this thesis to understand how modification by microtubule actives affects the immune system.

1.1.2 Microtubule Destabilising Drugs

DSD interact with microtubules in numerous ways, all of which have the net effect of reducing microtubule dynamicity by destroying the microtubule network (Jordan and Wilson, 2004; O'Brien Jr et al., 1995). These drugs have been successfully employed as anti-cancer or anti-inflammatory drugs (Ahern et al., 1987; Nole et al., 2009). DSD commonly used in the laboratory are colchicine, the vinca alkaloids (vincristine, vinblastine and vinorelbine), nocodazole and podophyllatoxin (Ding et al., 1990a).

1.1.3 Microtubule Stabilising Drugs

In contrast to DSD, MSD have the ability to bind to and stabilise microtubules. At low concentrations this suppresses dynamic instability, and at higher concentrations the structural arrangement of the network is altered (Hood et al., 2002; Jordan et al., 1993; Jordan and Wilson, 2004; O'Brien Jr et al., 1995). MSD cause mitotic block, the appearance of multiple mitotic asters, and the induction of apoptosis in dividing cells as well as cause microtubule bundling in interphase cells (Hood et al., 2002; Jordan et al., 1993; O'Brien Jr et al., 1995). Such drugs have been applied as chemotherapeutics and are still in wide clinical use. MSD include paclitaxel, docetaxel, the epothilones, TTI-237, discodermolide, laulimalide and peloruside A (peloruside) (Beyer et al., 2008; Buey et al., 2005; Mooberry et al., 1999; West et al., 2000). The microtubule stabilising activity of paclitaxel and peloruside are discussed in more detail below.

1.1.3.1 Paclitaxel

The first discovered MSD, paclitaxel, was isolated from the pacific yew tree *Taxus brevifolia* (Schiff et al., 1979; Wani et al., 1971). Low nanomolar concentrations of paclitaxel induce apoptosis and cause mitotic block at the G_2/M-phase transition of the cell cycle and induce bundling in interphase cells (Jordan et al., 1993; Schiff et al., 1979). Paclitaxel binds to the taxane site on microtubules, a site shared by most other MSD (Buey et al., 2005; Nogales et al., 1998). Paclitaxel, marketed as Taxol®, is used clinically to treat a wide range of solid tumour cancers, including breast, endometrial and non-small cell lung carcinoma (Connelly et al., 1996; Holmes et al., 1991; Kelly et al., 2001). Some cancers are resistant to a broad spectrum of chemotherapeutic agents, including paclitaxel, which is associated with overexpression of the MDR-1 gene encoding the P-glycoprotein efflux pump (P-gp) (Gaitanos et al., 2004; Goldstein et al., 1989; Newman et al., 2000; Parekh et al., 1997). Further, due to limited solubility, paclitaxel is administered using Cremophor EL® as a vehicle which is associated with deleterious side effects

(Gelderblom et al., 2001; Goldstein et al., 1989; Newman et al., 2000; Parekh et al., 1997). Due to limitations of delivery and multi-drug resistance, alternative MSD and delivery mechanisms for paclitaxel are currently under development.

1.1.3.2 Peloruside

A recently discovered MSD, peloruside, was isolated from the New Zealand marine sponge *Mycale hentscheli* (West et al., 2000). Like paclitaxel, peloruside causes mitotic block at low nanomolar concentrations and induces microtubule bundling at higher concentrations (Crume et al., 2007; Gaitanos et al., 2004; Hood et al., 2001; Hood et al., 2002; Miller et al., 2004; Wilmes et al., 2007). Peloruside binds to a site on microtubules distinct from the taxane site that shows overlap with laulimalide (Gaitanos et al., 2004; Hamel et al., 2006; Huzil et al., 2008). The compound is a potent inducer of apoptosis in P-gp-expressing cell lines and synergises with a number of taxane-site MSD in the polymerisation of tubulin and killing of cell lines *in vitro* (Gaitanos et al., 2004; Hamel et al., 2006; Wilmes et al., 2007). Currently, it shows great promise for development as an alternative chemotherapeutic agent to paclitaxel.

1.1.4 *In vivo* Immunomodulation by Microtubule Stabilising Drugs

As mentioned in section 1.1.3, MSD are used clinically in the treatment of a variety of cancers. Chemotherapy involving taxanes (paclitaxel or docetaxel) can substantially modify the human immune system. First and foremost, the agents cause general leukopenia (Tong et al., 2000). $CD8^+$ T cells, however, survive better than other lymphocyte subsets and replenish comparatively faster post-therapy (Westerterp et al., 2008; Zhang et al., 2008). Increased numbers of IFN-γ^+- and activated $CD44^{High}$-$CD8^+$ T cells have also been reported following taxane therapy (Zhang et al., 2008). In contrast, paclitaxel causes a selective inhibitory effect on T_{REG} function (Zhang et al., 2008). Taxane therapy also modifies the

cytokine environment of cancer patients, suggesting that MSD induce a variety of effects on the immune system (Penson et al., 2000; Tong et al., 2000; Tsavaris et al., 2002; Zhang et al., 2008).

Recent investigations in mice combining immunotherapies with taxane treatment have consistently found positive effects of the combined therapy on tumour regression (Chu et al., 2006; Emens et al., 2001; Yu et al., 2003; Zhong et al., 2007). These positive outcomes are associated with decreased T_{REG} function and increased anti-tumour cytotoxic T lymphocyte (CTL) responses (Chu et al., 2006; Garnett et al., 2008; Vicari et al., 2009; Yu et al., 2003; Zhong et al., 2007). It is apparent that MSD can alter the immune system, but few studies distinguish functional modifications to immune cells caused by MSD from anti-proliferative properties. The immune responses of macrophages (MØ) and cytotoxic T lymphocytes (CTL) involve microtubules either after or without entering mitosis, making it possible to investigate the functional effects of MSD on these cell types.

1.2 Macrophage function: Role and Responses

1.2.1 Macrophage Function

MØ are terminally-differentiated phagocytic cells of the innate immune system. MØ are one of the first cells to respond to infection and act predominantly through pattern recognition receptors, such as the toll-like receptors (TLR). TLR recognise conserved carbohydrate, nucleic acid and lipotechoic acid motifs, collectively termed pathogen-associated molecular patterns (PAMP) (Akira et al., 2001). One of the major receptors involved in MØ responses is TLR-4, which is stimulated by bacterial lipopolysaccharide (LPS) (Akira et al., 2001; Hirschfeld et al., 2000). Optimal activation of TLR-4 is conferred when TLR-4 associates with MD-2, CD14, and LPS-bound LPS-binding protein to form the TLR-4 signalling complex (da Silva Correia et al., 2001; Wright et al., 1990). Stimulation of the TLR-4

complex by LPS causes MØ to produce high levels of the proinflammatory mediators TNF-α, IL-1β, IL-6, IL-8, IL-12p40, MMP-9, and nitric oxide (NO); to upregulate MHC-II; and also alters tissue trafficking of the cells (Chow et al., 1999; Crume et al., 2007; Fiorentino et al., 1991; Hirschfeld et al., 2000; Hoshino et al., 1999; Kawai et al., 1999; Kincy-Cain and Bost, 1997; Marikovsky et al., 2003; Nakano et al., 1999; Schartner et al., 2005; Stuehr and Marletta, 1985; Tamandl et al., 2003; Tobias et al., 1993; Woo et al., 2004; Xie et al., 1994). Priming MØ with IFN-γ augments production of these mediators. Most importantly, pre-treatment with IFN-γ enhances production of TNF-α and NO in response to LPS (Ding et al., 1988; Gifford and Lohmann-Matthes, 1987; Stuehr and Marletta, 1985). Furthermore, IFN-γ also synergises with TNF-α to enhance the production of NO (Vila-del Sol et al., 2006).

1.2.2 Tumour Necrosis Factor-α

TNF-α signalling is important in the host response to infection, functioning as both a signalling molecule and an inducer of apoptosis (Carswell et al., 1975; Havell, 1989; Rothe et al., 1993). TNF-α is an early onset cytokine that is rapidly produced by LPS-activated MØ. TNF-α mRNA can be detected in MØ as little as 30 minutes after LPS activation and most protein production occurs in the first 2-10 hours (Crume et al., 2007; Sander et al., 1991; Takasuka et al., 1995). Prolonging culture generally leads to decreases in bioactive protein (Fujihara et al., 1994; Virca et al., 1989). It was first identified as an LPS activation product with tumoricidal properties, and later as a chemotactic agent capable of inducing migration of monocytes and neutrophils (Carswell et al., 1975; Ming et al., 1987). There are two signalling receptors for TNF-α: TNF-RI and TNF-RII. While both TNF-RI and TNF-RII stimulate proinflammatory immune signalling through nuclear factor–κβ (NF-kβ) and c-Jun N-terminal kinase (JNK)/MAP-kinase (MAP-K) pathways (Liu et al., 1996; Tartaglia et al., 1993), TNF-RI is the predominant

effector of apoptosis in non-haematopoetic cells (Beg and Baltimore, 1996; Vandenabeele et al., 1995a). TNF-RI expresses a cytoplasmic death domain signal sequence which activates the caspase cascade (Nagata, 1997; Wang et al., 1998). However, NF-kB signalling blocks TNF-α-induced apoptosis and is thus anti-apoptotic (Beg and Baltimore, 1996; Wang et al., 1998). In contrast to TNF-RI, TNF-RII lacks the cytoplasmic death domain, and while it synergises with TNF-RI in the induction of apoptosis (Vandenabeele et al., 1995b), TNF-RII is primarily involved in immune signalling (Rothe et al., 1994).

Recently it has been identified that secretion of TNF-α occurs in a unique fashion, as it associates with recycling endosomes. When MØ are activated, these endosomes fuse with the plasma membrane facilitating rapid release of TNF-α (Manderson et al., 2007; Murray et al., 2005). Once released, as NF-kβ activation stimulates TNF-α gene transcription, TNF-α can enhance its own production (Collart et al., 1990).

1.2.3 Nitric Oxide

Like TNF-α, NO is involved in the host response against microbial infection (Stenger et al., 1996). NO is produced by the enzyme nitric oxide synthase (NOS). Three distinct isoforms of NOS exist – neuronal NOS (nNOS; NOS1), inducible NOS (iNOS; NOS2) and endothelial NOS (eNOS; NOS3) (Bredt et al., 1991; Marsden et al., 1992; Xie et al., 1992). nNOS and eNOS are constitutively active and produce NO in a calcium dependent manner, but operate in different tissue types and have different functions to iNOS (Alderton et al., 2001; Bredt and Snyder, 1989, 1990; Janssens et al., 1992). Immune-mediated NO production occurs primarily via iNOS which has a minimal requirement for calcium and can induce much higher levels of NO than nNOS or eNOS (Lowenstein et al., 1992; MacMicking et al., 1997; Stuehr and Marletta, 1985; Xie et al., 1992). While IFN-γ

alone can induce iNOS mRNA activity, both LPS and TNF-α synergise with IFN-γ to enhance NO production (Ding et al., 1988; Geller et al., 1993; MacMicking et al., 1997). Compared to TNF-α, NO production occurs relatively later following LPS-activation, and is typically measured at later timepoints (Crume et al., 2007; Vila-del Sol et al., 2006).

1.2.4 Paclitaxel is a LPS Mimetic

Unique among MSD, paclitaxel mimics LPS *in vitro* by activating murine MØ to produce proinflammatory mediators including IL-1β, IL-12p40, TNF-α and NO (Bogdan and Ding, 1992; Crume et al., 2007; Ding et al., 1990b). Like LPS, paclitaxel-induced inflammation is dependent on signalling through the TLR-4 complex and is blocked in LPS-hyporesponsive and TLR-$4^{-/-}$ mice, as well as by antagonists of TLR-4 activation (Byrd-Leifer C.A. et al., 2001; Ding et al., 1992; Hoshino et al., 1999; Kawasaki et al., 2000; Manthey et al., 1993; Perera et al., 2001). No other MSD, including peloruside and the semi-synthetic paclitaxel analogue docetaxel, share this mimicry (Crume et al., 2007; Manthey et al., 1993). Importantly, paclitaxel specifically stimulates murine TLR-4/MD-2 and does not activate human monocytes or MØ (Allen et al., 1993), or cells transfected with human MD-2 (Kawasaki et al., 2000; Kawasaki et al., 2001).

Some work investigating the TLR-4-mediated effects of paclitaxel on LPS-tolerance has been conducted. LPS-tolerance is a state in which MØ responses to LPS are altered if the MØ have previously been exposed to low concentrations of LPS (Takasuka et al., 1991). The low-dose LPS-priming depresses transcriptional activity and alters the proinflammatory cytokine response (Shnyra et al., 1998; Tominaga et al., 1999). Most significantly, LPS-primed MØ are reciprocally rendered predominant producers of either TNF-α or NO, relating directly to the priming dose of LPS (Hirohashi and Morrison, 1996; Shnyra et al., 1998; Zhang

and Morrison, 1993a, b). In a similar fashion, when MØ are pretreated with either LPS or paclitaxel, paclitaxel-induced TNF-α production is reduced, and the production of NO is reciprocally enhanced (Nakano et al., 1999). Further studies show that paclitaxel, likely due to its TLR-4 mimicry, depresses NF-kB and MAP-K phosphorylation in LPS-tolerant MØ (Tominaga et al., 1999), and a similar state of tolerance is induced by paclitaxel on LPS responses in B-cells (Lee and Jeon, 2001; Lee et al., 2000).

1.2.5 Involvement of the Microtubule Network in LPS Signalling

Activation of the TLR-4 complex by paclitaxel has been heavily investigated, but only a small body of literature has examined the combined effects of simultaneous exposure to LPS and microtubule actives on TLR-4 responses. The most recent studies by our group investigated the effects of paclitaxel and peloruside on IFN-γ-primed murine bone-marrow derived MØ (BMMØ) and demonstrated that while peloruside does not activate TLR-4 like paclitaxel, both peloruside and paclitaxel inhibit LPS-induced TNF-α and NO production (Crume et al., 2007). Earlier work using LPS-activated peritoneal MØ (PMØ) assessed only low concentrations of paclitaxel that did not inhibit TNF-α production, but did not assess higher concentrations which may have revealed an effect (Manthey et al., 1992).

Similar effects on LPS-induced cytokine production are seen with DSD. DSD diminish LPS-induced TNF-RI expression, TNF-α protein production, iNOS activity and NO production in PMØ (Ding et al., 1990b; Kirikae et al., 1996; Li et al., 1996). In the RAW MØ cell line, LPS-induced production of TNF-α and GM-CSF are inhibited, but in contrast to PMØ, iNOS activity is unaltered (Isowa et al., 1999; Rao et al., 1997). Thus murine MØ responses to LPS are similarly inhibited by DSD and MSD.

In general, DSD & MSD affect human and murine MØ similarly, but some differences between species do occur. Studies into DSD show that colchicine inhibits LPS-induced peripheral blood mononuclear cell (PBMC) TNF-α production, but enhances IL-1β production (Allen et al., 1991). Similar inhibitory effects of the DSD nocodazole on IL-1β and TNF-α are observed in PMA-stimulated human monocytes (Rammes et al., 1997). Interestingly, while paclitaxel does not directly activate human TLR-4 (Kawasaki et al., 2000; Resman et al., 2008), in the presence of paclitaxel, PBMC production of both IL-1β and TNF-α are increased (Allen et al., 1993). This is the opposite effect of paclitaxel on TNF-α production to that seen in murine BMMØ (Crume et al., 2007), and the opposite effect on TNF-α production from DSD (Allen et al., 1991).

Here, it is apparent that species and cell type can lead to different effects of microtubule actives on cytokine production. Microtubules are involved in almost every facet of cellular function (section 1.1.1) so targeting them causes relatively non-specific pathway inhibition. It is the combined effect of all such modified interactions that render the final phenotype; altering the microtubule network can have drastic consequences on the inflammatory response. With this in mind, it is important to understand the pathways that are most crucial for immune signalling that we may better understand the immunological implications of MSD therapy.

1.3 $CD8^+$ T Cells: Activation & CTL-Mediated Cell Death

1.3.1 The role of $CD8^+$ T Cells

Cytotoxic T lymphocytes (CTL) are cells of the adaptive immune system that function primarily to kill virally-infected and cancerous cells (Abougergi et al., 2005; Breart et al., 2008; Kagi et al., 1994; Shimizu et al., 1999). Naïve $CD8^+$ T

cells are the precursors to CTL, both of which express T cell receptors (TCR) specific for the same short peptide presented in the context of MHC-I (Townsend et al., 1986). Such short peptides are termed ‘antigens’ (Janeway et al., 2001). Typically the TCR repertoire of an individual mouse or human is enormous and allows the immune system to direct responses against pathogens expressing many different antigens. However, transgenic mice have been generated that express limited and peptide-specific TCR. For example, OT-I mice are modified such that a large proportion of T cells express CD8 and $V_{\alpha 2}/V_{\beta 5.1/5.2}$-TCR that recognise the SIINFEKL peptide of OVA protein, allowing for great enrichment of these T cells and tight control of the experimental immune response (Hogquist et al., 1994).

For both normal and transgenic $CD8^+$ T cells, recognition of the TCR-specific antigen in the context of MHC-I is required to activate the T cell and generate an effective immune response. To differentiate into effector CTL, naïve $CD8^+$ T cells encountering an antigen presenting cell (APC) in the lymph node scan the APC surface for antigen-MHC-I complexes. When the specific antigen is recognised, formation of a signalling complex including the TCR, MHC-I, CD8 and costimulatory molecules activate the T cell (Albert et al., 1998; Bachmann et al., 1997; Cottalorda et al., 2006; Luescher et al., 1995). This leads to large-scale proliferative expansion and activation of the $CD8^+$ T cell population (Tanchot et al., 1997).

As the $CD8^+$ T cells replicate they undergo characteristic functional changes that alter their activity and tissue homing properties. Immature, antigen inexperienced, naïve $CD8^+$ T cells are required to divide at least once to reach effector status, both *in vitro* and *in vivo* (Oehen and Brduscha-Riem, 1998). During progressive

divisions, the lytic machinery of the $CD8^+$ T cell is upregulated and the cells increase in cytolytic capacity (Oehen and Brduscha-Riem, 1998; Wolint et al., 2004). With later cell divisions, CTL granule potency reduces, and the CTL develop into a memory phenotype (Oehen and Brduscha-Riem, 1998).

The effector status of $CD8^+$ T cells can be determined by surface markers involved in tissue homing and intercellular recognition (Table 1.1). *In vivo*, naïve $CD8^+$ T cells are stereotypically $CD44^{low}$, $CD45RA^+$, $CD62L^{high}$, and $CD69^{low}$ (Hamann et al., 1997; Oehen and Brduscha-Riem, 1998). After antigenic stimulation, naïve $CD8^+$ T cells immediately upregulate CD69 and integrins, and begin to divide (Hamann et al., 1997; Oehen and Brduscha-Riem, 1998). It takes at least 24 hours for $CD8^+$ T cells to divide and become CTL capable of rapidly killing target cells (Boissonnas et al., 2004; Hwang et al., 2006; Oehen and Brduscha-Riem, 1998). CTL are characteristically $CD44^{High}$, $CD62L^{Low}$, and express reduced levels of TCR as well as increased levels CD25 (Oehen and Brduscha-Riem, 1998). Further divisions convert the CTL population into a memory phenotype. Two related classes of memory T cells exist – Effector memory T cells (T_{EM}), and central memory T cells (T_{CM}). Both classes are $CD44^{High}$, $CD11A^{High}$, $CD69^{Low}$ and $CD25^{Low}$. T_{CM} are stereotypically $CD45RO^+$, $CD62L^+$, $CCR7^+$, and $CD27^{High}$, while T_{EM} are $CD62L^-$, $CCR7^-$ and $CD27^{Low/Mid}$ (Geginat et al., 2003; Hamann et al., 1997; Masopust et al., 2001; Wherry et al., 2003). On antigenic stimulation, CTL, T_{EM} and T_{CM} release granules, but the granules of T_{CM} are deficient in lytic proteins, and they do not induce lysis (Wolint et al., 2004). Thus, while CTL and T_{EM} can immediately induce death of target cells, T_{CM} are primarily involved in ongoing immunological surveillance, as they can revert to a CTL phenotype on re-exposure to antigen (Oehen and Brduscha-Riem, 1998; Wherry et al., 2003). The different phenotypes provide tight

immunological surveillance – CTL, T_{EM} and T_{CM} can circulate through the periphery and respond to current and future infection, while naïve T cells localise in the lymphoid tissues awaiting activation (Wherry et al., 2003). In mouse models, 6-8 days after initial antigen exposure generates an optimal CTL response with minimal proliferation (De Boer et al., 2001).

Table 1.1

			T-MEM	
Class	Naïve	CTL	T-EM	T-CM
TCR Specificity	All Identical			
CD8	+	+	+	+
Differentiate into:	CTL	T-EM	T-CM	CTL
CD62L	High	Low	Low	High
CD44	Low	High	High	High
CD69	Low	High	Low	Low
Degranulate	No	Yes	Yes	Yes
Immediately Cytolytic	No	Yes	Yes	No
Long lived	Yes	No	No	Yes

$CD8^+$ T Cell Surface Phenotype Determines Effector Status. Naive $CD8^+$ T cells reside in lymphoid tissues until they are stimulated by APC to divide into CTL which rapidly kill target cells. CTL eventually divide to establish transient T_{EM} or long-lived T_{CM} populations. T_{EM} also have lytic capabilities. Over a period of time T_{EM} also divide into T_{CM}. T_{CM} are unable to immediately kill TC and must first divide and return to a CTL phenotype.

1.3.2 Death Mediated by CTL

On encounter of a specific target cell (TC), CTL employ two major pathways to mediate the removal of such cells. The primary pathway requires the delivery of perforin and granzyme-containing lytic granules to the TC. The second is dependent on the ligation of Fas receptors (Fas) on the surface of the TC by Fas-Ligand (FasL) expressed by CTL. Both mechanisms have the net result of induction of apoptosis in the TC, and are discussed in more detail in sections 1.3.4 and 1.3.5 respectively.

1.3.3 Formation of the Immunological Synapse

Once a T cell recognises an appropriate TC, TCR-conjugation initiates binding and segregation of signalling components. This leads to the formation of two distinct supramolecular activation clusters (SMAC) at the CTL:TC interface and concurrent increases in affinity at the contact site, which becomes known as the immunological synapse (IS) (Bunnell et al., 2001; Monks et al., 1998; Stinchcombe et al., 2001b; Stinchcombe et al., 2006). Analogous to $CD4^+$ T cell immunological synapses, CTL:TC conjugates form a tight central ring enriched in TCR, CD3, Lck, and PKC-θ, comprising the central SMAC (cSMAC) (Monks et al., 1998; Stinchcombe et al., 2001b; Stinchcombe and Griffiths, 2003; Wiedemann et al., 2006). The cSMAC is surrounded by a dense ring of LFA-1 and talin, comprising the peripheral SMAC (pSMAC) (Grakoui et al., 1999; Monks et al., 1998; Stinchcombe et al., 2001b; Stinchcombe and Griffiths, 2003). In $CD8^+$ IS, some PKC-θ is present in the pSMAC, but the relevance of this is not known. More importantly for effective signalling, CD45 is excluded from the cSMAC, which allows for optimal TCR/CD3 stimulation (Stinchcombe et al., 2001b), and downstream stimulation of signalling events (Janes et al., 1999; Janes et al., 2000). While formation of an IS is requisite to successful killing by CTL, large

enrichment of TCR/CD3 in the cSMAC is not necessary for the initiation of apoptosis in the target, suggesting that signalling and lysis are separately regulated in CTL (Faroudi et al., 2003; Stinchcombe et al., 2001b; Wiedemann et al., 2006). Thus, CTL stimulation can be separated into two stages: first, degranulation by CTL to kill TC; and second, activation of immune signalling (i.e., IFN-γ production). As the threshold required to induce cytokine production is higher than that of degranulation (Faroudi et al., 2003; Wherry et al., 2003), the lytic and stimulatory events of CTL activation may be differentially susceptible to the effects of MSD.

1.3.4 Inducing Cell Death via Granule Exocytosis

In conjunction with IS formation, large scale cytoskeletal remodelling occurs in CTL (Figure 1.1). Actin microfilaments are excluded from the cSMAC along with talin and terminate at the outer edge of the pSMAC (Kuhn and Poenie, 2002; Stinchcombe et al., 2001a; Stinchcombe et al., 2001b; Stinchcombe et al., 2006). The microtubule network at this point is comprised of two distinct types of microtubules – The first type are long sweeping microtubules, of which the plus ends contact the plasma membrane within the pSMAC and terminate peripheral from the IS; The second type are short straight microtubules that extend from the MTOC and terminate within the IS at sites away from the cSMAC (Kuhn and Poenie, 2002; Stinchcombe et al., 2006). Simultaneous with pSMAC/cSMAC partitioning, the MTOC and associated golgi-apparatus vectorially translocate down the long sweeping microtubules to associate with the IS, localising at or near the cSMAC (Geiger et al., 1982; Stinchcombe et al., 2001b). Thus, by the time the MTOC associates with the IS, actin filaments and microtubule plus-ends have been cleared from the site of lytic granule delivery (Kuhn and Poenie, 2002; Stinchcombe et al., 2006).

After MTOC polarisation, preformed lytic granules stored in the cell periphery traffic down microtubules and cluster around the MTOC (Stinchcombe et al., 2001b; Stinchcombe et al., 2006). Lytic granule mediated cytolysis can take place in the absence of plus-end movements of lytic granules, suggesting a unique exocytosis mechanism, likely involving dyneins, in lytic granule delivery (Kuhn and Poenie, 2002; Stinchcombe et al., 2006). During killing, the CTL MTOC dynamically oscillates across the IS in single CTL:TC conjugates, at times contacting the plasma membrane (Kuhn and Poenie, 2002). Lytic granules detach from the microtubule network to be delivered to the TC via the golgi apparatus (Bossi and Griffiths, 2005; Stinchcombe et al., 2001a). As lytic granules dissociate from the microtubule network they release their contents in a static secretory domain between the cSMAC and pSMAC, defined visually by a pre-formed invagination in the TC membrane (Stinchcombe et al., 2001b; Stinchcombe and Griffiths, 2003). The high concentration of lytic proteins found within lytic granules, including a range of granzymes (primarily A,B,C) and perforin (cytolysin), induces apoptosis in the TC (Konigsberg and Podack, 1986; Macdermott et al., 1986; Munger et al., 1986; Peters et al., 1991; Podack and Dennert, 1983; Podack and Konigsberg, 1984). After granule delivery, CTL can dissociate from TC and recirculate to kill multiple TC in a similar manner (Chuang, 1994; Chuang et al., 1994). The whole process occurs very rapidly, with the time from initial antigen encounter to measurable apoptosis generally occurring in less than 20 minutes *in vitro* and *in vivo* (Mempel et al., 2006; Stinchcombe et al., 2001b).

The importance of degranulation is demonstrated in both *in vitro* and *in vivo* processes. *In vitro*, CTL deficient in perforin, one of the key lytic granule proteins, are severely impaired in lytic capacity (Kagi et al., 1994; Lowin et al., 1994). *In vivo,* Tumour-infiltrating lymphocytes (TIL) are rendered unable to polarise and

deliver granules to TC and are accordingly unable to elicit killing (Radoja et al., 2001); and T_{REG} greatly impair TC killing by CTL by inhibiting granule release (Mempel et al., 2006). However, the most striking example of the involvement of degranulation in CTL-mediated cytolysis is demonstrated by CTL generated from *Ashen* mice. CTL from these mice lack the small Ras-like GTPase Rab27a, which is required for lytic granules to dock and release their contents at the CTL:TC interface (Stinchcombe et al., 2001a). Because of this deficiency, CTL from *Ashen* mice are rendered incapable of killing certain types of TC (Stinchcombe et al., 2001a).

Figure 1.1

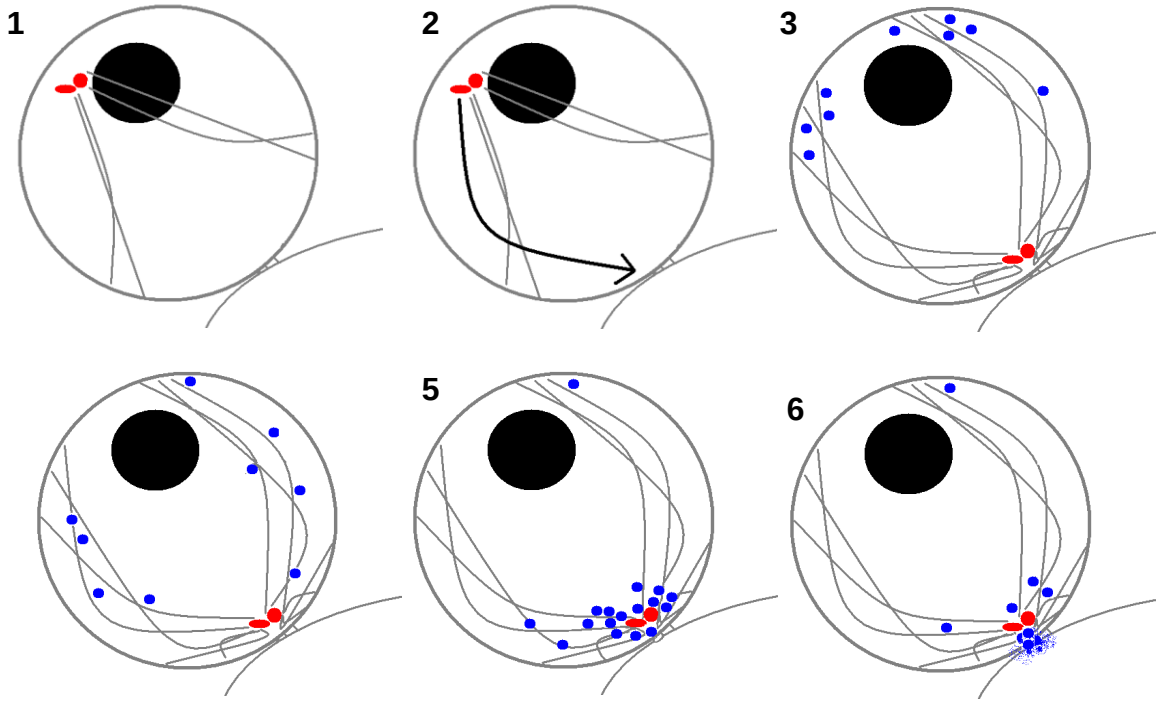

Involvement of the microtubule network in lytic granule delivery. (**1**) When a CTL (whole cell) recognises a TC (shown in part) an IS is formed and the MTOC (red) relocalises and associates with the CTL:TC interface, known as the immunological synapse (**2**). (**3**) Lytic granules (blue) traffic down microtubules (**4**) and cluster around the MTOC (**5**) for delivery to and induction of apoptosis in the TC (**6**).

1.3.5 Fas-Ligand Mediated Cell-Death

The second pathway CTL employ to kill TC involves the ligation of Fas on the TC by Fas Ligand (FasL) expressed on the surface of the CTL. FasL exists in two forms: As either membrane bound FasL or soluble FasL (sFasL). While in humans sFasL can induce diapedesis and has cytolytic activity (Seino et al., 1998; Tanaka et al., 1995), murine sFasL is minimally active, operating solely as a competitive inhibitor for Fas binding (Hohlbaum et al., 2000; Tanaka et al., 1995).

The intracellular domain of Fas shares sequence homology with the apoptosis-inducing death domain of TNF-RI (Itoh and Nagata, 1993; Nagata and Golstein, 1995). When expressed in non-haematopoietic cells, FasL is constitutively expressed and limits autoimmunity at immunologically priviledged sites (Bossi and Griffiths, 1999; Bossi et al., 2000). In contrast, FasL is only expressed by CTL on CD3/TCR activation (Vignaux et al., 1995). FasL can compensate for deficiencies in the perforin/granzyme (i.e., lytic granule) pathway (Kagi et al., 1995; Lowin et al., 1994), and is essential in the clearance of some viral infections (Abougergi et al., 2005). While only expressed in CTL on activation, control of FasL expression in CTL is biphasic. Pre-formed FasL is stored in lytic granules and on CTL activation is delivered to the surface in lytic granules (Blott et al., 2001; Bossi and Griffiths, 1999; Bossi et al., 2000). FasL synthesised thereafter, however, is expressed directly on the CTL surface (He and Ostergaard, 2007). This second phase of FasL expression bypasses the granule component and does not require the microtubule network (He and Ostergaard, 2007). Thus, to be functional, murine FasL needs to be present on the plasma membrane of CTL, but can be expressed in the absence of degranulation and compensate for deficiencies in the perforin/granzyme pathway (He and Ostergaard, 2007; Lowin et al., 1994).

1.3.6 The Known Effects of Microtubule Actives on Lymphocyte Function

Early work investigating the role of the microtubule network in CTL function primarily employed DSD. While actin microfilaments, and not microtubules, are involved in initial TC recognition (Bunnell et al., 2001; Plaut et al., 1973), microtubules are involved in stabilising the IS (Bunnell et al., 2001). DSD also reduce the TCR turnover rate at the IS, which may affect signalling events (Das et al., 2004). Most importantly, destroying the microtubule network prevents lethal hit delivery and inhibits cytolysis *in vitro* (Plaut et al., 1973). The inhibitory effect DSD have occurs primarily because they block CTL polarisation by preventing relocalisation of the MTOC adjacent to the TC, precluding all the downstream events involved in killing (Geiger et al., 1982; Kupfer and Dennert, 1984; Kupfer et al., 1985).

Studies into the effects of MSD on lymphocytes have concentrated on the use of paclitaxel. Paclitaxel induces G_2/M-phase block in proliferating lymphocytes *in vitro* (Brown et al., 1985). Paclitaxel also inhibits allogeneic activation of cells in the mixed lymphocyte reaction (MLR), but only when responding cells, not stimulators, are treated with paclitaxel (Roy et al., 1988). In human NK T cells, paclitaxel inhibits TC death without killing the effector cells (Markasz et al., 2007). Two separate studies have analysed paclitaxel in human CTL, both showing that the ability of CTL to kill multiple targets is inhibited at low micromolar concentrations *in vitro* (Chuang et al., 1994; Markasz et al., 2008). However, in the murine system micromolar concentrations of paclitaxel induce microtubule bundling in interphase CTL, but do not inhibit *in vitro* cytolysis by CTL (Brown et al., 1985; Knox et al., 1993). Further, low-dose paclitaxel can partially abrogate the inhibitory effects of DSD on killing (Kupfer et al., 1983; Wolberg et al., 1984).

The immunological effects of peloruside on lymphocytes are less widely explored. Peloruside is known to inhibit IL-2 and IFN-γ production by killing splenocytes stimulated with T cell mitogens, as well as in the MLR (Crume et al., 2007; Hood et al., 2001; Miller et al., 2004). Aside from this, little is known about the effects the compound has on immediate processes, such as CTL-mediated cytolysis.

In contrast to human CTL, studies into the effects of paclitaxel did not demonstrate effects on murine CTL function (Knox et al., 1993). However, the initial study by Knox et al. only investigated the effects at high CTL:TC ratios (Knox et al., 1993). Due to the known importance of dynamic instability in other cell transport mechanisms and the involvement of the cytoskeleton in lytic granule delivery, it is possible that under more limited circumstances such as at lower CTL:TC ratios, or in an *in vivo* setting, effects of MSD may become more apparent. Further, because the mechanisms of microtubule stabilisation by paclitaxel and peloruside differ, these two agents may differentially affect degranulation and cell death. Thus, there is reason to believe paclitaxel and peloruside may differently or similarly affect CTL function *in vitro* and MSD may alter killing processes *in vivo*. Determining how these agents affect CTL function will identify immediate effects of MSD therapy on the immune system and better clarify the involvement of microtubules in the normal immune response.

2 Methods

2.1 Mice

BALB/c mice were from breeders at VUW. C57BL/6 mice were purchased from the Otago School of Medicine Biomedical Research Unit, Wellington, New Zealand. OT-I and OT-I/ptp-rc^a mice were kindly provided by Prof. Franca Ronchese at the Malaghan Institute of Medical Research (MIMR). OT-I mice possess an enriched population of T cells expressing $V_{\alpha 2}/V_{\beta 5.1/5.2}$-TCR specific for the SIINFEKL peptide of OVA (Hogquist et al., 1994). T cells from OT-I/ptp-rc^a mice are SIINFEKL-peptide specific and CD45.1$^+$/CD45.2$^+$, whereas C57BL/6 T cells only express CD45.2. Thus, populations of OT-I/ptp-rc^a T cells can be tracked in C57BL/6 mice by measuring CD45.1 expression. Mice used for *in vivo* work were housed in a 12-hour light/dark cycle and experiments started early in the light cycle. Mice were euthanized by CO_2 asphyxiation and tissues removed by blunt dissection with forceps and scissors sterilised in 100% ethanol. All mouse work was done in accordance with the guidelines of the Victoria University of Wellington Animal Ethics Committee.

2.2 Reagents

Paclitaxel purified from *Taxus yannanensis,* colchicine and LPS (from *E. coli*) were purchased from Sigma Chemical Company (St. Louis, MO, USA). Taxol® (Taxol; in Cremophor; Bristol Myers Squibb, New York City, NY, USA) was purchased from Capital Coast Chemists (Wellington, New Zealand). Cremophor EL® was purchased from Sigma-Aldrich-Fluka (Taufkirchen, Germany). Peloruside was provided by Dr. Peter Northcote (Victoria University of Wellington, School of Chemical and Physical Sciences). Paclitaxel and peloruside stocks

were dissolved in ethanol at 1 mM and stored at -80°C. Colchicine was dissolved in ethanol at 1 mM and stored at room temperature protected from light.

2.3 Cell Culture

2.3.1 BMMØ Culture

BMMØ culture has been described previously (Crume et al., 2007). Femurs and tibias were excised from euthanised C57BL/6 or BALB/c mice and 5 mL Dulbecco's phosphate buffered saline (dPBS; Invitrogen, Auckland, New Zealand) was flushed through each bone. The elute was collected into a 50 mL polystyrene tube (Falcon, Franklin Lakes, NJ, USA). Clumps of marrow were disrupted and red blood cells were lysed with 2 mL Red Blood Cell Lysing Buffer (Sigma). Cells were seeded in 10 or 30 mL volumes in T-25 or T-75 tissue culture flasks (Greiner, Monroe, NC, USA) respectively at $4x10^5$-$1x10^6$/mL in complete T cell medium (CTCM; see Appendix A) overnight. The following day GM-CSF and IL-3 (from supernatants from the GM-KLON and WEHI-3 cell lines respectively) were added and the non-adherent population cultured for a further 7-9 days. Cells were fed on day 4 or day 5 with the original volume of CTCM and cytokines. After a total of 8-10 days culture the non-adherent fraction was removed, the plates washed briefly with dPBS and vigorously blasted with ice-cold dPBS to remove the adherent population. These cells were deemed 'BMMØ'. BMMØ were washed once in handling medium (Appendix A) prior to use. In all experiments BMMØ were checked visually for large, adherent granular cells. Cultures were typically 80-95% $CD11b^+$, $F4/80^{high}$, $I\text{-}Ab^+$, $GR\text{-}1\text{-}PE^{low/mid}$ as determined by flow cytometry.

2.3.2 LPS Stimulation of BMMØ

Following culture, $5x10^4$ BMMØ were seeded at $2.5x10^5$/mL in 96-well flat-bottomed plates (Falcon). Unless otherwise stated, BMMØ were stimulated

overnight with 40 U/mL IFN-γ. After 12-18 hours, 100 µL of the supernatant was replaced with CTCM or CTCM+LPS with or without paclitaxel or ethanol (as vehicle control). Final concentrations are stated in figures. For TNF-α analysis, 100 µL supernatant from each well was removed and frozen at -20°C for TNF-α ELISA. The cells were incubated for a final total of 72 hours and subjected to the Greiss Reaction and the MTT Assay (described below).

2.3.3 BMDC Culture

BMDC were cultured from C57BL/6 mice as previously described (Yang et al., 2006). Femurs and tibias were flushed with 5mL Iscove's modified Dulbecco's medium (IMDM; Invitrogen), the cells washed once in IMDM and cultured in cIMDM (Appendix A) in 5 mL aliquots at $4x10^5$/mL in 6-well tissue culture plates (Invitrogen) in the presence of 20 ng/mL recombinant murine GM-CSF and 20 ng/mL recombinant murine IL-4. On days 3 and 5 of culture 2 mL of the supernatant was carefully replaced with 2 mL cIMDM containing the original volume of cytokines. On day 6 BMDC were matured with 100 ng/mL LPS for 16-20 hours before use in further experiments. The majority of LPS-matured BMDC were typically $CD11b^{high}$, $I\text{-}Ab^{+}$ and $CD11c^{Mid}$. Cultures were also checked visually for typical BMDC morphology (medium to large cells extending whispy dendrites).

2.3.4 CTL Culture

For *in vitro* CTL culture, OT-I or OT-I-$ptprc^a$ mice were euthanized and inguinal, brachial, axillary, cervical and mesenteric lymph nodes (LN) were excised. Cells were separated by disrupting the LN capsules and passing through 70 µm pore size strainers (Falcon). LN cells were washed once in IMDM and combined with LPS-matured BMDC that had been incubated with 0.1 µM SIINFEKL peptide (JPT Peptide Technologies GmbH, Berlin, Germany) for 4 hours. Cells were incubated at final concentrations of $1.25x10^4$/mL (BMDC) and $1x10^5$ /mL (LN cells) in 5 mL

aliquots of cIMDM in 6-well plates. After 4 days the non-adherent fraction was removed, washed once and cultured at $2.5x10^5$/mL in cIMDM containing 100U/mL recombinant human IL-2 in T-75 tissue culture flasks. IL-2 was replaced after 24 hours of culture and CTL were used the following day. CTL were generally >99% $V_{\alpha 2}/V_{\beta 5.1/5.2}$-TCR-specific, of which 98-99% were $CD8^+$, 98% $CD44^{high}$ and >90% $CD62L^{low}$ as determined by flow cytometry. Visually, CTL were larger and less spherical than naïve T cells.

2.3.5 EL-4 Cell line maintenance

Seeder stocks of the murine T-cell hybridoma/thymoma EL-4 were grown from a stock from the MIMR and stored in Freezing Medium (Appendix A) in liquid nitrogen. Cells were maintained in T-25 and T-75 tissue culture flasks at a density of $2x10^5$-$2x10^6$/mL for a maximum of 20 passages in cIMDM.

2.4 MTT Assay

The MTT assay was used to determine metabolic activity of cell cultures as described previously (Crume et al., 2007). In experiments with BMMØ, after the removal of supernatant for the Greiss Reaction, 50 µL CTCM and 20 µL sterile filtered 5 mg/mL (3-(4,5-dimethylthiazoyl-2-yl)-2,5-diphenyltetrazolium bromide) (MTT; Sigma) in dPBS was added to each well. For JAM assay controls (refer to page 38), after a 4 hour pre-treatment with 1 µM paclitaxel, 1 µM peloruside or 0.1% ethanol as vehicle control, CTL ($1x10^5$/well) were washed once and incubated in 100 µL fresh medium in 96-well flat bottomed plates for 4 hours. When JAM plates were harvested, 20 µL MTT was added to each well of the MTT plate. For degranulation assay controls, after pre-treatment CTL were overlayed with 100 µL cIMDM and incubated until the end of the degranulation assay (4 or 6 hours). While degranulation plates were being stained MTT plates were spun for 60 seconds at 50*g* to settle the cells to the bottom of wells, 100 µL supernatant

carefully removed and 20 µL MTT was added to each well. In all cases plates were incubated for 2-2.5 hours with MTT and the reaction was stopped with 100 µL 10% weight/volume sodium dodecyl sulfate (Sigma) in 0.01N HCl. Plates were incubated overnight to allow the crystals to solubilise and read on a Versamax plate reader (Molecular Devices; Sunnyvale, CA, USA) at 570 nanometers the following day.

2.5 ELISA

Enzyme-linked Immunosorbant Assays (ELISA) were run as per the manufacturer's recommendations and unless stated ELISA reagents were from BD Bioscience. Washes were in 0.05% Tween-20 (Sigma) in phosphate buffered saline (PBS; Appendix A). Capture antibodies used were Rat-anti-mouse-TNF-α or Rat-anti-mouse-IFN-γ. Capture was done in 96-well ELISA plates (Greiner) overnight at 4°C by diluting the capture antibody in sodium phosphate buffer pH=6.0 for TNF-α and pH=9.0 for IFN-γ. All subsequent steps were done at room temperature. Plates were blocked with blocking buffer (5% foetal calf serum (FCS; Invitrogen) in PBS) for 2 hours. After four washes; standards and samples (either neat or diluted in blocking buffer) were added to wells for 2 hours. Plates were washed four more times and incubated with a biotinylated detection antibody for TNF-α or IFN-γ; incubated for 1 hour then washed six more times. Plates were then incubated with streptavidin-horse radish peroxidase for 1 hour and washed 8 times. TMB reagents "A" and "B" were combined and added to each well. After sufficient colour development the reaction was stopped by the addition of 100 µL 0.18 M sulfuric acid. Plates were read at 450 nanometers and cytokine concentrations were calculated by comparing sample absorbances to the standards.

2.6 Greiss Reaction

The Greiss Reaction was used to measure NO production as described previously (Crume et al., 2007). NO gas is unstable and breaks down rapidly to form nitrite (NO_2^-) and nitrate which accumulate in culture (Stuehr and Marletta, 1985). By measuring NO_2^-, the Greiss reaction provides a relative measure of NO production. 72 hours after BMMØ were activated with LPS 50 µL of culture supernatants were removed to wells of a 96-well flat-bottomed ELISA plate. Greiss reagents A and B (Appendix A) were combined in equal volumes and 50 µL added to each sample well; each plate contained a row of titrated standards. Plates were read at 570 nanometers in a plate reader and NO production calculated by comparing to the standard curve.

2.7 JAM assay

The Just Another Method (JAM) assay has been described previously (Matzinger, 1991; Usharauli et al., 2006). When radioactively-labelled TC are induced to apoptose by effector cells, TC DNA is cleaved to a size that passes through a filtermat while intact DNA is trapped (Matzinger, 1991). This results in a reduction in radioactivity in wells with specific killing. OT-I CTL were used as effector cells and EL-4 cells were TC. TC split the day before were incubated overnight in 6-well plates in cIMDM containing 2 µCi/mL [*methyl*-^{3}H]Thymidine (GE Healthcare, Auckland, New Zealand). The following day TC were washed twice and incubated for 60-90 minutes at $5x10^4$/mL in cIMDM with (Ag^+) or without (Ag^-) 10 ng/mL SIINFEKL peptide. $5x10^3$ Ag^+ TC or $5x10^3$ Ag^- TC were combined with CTL titrated out in half-logs to give final CTL:TC ratios of 50:1-0.4:1 in a volume of 200 µL in 96-well round bottomed plates. In some assays CTL were pre-treated for 4 hours at $1x10^6$/mL with 1 µM paclitaxel, 1 µM peloruside or 0.1% ethanol (as vehicle control) in 5 mL polystyrene tubes (Falcon). Following pre-treatment CTL

were washed and resuspended to the specified ratios in drug-free medium. After combining CTL and TC, plates were spun for 60 seconds at 50*g* to promote CTL:TC conjugation. Plates were incubated at 37°C for 4-4.5 hours and immediately harvested onto 96-well plate glass fibre filters (Wallac, Perkin Elmer, Boston, USA) in an automated Mach-III-FM cell harvester (Tomtec, Hamden, CT, USA). Radioactivity was measured in scintillations per minute (cpm) determined by liquid scintillation counting in Betaplate Scint (Wallac). Specific Lysis was calculated as: Specific Lysis = 100 - % Specific Survival; % Specific Survival was normalised to Ag^+ TC without effectors as: % Specific Survival = $(x/\mu_y) * 100$; Where x = cpm of wells with CTL and μ_y = mean cpm wells without effectors. Spontaneous lysis was controlled for by harvesting a TC-only plate at the start and comparing cpm to control wells at the end of the assay. Spontaneous lysis was generally 5-30%.

2.8 Degranulation assay

CTL ($1x10^5$/well) were pre-treated for 4 hours with peloruside, paclitaxel, colchicine or ethanol in 100 µL at concentrations specified in the text. At the start of the assay, wells were topped up with an equal volume of media containing CD107a-Fitc (final concentration 2.5 µg/mL) or non-specific IgG2α-Fitc antibody with or without SIINFEKL peptide to a final concentration of 25 nM, thus halving the drug concentration for the remainder of the assay. When a pre-treatment step was not used the final concentration of colchicine relates to the final 200 µL volume. After 2, 4 or 6 hours as stated in the text, plates were spun down, 100 µL of the supernatant was removed from each well and frozen at -20°C for IFN-γ ELISA. The cells were then stained for CD8 and subjected to flow cytometry procedures. Live gates were set with control antibodies and IFN-γ production was

determined by combining results from all peptide-treated wells. The antibody used did not affect IFN-γ production at any timepoint (data not shown).

2.9 Confocal Microscopy

2.9.1 Coverslip preparation for CTL

Thirteen millimetre round glass coverslips were stored in 70% ethanol and on the day before use sterilised by flaming. When dry, coverslips were put into 6-well plates, and coated with 200 µL 10 µg/mL poly-$_{D/L}$-lysine hydrobromide (PDL; Sigma). PDL was removed, coverslips were washed twice in double-distilled water, and dried under sterile conditions. Coverslips were stored under sterile conditions at 4°C until use.

2.9.2 Staining of CTL

CTL were incubated with drug as specified in figure legends. After 4 hours, $1x10^5$ cells (100 µL) were aliquoted onto coverslips and allowed to adhere for 30 minutes. Coverslips were transferred directly into ice-cold 1:1 Acetone:Methanol and fixed for 7 minutes at room temperature. Coverslips were washed twice for 5 minutes in PBS and permeabilised in permeabilisation buffer (0.25% Triton-X 100 (Sigma) in 1% bovine serum albumin (Invitrogen) in PBS) for 30 minutes. Coverslips were then incubated overnight at 4°C with 30 µL 1 µg/mL polyclonal rabbit anti-alpha-tubulin-IgG (Abcam; Sapphire Biosciences, Redfern, Australia) in permeabilisiation buffer. The following day coverslips were washed three times for 5 minutes in PBS and incubated for 1 hour at room temperature in the dark with 30 µL 1 µg/mL Alexafluor-488 goat-anti-rabbit-IgG (Invitrogen). Coverslips were washed three times for 5 minutes in PBS, overlayed with 10 µL Prolong Gold® antifade with DAPI (Invitrogen) and sealed with nail polish. Microtubules and nuclei were visualised with a 60 x oil immersion objective lens using an Olympus

FluoView FV1000 confocal laser scanning biological microscope (inverted model IX81) using sequential frame acquisition. Images were acquired using Olympus FV10-ASW software.

2.10 *In Vivo* Assay of Cell Death

2.10.1 Immunisation

The *in vivo* VITAL assay was adapted from Hermans et al. (Hermans et al., 2004). BMDC were incubated for 2 hours at $1x10^6$/mL in cIMDM with or without 1 µM SIINFEKL peptide, washed once and resuspended in IMDM at $1x10^6$/mL. $1x10^5$ Ag^+-BMDC or $1x10^5$ Ag^--BMDC were injected subcutaneously into the right flank of C57BL/6 mice for immunised and unimmunised groups respectively. For adoptive transfer experiments, $1x10^6$ LN cells from naïve OT-I-ptprc^a mice were injected into congenic C57BL/6 recipients via the lateral tail vein 1 day prior to immunisation.

2.10.2 CFSE & CTO labelling of splenocytes

Splenocytes from naïve syngenic C57BL/6 mice were harvested and flushed through 70 µm pore size strainers. Red blood cells were lysed and cells resuspended at $1x10^6$/mL in cIMDM and incubated for at least 60 minutes with or without 1 µM SIINFEKL-peptide for Ag^+ TC and Ag^- TC respectively. Ag^- TC were washed once in IMDM and incubated in cIMDM with 10 µM Cell Tracker Orange® (CTO; Invitrogen) for 15 minutes at $2x10^7$/mL, and then incubated in medium alone for 15 minutes. Ag^+ TC were washed in dPBS and incubated at $2x10^7$/mL in dPBS with 200 nM 5,6-carboxyfluorescein succinimidyl ester (CFSE; Sigma) for 8 minutes at room temperature. CFSE labelling was quenched with 2.5 volumes of FCS. Both Ag^+ TC and Ag^- TC were washed twice in IMDM, resuspended at $4x10^7$/mL in IMDM and combined for adoptive transfer.

2.10.3 The *in vivo* VITAL assay

One week after immunisation mice were given a single intraperitoneal dose of 20 mg/kg or 30 mg/kg Taxol or an equivalent dose Cremophor EL® (as vehicle control). Groups were sib- and weight matched; drug doses were based on average weight to the nearest 2.5g in a given experiment. The drug dose was based on the work of Innocenti et al., suggesting that intraperitoneal administration of 18-36 mg/kg Taxol results in plasma concentrations of >1 µM for the first few hours after injection (Innocenti et al., 1995), and thus was likely to provide comparable concentrations to those used in *in vitro* CTL work (chapter 4).

Approximately 2 hours after drug administration 200 µL ($8x10^6$) TC were injected into each mouse via the lateral tail vein. The TC contained an equal mix of CFSE-labelled SIINFEKL$^+$ (Ag^+) TC and CTO-labelled control (Ag^-) TC prepared as outlined in the previous section. After 8 or 10 hours as specified in the text mice were euthanized and splenocytes stained for CD8 or CD8+CD45.1 and subjected to flow cytometric analysis. Total $CD8^+$ or $CD8^+/CD45.1^+$ T cell number was calculated by multiplying the proportion of $CD8^+$ or $CD8^+/CD45.1^+$ splenocytes determined from flow cytometry data by the total number of splenocytes determined by the Trypan Blue Exclusion test. One control mouse in adoptive transfer experiments was excluded as its $CD45.1^+/CD8^+$ T cell numbers and killing profile matched that of unimmunised mice. Mice with <400 events in the Ag^- gate were also excluded from analyses. Specific Lysis was determined by subtracting Specific Survival from 100%. Specific Survival was calculated as the proportion of Ag^+/Ag^- splenocytes in immunised mice normalised to unimmunised mice with the same drug treatment multiplied by 100. The final calculation is as follows:

$$SL_A=100-(Ag^+_A/Ag^-_A)/(\mu_{DU})*100$$

Where SL_A= Specific Lysis in mouse A;

μ_{DU}= mean Ag^+/Ag^- of unimmunised mice receiving the same drug treatment.

2.11 General Flow Cytometry

Staining for flow cytometry was done in eppendorfs or 96-well round bottomed plates (Falcon). Samples were washed twice in FACS buffer (Appendix A) and Fc-Receptors blocked with 1 µg/mL 24G2 antibody for 5 minutes prior to the addition of primary antibodies. Samples were incubated with primary antibodies or relevant isotype controls at 4°C for 30 minutes (Appendix B contains sources of all antibodies). Samples were washed twice in FACS buffer and resuspended for flow cytometry. When a secondary antibody (Streptavidin-Cyc) was used, cells were incubated with the antibody at 4°C for 10 minutes, washed twice and resuspended for flow cytometry. In some assays samples were stored overnight at 4°C prior to collection. Samples were collected with a FACSScan, FACScalibur or FACSort flow cytometer mounted with Cellquest*pro* (Becton Dickinson, Franklin Lakes, NJ, USA). Background fluorescence was set with isotype controls, and compensation was done with single antibody stains. FLOWJO 8.8.4 (Tree Star, Ashland, OR, USA) or Cellquest*pro* were used to graph data.

2.12 Trypan Blue Exclusion Test

Viable cell number was determined by mixing a known volume of cells with 0.4% trypan blue (Sigma). 2 to 4 fields were counted and multiplied by the dilution factor field volume, and total volume to determine overall cell number. In *in vivo* assays, total numbers of $CD8^+$ and $CD8^+/CD45.1^+$ CTL were back-calculated after determining relative proportions of total live cells.

2.13 Statistics

Data were graphed in Graphpad*prism* 4.0 (Graphpad Software Inc., San Diego, CA, USA). Student's *t*-test, One-way ANOVA with Bonferroni correction, Two-way ANOVA with Bonferroni correction and linear regression analysis were performed in Graphpad*prism.* Student's *t*-test was used in adoptive transfer experiments due to low group numbers. In JAM assays, after calculating mean % specific lysis, group means at different CTL:TC ratios were ranked and compared using Friedman's mean rank sum test against a table of Chi(X)-square statistics by the formula:

$X^2=12*S/(n*g*(g+1))$

Where n=number of means in samples; g=number of drug treatments; and

$S=(Ranksum_A)^2+(Ranksum_B)^2+(Ranksum_C)^2-(Sumranksum)^2$

Where $Ranksum_A$=The total of the ranked means for drug A; and

Sumranksum=The sum of all the ranked sums for all the groups

Unless otherwise stated, bar graphs show group mean plus standard error of the mean (SEM).

3 Interactions of Lipopolysaccharide and Paclitaxel on Proinflammatory Processes in Macrophages

3.1 Introduction

Paclitaxel stimulates proinflammatory pathways, especially those leading to TNF-α and NO production in BMMØ, by binding to and activating TLR-4 in a manner similar to LPS (Bogdan and Ding, 1992; Byrd-Leifer C.A. et al., 2001; Crume et al., 2007; Ding et al., 1990b; Kawasaki et al., 2000; Kirikae et al., 1996; Manthey et al., 1994; Manthey et al., 1993). Figure 3.1A illustrates the ability of paclitaxel to induce TNF-α production by IFN-γ-primed BMMØ. In contrast, when IFN-γ-primed BMMØ are activated with LPS, production is dose-dependently inhibited by both paclitaxel (Figure 3.1B; (Crume et al., 2007)) and peloruside (Crume et al., 2007). To better understand the contradictory effects of paclitaxel on TNF-α production, we investigated the relationship between LPS concentration and paclitaxel-mediated inhibition to determine the conditions that induce the optimal inhibitory response.

3.2 Results

3.2.1 Paclitaxel inhibits IFN-γ-primed BMMØ responses to LPS in a broad time window

The first set of experiments aimed to determine if IFN-γ priming was essential to the observed inhibitory effects of paclitaxel on LPS-stimulated BMMØ. Previous studies have shown that BMMØ primed with IFN-γ are far more responsive to LPS than unprimed MØ (Gifford and Lohmann-Matthes, 1987; Yamamoto et al., 1994). As shown in Figure 3.2, when primed, BMMØ respond strongly to lower levels of LPS than unprimed MØ. IFN-γ renders cells increasingly sensitive to LPS and this augmentation reaches its maximum between 8 and 12 hours (Chung and Benveniste, 1990; Ma et al., 1996). Thus, we wished to determine if the inhibition of LPS-stimulated TNF-α production by MSD was due to a delay or defect in the IFN-γ priming response. By priming BMMØ for various times after the previous period of 12 hours we saw no shift in inhibition by paclitaxel (Figure 3.3A&B). This suggests that paclitaxel does not defer augmentation by IFN-γ and that the interaction of paclitaxel and IFN-γ is consistent after 12 hours priming.

3.2.2 Altered Production Kinetics do not Explain Inhibition of TNF-α production

One possible explanation for paclitaxel-mediated inhibition of TNF-α production by LPS-stimulated BMMØ is that the kinetics of TNF-α production are altered. TNF-α feeds back on TNF-RI and TNF-RII expressed by MØ which can induce NO and further augment TNF-α production (Miller et al., 1996; Vila-del Sol et al., 2006). Moreover, bioactive TNF-α bound by TNF receptors can be taken up and removed from culture by MØ (Fujihara et al., 1994; Virca et al., 1989). Thus, we postulated MSD may lead to an early peak in extracellular TNF-α and subsequent reduction in detectable levels by 8 hours. However, while TNF-α production by LPS-stimulated, IFN-γ-primed BMMØ increases between 2 and 8 hours (Figure

3.4A), the addition of paclitaxel does not alter the time of peak production (Figure 3.4B). Instead, paclitaxel significantly inhibited production of TNF-α at 6 and 8 hours. This finding suggests that paclitaxel does not alter the kinetics of LPS-induced TNF-α production by promoting early enhanced production.

3.2.3 Paclitaxel inhibits TNF-α and NO production in a manner dependent on LPS-responsiveness

Work by other groups suggests that TNF-α production can decrease above an optimal concentration of LPS (Chung and Benveniste, 1990; Kastenbauer and Ziegler-Heitbrock, 1999; Kikkawa et al., 1998; Takasuka et al., 1991). Further, pre-treatment of MØ with low-dose LPS can exacerbate this decrease, inhibiting and even ablating TNF-α production on restimulation with LPS (Hirohashi and Morrison, 1996; Nakano et al., 1999; Shnyra et al., 1998; Zhang and Morrison, 1993a, b). Thus, we sought to determine if there was a concentration-dependent interaction for TNF-α with LPS, and whether altering this LPS concentration affected the inhibition seen by paclitaxel. BMMØ primed with IFN-γ for 18 hours were treated with 10 µM paclitaxel, an equivalent concentration of ethanol (vehicle) or medium alone and activated with concentrations of LPS ranging from 0.5 ng/mL to 128 ng/mL for 8 hours. As shown in Figure 3.5A, TNF-α produced by LPS-stimulated BMMØ peaked at 4 ng/mL and above this LPS concentration, TNF-α production decreased to a basal level. As shown by other groups, it is also observed that the presence of ethanol affected TNF-α production on LPS activation (Feng et al., 2002; Fernandez-Lizarbe et al., 2008; Kolls et al., 1995; Shi et al., 2002; Stoltz et al., 2000; Xie et al., 1995). While inhibition by ethanol was not always this pronounced (*c.f.* Figure 3.3A), peak TNF-α production by LPS-stimulated BMMØ occurred at the same concentration as medium alone (4 ng/mL), and also decreased to basal levels above 4 ng/mL. Paclitaxel inhibited TNF-α production compared with vehicle control at concentrations of LPS where

TNF-α production was highest (i.e., 1-8 ng/mL). Above 8 ng/mL LPS and below 1 ng/mL, no inhibition of TNF-α could be seen by paclitaxel against vehicle or medium alone. From these studies we conclude that the greatest level of inhibition of TNF-α production by paclitaxel is found at optimal LPS responsive levels.

Additionally, because TNF-α production peaked similarly (<16 ng/mL LPS) in all three conditions, this experiment supports our previous finding that paclitaxel does not shift LPS-responsivity of BMMØ. That is, paclitaxel did not alter TNF-α production such that peak production occurred at a lower or a higher concentration of LPS, but paclitaxel generally depressed TNF-α production at optimal LPS responsive levels. Therefore we conclude that a shift in peak LPS responsiveness by paclitaxel does not explain inhibition by MSD.

3.2.4 NO Production is inhibited by Paclitaxel at LPS Concentrations above which TNF-α Inhibition is seen

iNOS is the main enzyme responsible for the production of inducible NO and it is expressed by LPS-activated IFN-γ-primed BMMØ (Santos et al., 2006). IFN-γ also operates in synergy with TNF-α to produce large amounts of NO (Geller et al., 1993; Vila-del Sol et al., 2006). It has therefore been suggested that inhibiting TNF-α production may cause a subsequent decrease in NO production by LPS-stimulated BMMØ (Crume et al., 2007).

After removal of a portion of the supernatant at 8 hours to measure TNF-α, cells were incubated for a further 64 hours and assayed for NO production (Figure 3.5B). Unlike TNF-α, NO breaks down to form nitrate and NO_2^- which cannot be removed by BMMØ and accumulate over the course of the assay (Stuehr and Marletta, 1985; Stuehr and Marletta, 1987). Thus by measuring NO_2^- the total

amount of NO produced can be determined at later times than TNF-α. In the presence of 10 μM paclitaxel, IFN-γ-primed BMMØ NO production was significantly inhibited at 4 ng/mL LPS and above ($p<0.05$, Two-way ANOVA with Bonferroni correction). By comparing TNF-α and NO production from these cells (Figure 3.5A & Figure 3.5B) there was overlap in inhibition where control TNF-α production was optimal, but at concentrations above 16 ng/mL, where TNF-α production reduced to basal levels, NO production became increasingly inhibited. When assessed together these findings may suggest that NO production is inhibited by paclitaxel in a manner independent of generation by TNF-α.

3.2.5 Myeloid-derived cells show increased metabolism in the presence of paclitaxel

One previously noted phenomenon is the specific increase in metabolic activity of BMMØ treated with high dose (1-10 μM) paclitaxel (Crume et al., 2007). Figure 3.6A shows a 10 μM dose of paclitaxel pronouncedly increases metabolic activity of BMMØ ($p<0.01$ by Student's *t*-test; paclitaxel vs. vehicle). In like fashion, LPS-matured BMDC also show enhanced metabolism in the presence of paclitaxel (Figure 3.6B; $p<0.01$ by Student's *t*-test; paclitaxel vs. vehicle). Figure 3.6C demonstrates that with increasing concentrations of LPS BMMØ metabolic activity increases. It is also apparent that a 10 μM dose of paclitaxel does not inhibit metabolic activity of BMMØ at any concentration of LPS, nor does the addition of LPS to paclitaxel treated BMMØ additively increase MTT reduction by BMMØ. That is, BMMØ are similarly metabolically active regardless of the LPS concentration. Previously it has been demonstrated that paclitaxel induces a dose dependent increase in metabolism in LPS-activated BMMØ (Crume et al., 2007). Thus, it is possible that at 10 μM, paclitaxel induces maximal metabolic activity by BMMØ, and the addition of LPS cannot increase MTT reduction further. Finally, it also follows that at lower concentrations, such as those used by Crume et al.

(Crume et al., 2007), paclitaxel and LPS may show additive effects on metabolic activity.

Figure 3.1A

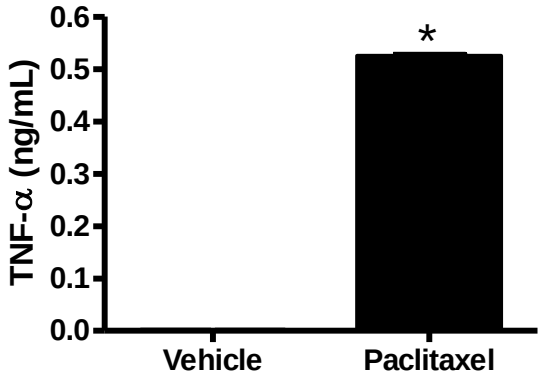

Figure 3.1B

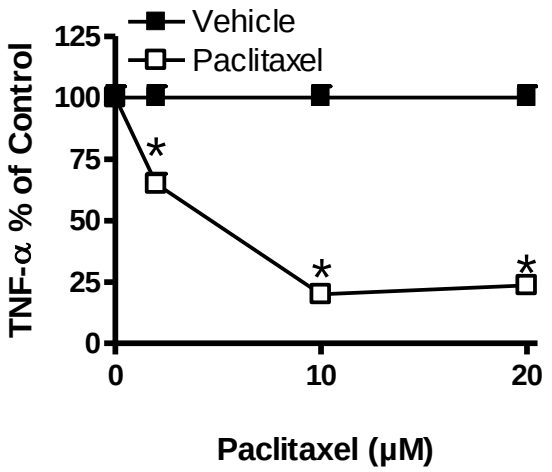

Paclitaxel exhibits dichotomous effects on BMMØ TNF-α production. (**A**) IFN-γ-primed BMMØ ($5x10^4$/well) were cultured with 10 μM paclitaxel or an equivalent concentration of ethanol (Vehicle). TNF-α production was measured in the supernatant by ELISA after 2 hours. *p<0.001; Student's *t*-test. (**B**) IFN-γ-primed BMMØ ($5x10^4$/well) were activated with 2 ng/mL LPS in the presence of paclitaxel or an equivalent concentration of ethanol (Vehicle). After 8 hours the supernatant was assayed for TNF-α production by ELISA. Control TNF-α production was 17.453 ± 1.4125 ng/mL in this experiment. *p<0.001; One-way ANOVA with Bonferroni correction; Vehicle vs. Paclitaxel. Data points represent mean+SEM of duplicate wells from one of two similar experiments.

Figure 3.2A

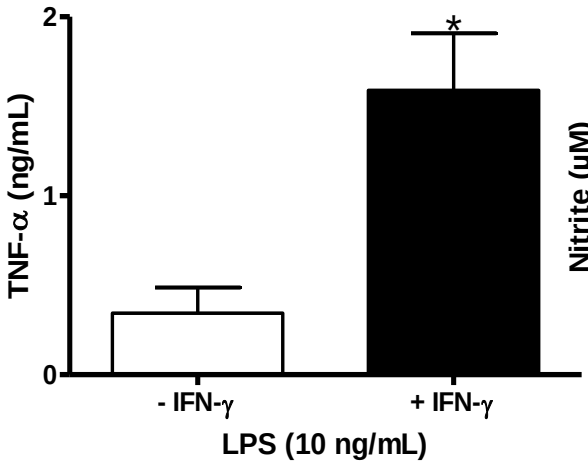

Figure 3.2B

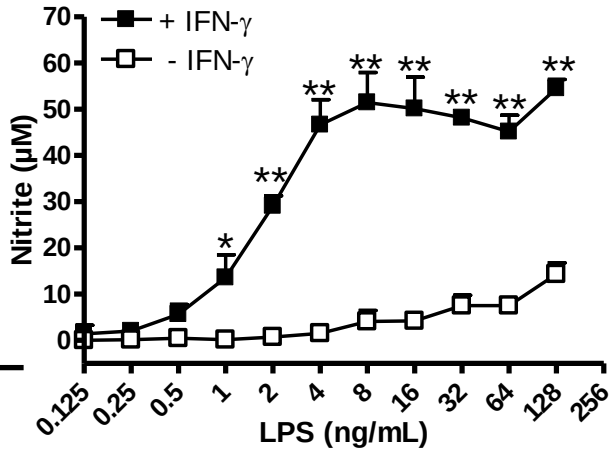

IFN-γ increases sensitivity of BMMØ to LPS. IFN-γ-primed (+ IFN-γ) or unprimed (- IFN-γ) BMMØ ($5x10^4$/well) were activated with LPS. (**A**) After 8 hours the supernatant was assayed by ELISA for TNF-α production. *p<0.01; Student's *t*-test vs. blank. (**B**) After 72 hours supernatants were assayed for nitric oxide production by the Greiss reaction. *p<0.05; **p<0.01; Two-way ANOVA with Bonferroni Correction, IFN-γ-primed vs unprimed. Data points and bars show mean+SEM of duplicate wells.

Figure 3.3A

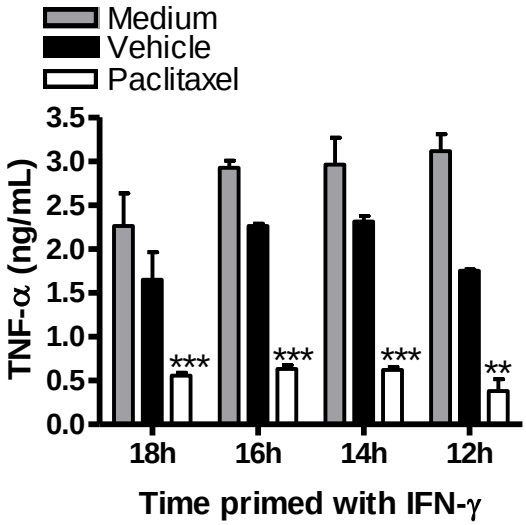

Figure 3.3B

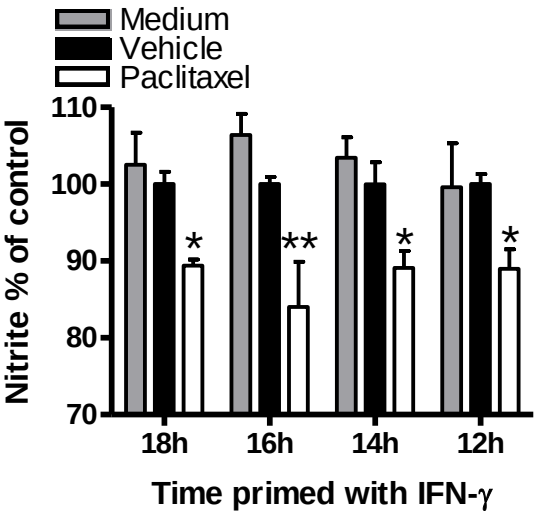

Duration of IFN-γ priming does not alter inhibition by paclitaxel. BMMØ ($5x10^4$/well) were primed with IFN-γ for various times prior to activation with 2 ng/mL LPS in the presence or absence of 10 µM paclitaxel or an equivalent concentration of ethanol (Vehicle). (**A**) Bars represent mean+SEM of duplicate wells. (**B**) Bars represent mean+SEM of duplicate wells combined from two experiments. *p<0.05; **p<0.01; ***p<0.001; Paclitaxel vs. Vehicle, Two-way ANOVA with Bonferroni correction.

Figure 3.4A

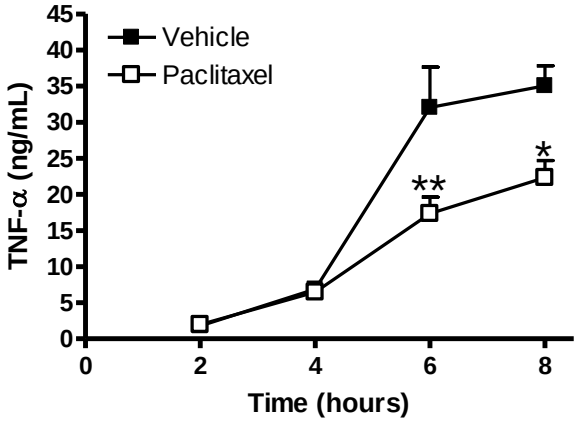

Figure 3.4B

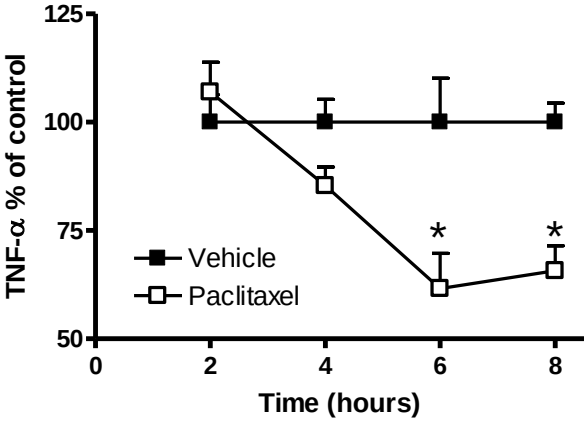

Paclitaxel does not cause an early shift in TNF-α production. IFN-γ-primed BMMØ ($5x10^4$/well) were activated with 2 ng/mL LPS in the presence of 10 µM paclitaxel or an equivalent concentration of ethanol (Vehicle). After 8 hours the supernatant was assayed by TNF-α ELISA. Data points represent mean+SEM of duplicate wells from one of three similar experiments (n=2) (**A**), all replicates were combined for values in (**B**) (n=6). *p<0.01; **p<0.001; Two-way ANOVA with Bonferroni correction.

Figure 3.5A

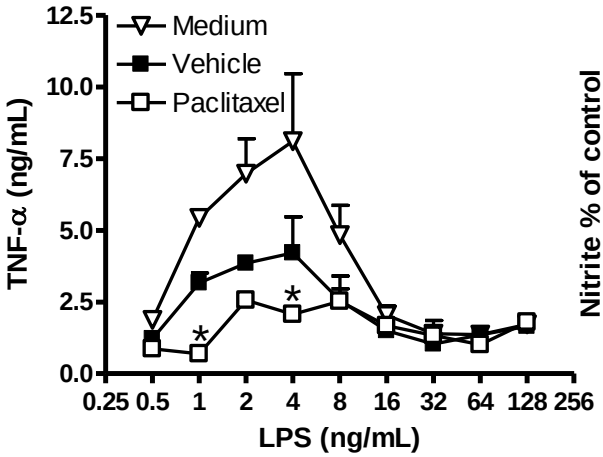

Figure 3.5B

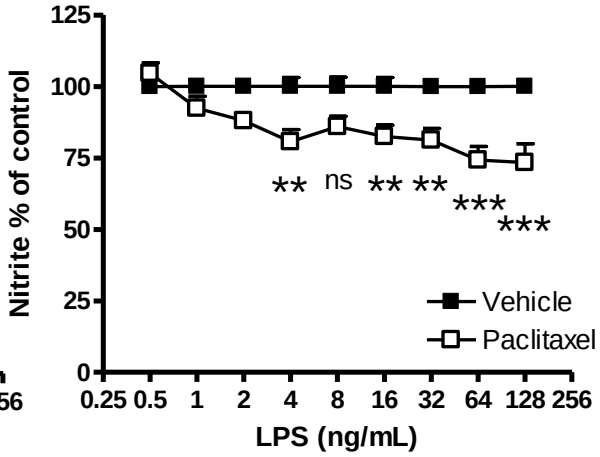

Paclitaxel inhibits TNF-α and NO production by BMMØ at optimal responsive levels. IFN-γ-primed BMMØ ($5x10^4$/well) were activated with LPS in the presence or absence of 10 μM paclitaxel or an equivalent concentration of ethanol (Vehicle). After 8 hours the supernatant was assayed for TNF-α by ELISA (**A**). Cultures were incubated for a further 64 hours and assayed by the Greiss reaction for NO production (**B**). (**A**) Data points represent mean+SEM of duplicate wells from one of two similar experiments (n=2). (**B**) Data points represent mean+SEM of duplicate wells combined from two experiments (n=4 wells). LPS concentrations at which inhibition was seen were assessed for significance. *p<0.05;**p<0.01;***p<0.001; Paclitaxel vs. Vehicle by Two-way ANOVA with Bonferroni correction.

Figure 3.6A

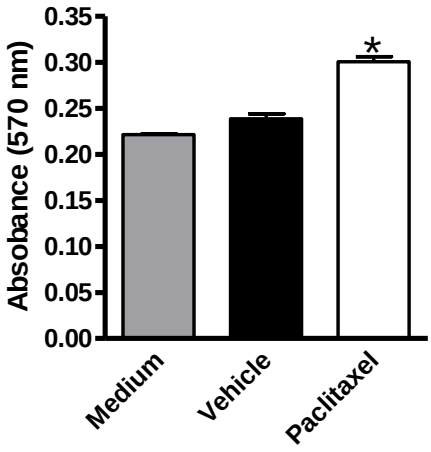

Figure 3.6B

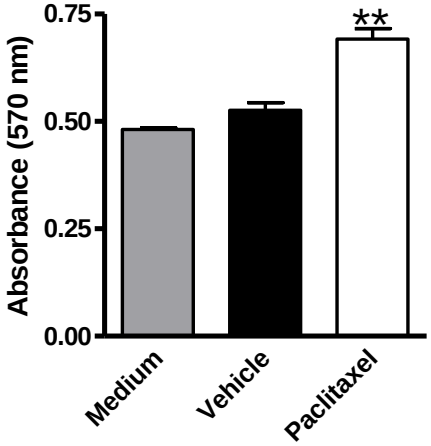

Figure 3.6C

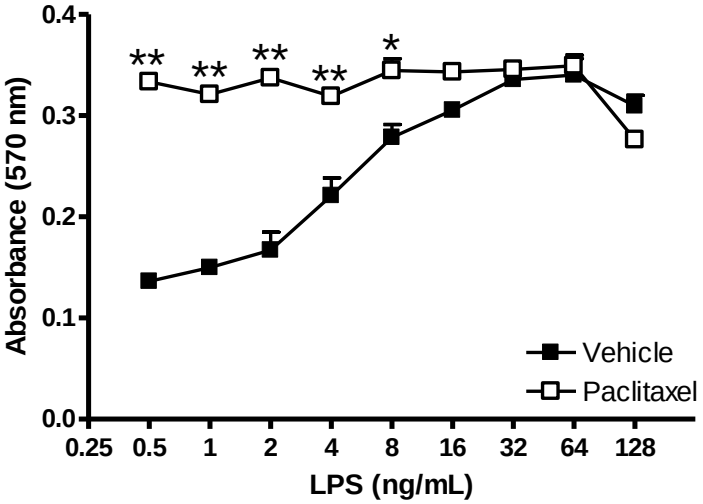

Paclitaxel enhances metabolic activity of Bone-Marrow Derived Cells. IFN-γ-primed BMMØ ($5x10^4$/well) (**A**) or LPS-matured BMDC ($1x10^5$/well) (**B**) were incubated for 72 hours in the presence or absence of 10 μM Paclitaxel or an equivalent concentration of ethanol (Vehicle) and subjected to the MTT assay. Bars show duplicate wells from one of three similar experiments (n=2). *p<0.01; Paclitaxel vs. Vehicle by Student's *t*-test. (**C**) IFN-γ-primed BMMØ were incubated for 72 hours with the stated concentrations of LPS in the presence or absence of 10 μM paclitaxel or an equivalent concentration of ethanol (Vehicle). Data points represent mean+SEM of duplicate wells from one of two similar experiments (n=2). *p<0.01;**p<0.001; Paclitaxel vs. Vehicle by Two-way ANOVA with Bonferroni correction.

3.3 Discussion

This study set out to determine why and how paclitaxel inhibits LPS-stimulated BMMØ TNF-α and NO production. An overnight stimulus of IFN-γ is commonly used as a stimulation step and requires 8-12 hours to fully augment LPS-responsivity (Chung and Benveniste, 1990; Ma et al., 1996). The first experiments asked if there was interplay between IFN-γ priming and paclitaxel's inhibitory effect. If this was the case, we expected to see a shift in inhibition with extended priming duration. However, we found that when primed for 12-18 hours with IFN-γ, BMMØ production of TNF-α and NO was depressed by paclitaxel similarly at all time points. This finding suggests that paclitaxel does not cause a delay in the IFN-γ priming response. However, these assays did not examine the effects of paclitaxel on unprimed BMMØ. It would be interesting to determine if IFN-γ priming is requisite for inhibition, or if the pathways to production are depressed whether or not BMMØ are first stimulated with IFN-γ.

Next we tested whether the drug was altering the temporal production of TNF-α. We postulated that a kinetic shift in production could induce an earlier peak in TNF-α production followed by a decrease in production by 8 hours. The results demonstrated that TNF-α increases with time in both drug-treated and vehicle-treated cultures. However, by 6 hours TNF-α production in the presence of paclitaxel was lower than in control BMMØ. This difference persisted until the end of the assay indicating that production was inhibited by paclitaxel and did not peak early.

Paclitaxel significantly reduced production of TNF-α and NO when BMMØ were stimulated with an optimal concentration of LPS. At low concentrations of LPS (<16 ng/mL) TNF-α production was inhibited by paclitaxel, but as LPS

concentrations increased, control BMMØ TNF-α production reduced to a basal level, masking paclitaxel's inhibitory effect. However, at all concentrations above 16 ng/mL LPS, NO production was significantly inhibited by paclitaxel. The different dose-responses of TNF-α and NO may relate to differences in the processing of the agents once in the supernatant. Extracellular TNF-α can be removed from culture by BMMØ (Crume et al., 2007; Fujihara et al., 1994), whereas NO breaks down rapidly and accumulates in culture as nitrite and nitrate (Stuehr and Marletta, 1985; Stuehr and Marletta, 1987). Further, TNF-α is an early onset cytokine, while NO production occurs later (Sander et al., 1991; Stuehr and Marletta, 1987; Vila-del Sol et al., 2006). It would be of interest to investigate the production of both TNF-α and NO at intermediary timepoints when both agents are present, such as 16 or 24 hours. This may reveal more precisely how paclitaxel affects the two mediators simultaneously and shed light on the mechanisms involved in its inhibitory activity. Furthermore, investigating the interdependence of TNF-α and NO by adding antibodies to TNF-α and iNOS inhibitors such as aminoguanidine hemisulfate will determine the involvement of feedback within the system.

The initial investigations by Crume et al. into the effects of LPS+paclitaxel on IFN-γ-primed BMMØ showed that exposure to paclitaxel can lead to reduced levels of TNF-α and NO (Crume et al., 2007). The present study extends this finding by indicating that this reduction is likely due to mechanistic inhibition rather than kinetic alteration of TNF-α production. The mechanism by which this inhibition occurs is not clear; however, there are a number of functional levels at which paclitaxel may be interrupting the process. Some ways paclitaxel may affect the process include competitive interactions with TLR-4; inhibiting TNF-α secretion; and inhibiting signalling pathways.

The first possibility is that paclitaxel directly inhibits the interaction of LPS with TLR-4. Paclitaxel is able to bind to and activate murine MD-2/TLR-4 complexes (Kawasaki et al., 2000; Kawasaki et al., 2001), so a mechanism of competitive inhibition for TLR-4 or other direct interactions may be involved. This possibility is unlikely for two reasons. Firstly, as peloruside demonstrates the same inhibitory properties as paclitaxel (Crume et al., 2007), it is likely that the microtubule network is involved in some way. Secondly, paclitaxel is seen to inhibit TNF-α and NO without altering IL-12p40 production, suggesting that the receptor is activated normally (Crume et al., 2007).

An alternative is that TNF-α secretion is blocked when the microtubule network is stabilised. While TNF-α and IL-12p40 are induced by the same transcription factors and processed by the golgi apparatus prior to secretion (Baumgartner et al., 1996; Ma et al., 2004; Trinchieri, 1995), only LPS-induced TNF-α production is inhibited by paclitaxel (Crume et al., 2007). Recently it has been shown that TNF-α release in MØ is controlled by the recycling endosome, and the phagosome is involved in its delivery to the recycling endosome (Manderson et al., 2007; Murray et al., 2005). There is evidence to suggest that suppressing microtubule dynamics with paclitaxel, colchicine or nocodazole causes inhibition of MØ phagosome movements and golgi transport (Blocker et al., 1998; Blocker et al., 1997; Peachman et al., 2004). It may be that by inhibiting these processes paclitaxel blocks TNF-α release. Furthermore, recycling endosome activity in T cells is inhibited by colchicine (Das et al., 2004), and if paclitaxel similarly represses recycling endosome activity in MØ it may directly inhibit TNF-α secretion. However, our results show that NO production is inhibited by paclitaxel at LPS concentrations where TNF-α production appears negligible. This does not rule out

that paclitaxel blocks TNF-α secretion but implicates other mechanisms in the inhibition of NO.

Another possibility is that stimulatory signals activated by LPS were altered by paclitaxel. LPS can directly associate with β-tubulin and microtubule-associated proteins such as *tau* (Bohm et al., 1999; Ding et al., 1992). LPS also induces microtubule stabilisation and enhances associations of microtubule associated proteins with microtubules (Allen et al., 1997a; Allen et al., 1997b). Furthermore, LPS causes preferential phosphorylation of p42/44 MAP-K (Ding et al., 1996) which regulates TNF-α secretion (Rousseau et al., 2008). Thus, the microtubule network is known to be involved and modified by LPS signalling, which may partially explain why microtubule actives alter LPS-induced cytokine production. Assessing TNF-α mRNA levels in LPS-activated BMMØ treated with paclitaxel will indicate if signalling, or at least pre-translational processes are affected by the compound. Further, examining intracellular versus extracellular protein expression may also provide insight into how release is affected. Together these tools may determine the functional level of inhibition.

TLR-4 signalling is also altered by DSD - Colchicine, nocodazole, podophyllotoxin and the vinca alkaloids affect MØ responses to LPS. These agents inhibit the LPS-induced formation of reactive oxygen species and NO, GM-CSF production and activity, and decrease TNF-α receptor, TNF-α protein and TNF-α mRNA expression (Allen et al., 1991; Ding et al., 1990a; Kirikae et al., 1996; Li et al., 1996; Rammes et al., 1997; Rao et al., 1997). The similarities in the interactions make it tempting to speculate that the effects of MSD and DSD are causally related. If this is the case, it would suggest that a dynamic microtubule network is requisite to adequate signalling, release and effective MAP-K activity. In support

of this theory, paclitaxel and colchicine both inhibit TNF-α production, and also act to enhance IL-1β production following LPS stimulation (Allen et al., 1991; Crume et al., 2007; O'Brien Jr et al., 1995). Unlike TNF-α, IL-1β is not processed through the golgi apparatus but is instead cleaved from pro-IL-1β which associates with microtubules (Auron et al., 1984; O'Brien Jr et al., 1995; Stevenson et al., 1992). These different exocytosis pathways may determine the way the microtubule network affects cytokine production by BMMØ.

We also investigated the metabolic activity of BMMØ in the presence of paclitaxel. As shown previously, paclitaxel increases BMMØ metabolic activity (Crume et al., 2007). We saw that overall metabolic activity by BMMØ increased with LPS concentration. Basal metabolic activity of BMMØ is decreased by addition of low concentrations of LPS (*c.f.* Figure 3.6.A & 3.6.C) but increases with ramping LPS concentrations. Previous work by other groups suggests that the decrease is due to apoptosis induced by NO (Yamamoto et al., 1994). Crume et al. showed that peloruside does not enhance BMMØ metabolic activity (Crume et al., 2007). Interestingly, in our experiments 10 µM paclitaxel induced the same metabolic activity irrespective of LPS concentration and it seems likely, as suggested previously (Crume et al., 2007), this may relate to its capacity to activate TLR-4. To determine if this alteration in metabolism correlates with changes in survival following LPS stimulation, looking at markers of apoptosis will be of value. Further, using LPS in combination with other ligands that stimulate TLR will help determine whether the increase in metabolic activity occurs in a TLR-dependent manner.

We have investigated the responses of BMMØ to LPS in the presence of the MSD paclitaxel. Our results indicate that inhibition is not due to an early peak in production of TNF-α, is independent of the duration of IFN-γ priming and is only

observed at optimal LPS responsive levels, which differ for TNF-α and NO. We also demonstrate that metabolic activity of BMMØ and BMDC is significantly enhanced in the presence of paclitaxel. Taken together our findings demonstrate that BMMØ TNF-α and NO synthesis in response to LPS is inhibited and metabolic activity enhanced by paclitaxel. This *in vitro* modulation suggests that paclitaxel can affect the immune system in ways distinct from its anti-mitotic properties and may be clinically relevant to cancer patients fighting infection.

4 Involvement of the Microtubule Cytoskeleton in CTL Function

4.1 Introduction

Relocalisation of the MTOC to the IS is a prerequisite for CTL-mediated cell death (Kupfer et al., 1985). DSD inhibit this process and preclude cytolysis by CTL (Kupfer and Dennert, 1984; Wolberg et al., 1984). In addition to polarisation toward the TC, the microtubule cytoskeleton is involved in many steps of CTL-mediated cytolysis. To induce TC death, the microtubule network is used as a scaffold along which lytic granules traffic *en route* to the IS (Stinchcombe et al., 2001b). In synapsed CTL:TC conjugates, the CTL MTOC shows dynamic oscillations at the IS (Kuhn and Poenie, 2002). Further, actin microfilaments and microtubule plus-ends are cleared from the IS during lytic granule delivery, and there is evidence to suggest dynein-mediated transport is sufficient to deliver lytic granules to the IS (Kuhn and Poenie, 2002; Poenie et al., 2004; Stinchcombe et al., 2006). We were interested to investigate how MSD affect CTL lytic granule delivery, and to determine if peloruside and paclitaxel elicit different effects on CTL function. Specifically we asked if CTL-mediated cell death, degranulation and cytokine production are altered by *in vitro* treatment with paclitaxel or peloruside.

4.2 Results

4.2.1 Short term paclitaxel treatment does not inhibit cytolysis *in vitro*

To begin to determine effects of MSD on CTL-mediated cell death *in vitro*, we compared killing by CTL in the presence of paclitaxel, a vehicle control (0.1% ethanol) or medium alone at a range of CTL:TC ratios (50:1-0.4:1). Figure 4.1A shows that when CTL were combined with TC in the absence of peptide they were unable to kill target cells. However, when TC were pre-incubated with SIINFEKL peptide, specific lysis of the TC by CTL increased with higher ratios of CTL:TC. The addition of 0.1 µM or 1 µM paclitaxel did not inhibit specific lysis ($p>0.05$; Friedman's mean rank-sum test). Although the drug was present for the duration of the assay, we did not observe any effect on TC survival as measured by cpm of TC at the end of the assay (Figure 4.1B, $p>0.05$; One-way ANOVA). These results demonstrate that TC killing by CTL *in vitro* occurs effectively in the presence of paclitaxel.

4.2.2 Pre-treatment with paclitaxel or peloruside does not inhibit CTL-mediated cell death *in vitro*

Concentrations of paclitaxel and peloruside above 100 nM can induce microtubule bundling (Hood et al., 2002; Jordan et al., 1993). Brown et al. have demonstrated that a 4-hour pre-treatment with 1 µM paclitaxel induces microtubule bundles in the majority of CTL (Knox et al., 1993), and these bundles remain stable, even after washing until the cells enter mitosis (Brown et al., 1985). As we observed no effect of paclitaxel on CTL lytic capacity without pre-treatment, we examined killing under conditions that induce microtubule bundling, potentially amplifying the effects of MSD on CTL. Because microtubule bundles caused by MSD are stable after drug washout (Brown et al., 1985), we were able to compare killing at a wide

range of CTL:TC ratios with limited amounts of MSD. CTL were pre-treated for 4 hours with 1 µM paclitaxel, 1 µM peloruside or an equivalent vehicle control (0.1% ethanol), washed and compared for their ability to lyse target cells *in vitro*. Figure 4.2A shows that, similar to the cytolytic assay in the continued presence of paclitaxel, a 4h pre-treatment with 1 µM peloruside or 1 µM paclitaxel did not inhibit CTL-mediated cytolysis *in vitro* ($p>0.05$; Friedman's mean rank-sum test). Additionally, we measured the metabolic activity of drug-treated CTL and saw no difference in the overall metabolism of CTL ($p>0.05$, One-way ANOVA). These results indicate that pre-treating CTL with MSD does not inhibit cytolysis of TC and is not directly cytotoxic to CTL.

4.2.3 Paclitaxel and Peloruside do not inhibit degranulation by activated CTL

Because FasL activity can compensate for deficiencies in the perforin/granzyme pathway (i.e., lytic granule delivery) (Lowin et al., 1994), and its expression does not require the microtubule network (He and Ostergaard, 2007), it was possible that increased FasL-induced apoptosis could mask any effect of MSD on lytic granule delivery. Thus, we directly assessed degranulation by measuring surface expression of the lysosomally-associated membrane protein CD107a (LAMP-1), which is indicative of lytic granule release (Betts et al., 2003). CD107a associates with lytic granules almost exclusively; however, during synthesis a small proportion transiently resides in the plasma membrane before trafficking to lytic granules (Carlsson and Fukuda, 1992), and thus can be detected at low levels on unactivated CTL.

Colchicine has previously been shown to inhibit degranulation by CTL (Betts et al., 2003). As shown in Figure 4.3A&B, pre-treatment with 1 µM colchicine inhibited degranulation. However, without pre-treatment degranulation was not

inhibited. Because pre-treatment with colchicine was required to inhibit degranulation, we used a pre-treatment step in all subsequent degranulation assays.

To determine the ability of lytic granules to traffic to the cell surface in the presence of MSD, CTL were pre-treated for 4 hours with 1 µM paclitaxel, 1 µM peloruside, 1 µM colchicine (as a positive control) or an equivalent vehicle control (0.1% ethanol), and then stimulated to degranulate. Neither paclitaxel nor peloruside inhibited degranulation by CTL (Figure 4.3C&D), whereas colchicine reduced degranulation by CTL at both 2 and 4 hours. Interestingly, pre-treatment with paclitaxel, peloruside or colchicine resulted in higher background MFI than control CTL (Figure 4.3A,C). We cannot explain why this occurs, but it may relate to CD107a trafficking or reinternalisation during synthesis (Carlsson and Fukuda, 1992).

4.2.4 Paclitaxel and Peloruside do not inhibit IFN-γ Production by activated CTL

The signals leading to cytokine production and degranulation are differentially regulated in CTL (Faroudi et al., 2003; Wiedemann et al., 2006), and therefore may be uniquely susceptible to modulation by MSD. Because CTL produce large amounts of IFN-γ upon activation, in addition to degranulation and cytolysis, we investigated whether paclitaxel or peloruside altered IFN-γ production by CTL. However, while IFN-γ production was significantly inhibited by colchicine at both 2 hours (Figure 4.4A; $p<0.001$) and 4 hours ($p<0.01$), it was not reduced by paclitaxel or peloruside (both $p>0.05$; Two-way ANOVA with Bonferroni correction, drug vs. vehicle). This suggests that pre-treating CTL with MSD does not inhibit their production of IFN-γ.

In parallel with assays of degranulation and IFN-γ production we examined metabolic activity of CTL. Neither paclitaxel nor peloruside altered metabolic activity, but some reduction in colchicine-treated cells was observed (Figure 4.4B; $p<0.05$, One-way ANOVA with Bonferroni correction, Colchicine vs. Vehicle). Together our data suggest that in the absence of anti-mitotic effects neither 1 µM paclitaxel nor 1 µM peloruside inhibit CTL-mediated cytolysis, degranulation or IFN-γ production *in vitro*. In contrast, colchicine, a known inhibitor of CTL function consistently reduced CTL degranulation, IFN-γ production and metabolic activity.

4.2.5 Paclitaxel and Peloruside induce microtubule bundling in OT-I T cells

As we observed no effect of MSD on CTL activity we determined the extent to which the microtubule network was modified by our drug regimen. CTL were pre-treated with 10 µM paclitaxel, 1 µM paclitaxel, 1 µM peloruside or 1 µM colchicine for 4 hours; adhered to coverslips for 30 minutes and stained for microtubules (green) and nuclei (blue). In control cells the microtubule network extends through the cytoplasm, radiating out from a dense core of microtubules which is likely to be the centrosome (Figure 4.5A,B). Examples of individual microtubules are demarcated by arrows. In contrast to control cells, 10 µM paclitaxel induces thick bundles of microtubules in almost all cells (Figure 4.5C; demarcated by asterisks). 1 µM paclitaxel and 1 µM peloruside also induced microtubule bundling in CTL (Figure 4.5D,E), but less extensively than 10 µM paclitaxel. Pre-treating CTL with colchicine caused diffuse staining across the cytoplasm (Figure 4.5F; cell with arrow), indicating the presence of solubilised α/β-tubulin heterodimers. These results suggest that a 4-hour pre-treatment with MSD can induce microtubule-bundling in CTL. However, because we observed stronger bundling at 10 µM paclitaxel than 1 µM it was possible that a high concentration (10 µM) of paclitaxel was required to alter degranulation and cytokine production by CTL.

4.2.6 10 µM Paclitaxel does not inhibit degranulation or IFN-γ production

As the confocal microscopy results revealed extreme bundling in CTL pre-treated for 4 hours with 10 µM paclitaxel, we pre-treated CTL with 10 µM paclitaxel, 10 µM colchicine or an equivalent vehicle control and assessed degranulation at 2, 4 and 6 hours. As shown in Figure 4.6A&B even at this high dose of paclitaxel degranulation was not altered, but was reduced by 10 µM colchicine. Furthermore, similar to the effects on degranulation, production of IFN-γ was inhibited by 10 µM Colchicine, but not by 10 µM paclitaxel (Figure 4.6C). Further, 10 µM paclitaxel did not alter CTL metabolism while 10 µM colchicine strongly reduced CTL metabolism (Figure 4.6D). These results support our previous findings that microtubule bundling does not inhibit peptide-induced degranulation or IFN-γ production by CTL.

Figure 4.1A

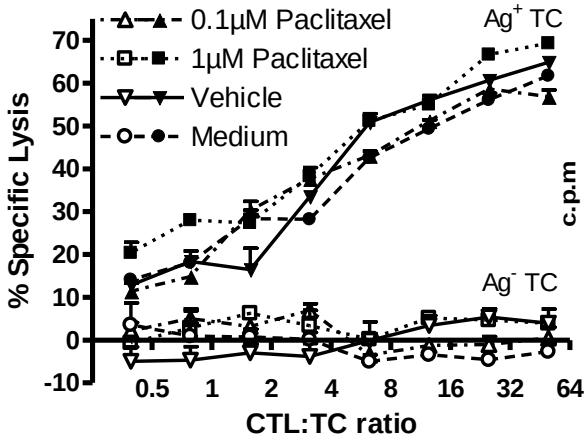

Figure 4.1B

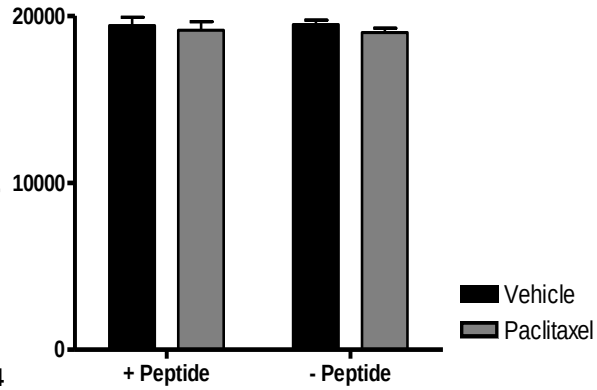

Paclitaxel does not inhibit CTL-mediated cytolysis *in vitro.* CTL were subjected to a 4 hour JAM assay against SIINFEKL-pulsed (Ag^+ TC) or control (Ag^- TC) EL-4 target cells (TC) at various ratios in the presence of 0.1 µM paclitaxel, 1 µM paclitaxel, 0.1% ethanol (Vehicle) or medium alone. (**A**) % Specific Lysis was calculated as stated in the methods section. Lysis was specific to peptide-pulsed TC and did not differ significantly between the four treatments ($p>0.05$, Friedman's mean rank sum test). (**B**) In the absence of CTL, TC survived equally well with or without 1 µM paclitaxel as no loss of radioactivity (cpm) at the end of the assay was observed ($p>0.05$, One-Way ANOVA). This indicates that paclitaxel was not directly toxic to the TC. Data points represent mean+SEM of triplicate wells from one experiment.

Figure 4.2A

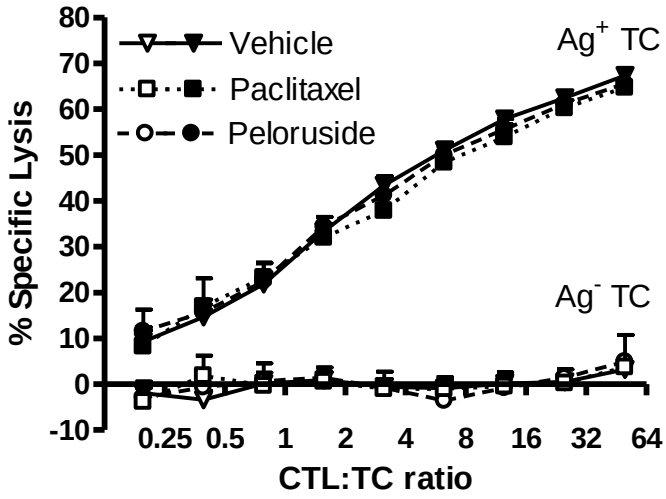

Figure 4.2B

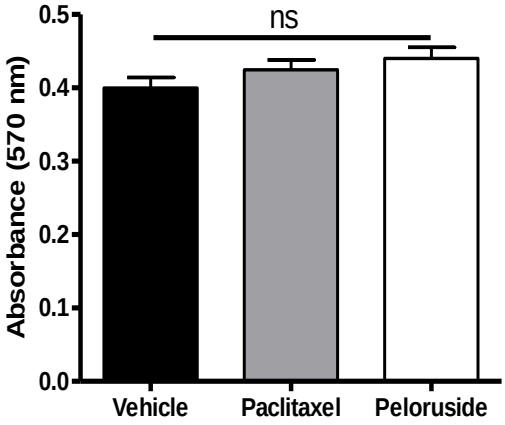

Pre-treatment with Paclitaxel or Peloruside does not inhibit CTL-Mediated Cytolysis *in vitro*. CTL were pre-treated for 4 hours with 1 µM paclitaxel, 1 µM peloruside or 0.1% ethanol as control (Vehicle) and combined with TC at various ratios in drug-free media. (**A**) Specific lysis was calculated as stated in the methods section. In the absence of peptide (Ag^- TC), no specific lysis was observed. In the presence of peptide (Ag^+ TC), specific lysis was higher in wells with more CTL. Neither paclitaxel nor peloruside inhibited specific lysis at 4 hours ($p>0.05$, Friedman's mean rank sum test). (**B**) Metabolic activity of CTL was measured in parallel by the MTT assay. Neither paclitaxel nor peloruside caused a reduction in metabolic activity at the end of the assay ($p>0.05$, One-Way ANOVA). (**A**) Data points represent two to four wells from one of three similar experiments. (**B**) Data points represent triplicate wells from one of three similar experiments.

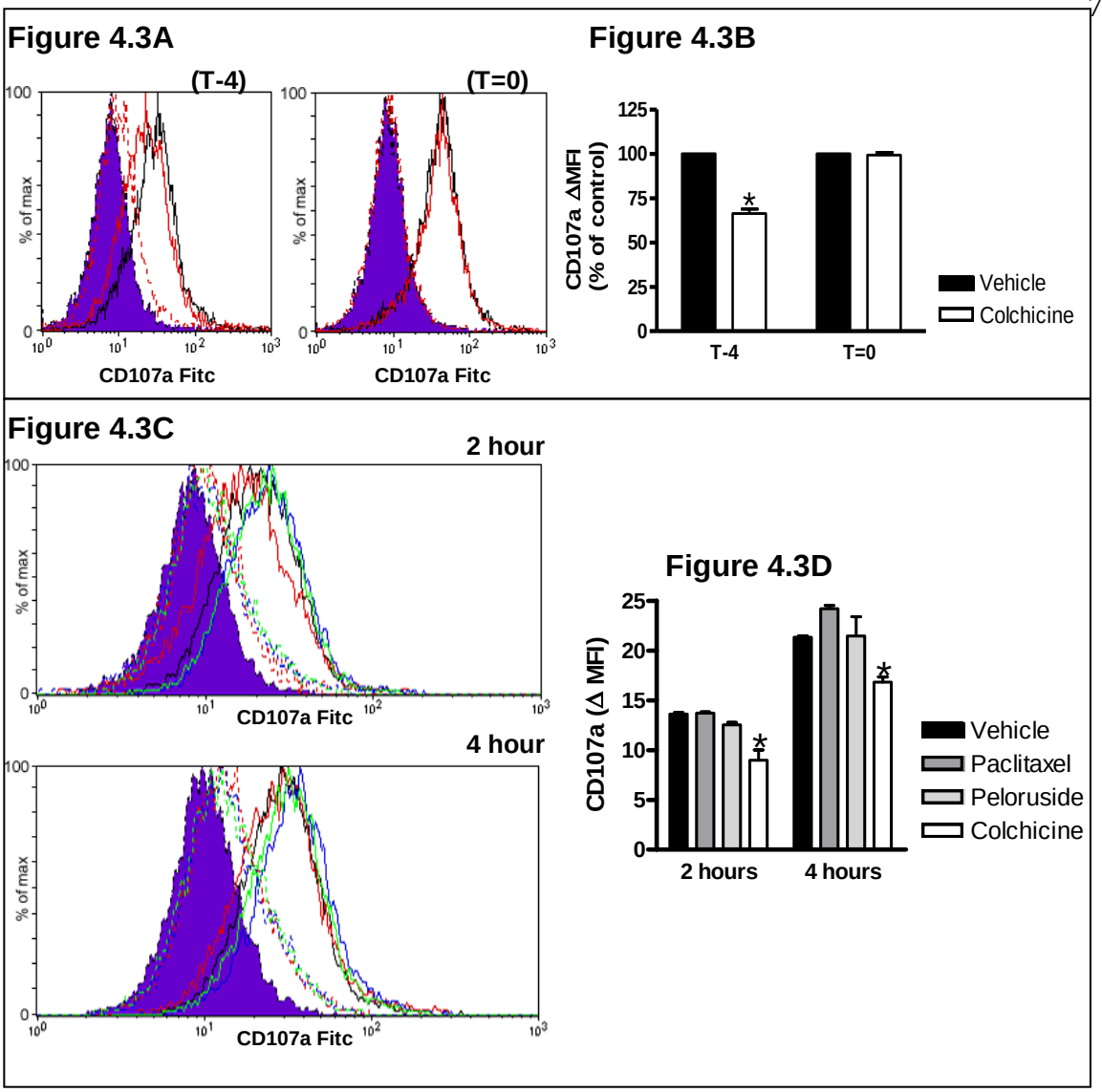

Paclitaxel and Peloruside do not inhibit degranulation *in vitro*. (**A**) CTL ($1x10^5$/well) were incubated with an antibody to CD107a with (solid lines) or without (dashed lines) SIINFEKL-peptide and assessed for their ability to degranulate as determined by MFI shift (**B**). All events were gated on $CD8^+$ live cells. Purple shading shows vehicle-treated CTL background CD107a expression. When added at the same time as peptide (T=0), 1 µM colchicine did not alter 2 hour degranulation compared to 0.1% ethanol (Vehicle). A 4-hour pre-treatment (T-4) with 1 µM colchicine inhibited degranulation at 2 hours. *p<0.001 One-way ANOVA with Bonferroni correction, Colchicine vs. Vehicle. Bars show mean+SEM of individual wells combined from two separate experiments. (**C**) CTL were pre-treated for 4 hours with 1 µM paclitaxel (blue lines), 1 µM peloruside (green lines), 1 µM colchicine (red lines) or 0.1% ethanol (vehicle; black lines) and subjected to

the degranulation assay as in (**A**). (**D**) Neither 1 µM paclitaxel nor 1 µM peloruside inhibited degranulation, whereas colchicine inhibited degranulation at both 2 and 4 hours. *$p<0.01$; Two-way ANOVA with Bonferroni correction, colchicine vs. vehicle. (**D**) Bars represent mean MFI shift + SEM of duplicate wells from one of three similar experiments; representative histograms from one such experiment are shown in (**C**).

Figure 4.4A

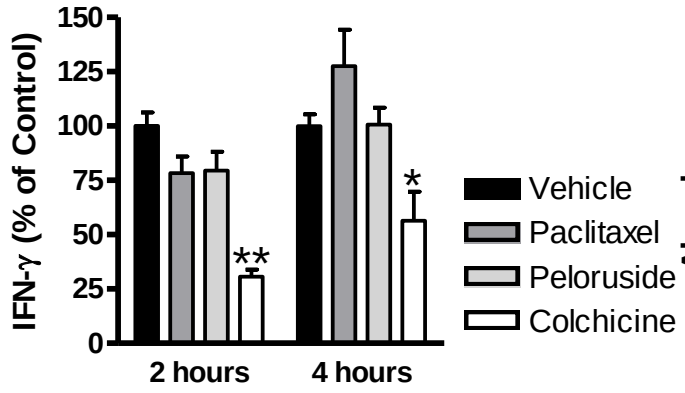

Figure 4.4B

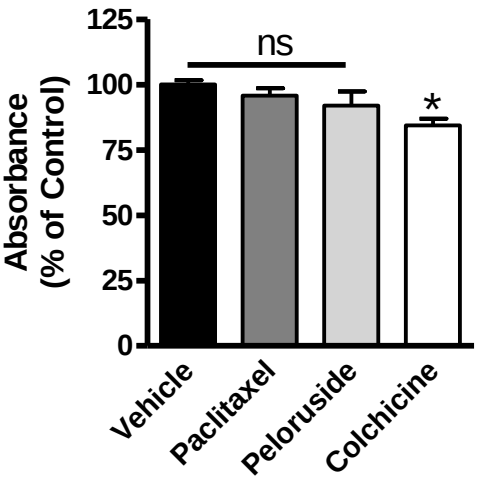

Paclitaxel and peloruside do not inhibit IFN-γ production and are not immediately cytotoxic to CTL. (**A**) CTL ($1x10^5$/well) were pre-treated for 4 hours with 1 µM paclitaxel, 1 µM peloruside, 1 µM colchicine or 0.1% ethanol (Vehicle) and then stimulated with SIINFEKL peptide. After 2 or 4 hours the supernatant was assayed for IFN-γ by ELISA. Neither paclitaxel nor peloruside inhibited IFN-γ production, whereas colchicine inhibited production at both 2 and 4 hours. Without SIINFEKL peptide no IFN-γ was produced (data not shown). *p<0.01, **p<0.001, Two-way ANOVA with Bonferroni correction, colchicine vs. vehicle. Bars represent mean+SEM of two to four wells combined from three similar experiments. In one experiment 4-hour supernatants were discarded prior to analysis. (**B**) Following pre-treatment as in (**A**) CTL were subjected to the MTT assay as described in the methods section. Metabolic activity was not altered by paclitaxel or peloruside, but was reduced by colchicine. *p<0.05, One-way ANOVA with Bonferroni correction vs. vehicle. Bars represent mean+SEM of triplicate wells combined from three similar experiments.

Figure 4.5A - Vehicle

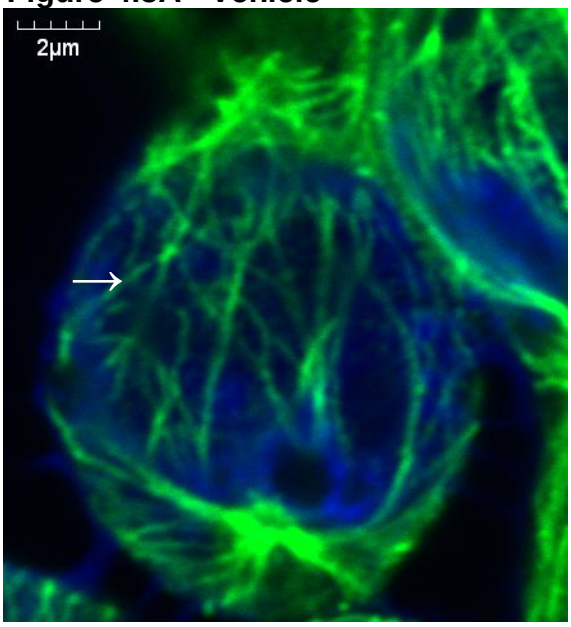

Figure 4.5B - Vehicle

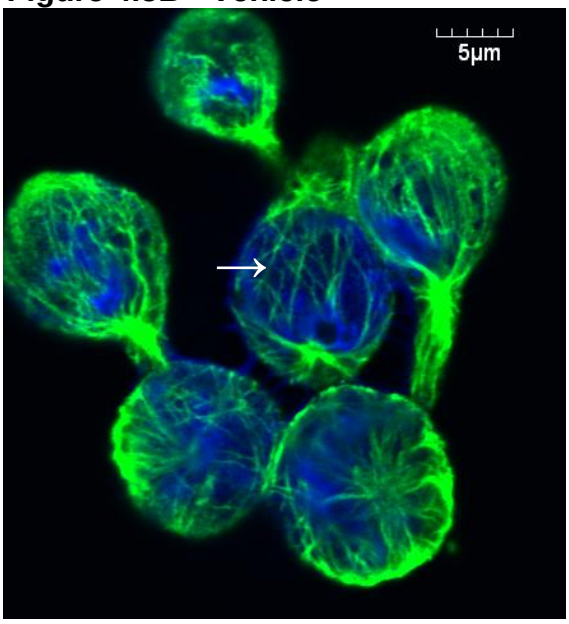

Figure 4.5C- 10 µM Paclitaxel

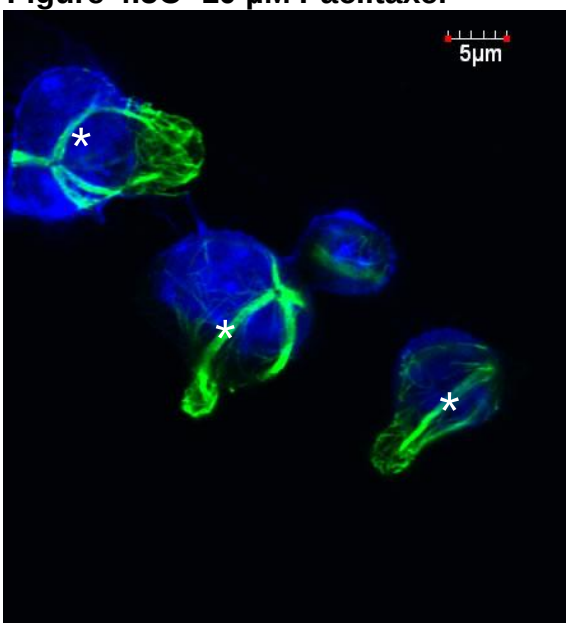

Microtubule Actives Modify the interphase CTL microtubule network. CTL were incubated for four hours in the presence of 0.1% ethanol, or the stated concentration of drug and subjected to immunocytochemistry. Microtubules were stained with rabbit anti-tubulin IgG and alexafluor-488 goat anti-rabbit IgG (green) and nuclei were identified using DAPI (blue). In control cells (A,B), individual microtubules (arrows) were seen extending through the cytoplasm. Some fragmented chromatin was observed, possibly an artefact of the sealing process. When treated with paclitaxel (C,D) or peloruside (E) microtubule bundles (asterisks) were observed. Bundling was more pronounced at 10 µM (C) than 1 µM paclitaxel (D) or 1 µM peloruside (E). In colchicine treated cells (F) diffuse staining (cell with arrow) was observed across the cell.

Figure 4.5D- 1 µM Paclitaxel

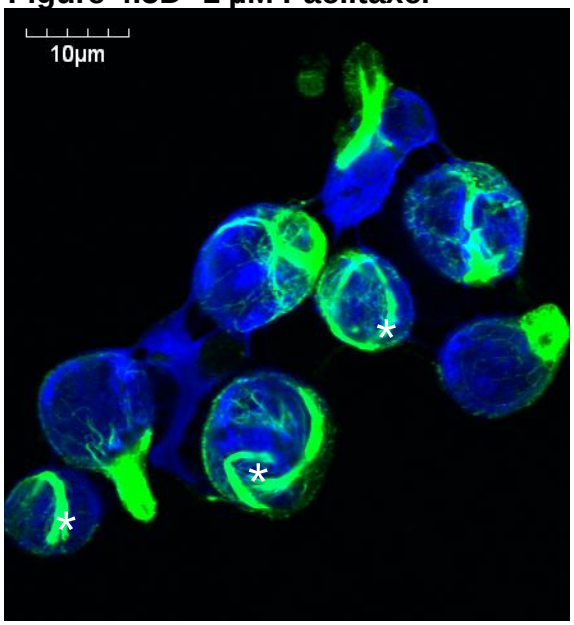

Figure 4.5E- 1 µM Peloruside

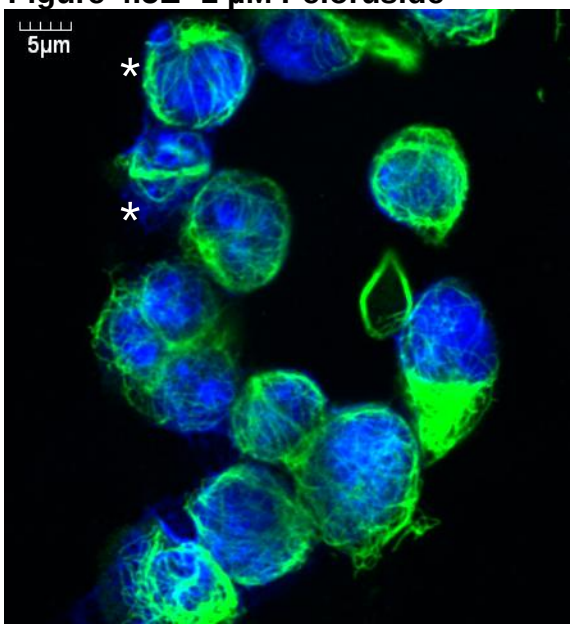

Figure 4.5F- 1 µM Colchicine

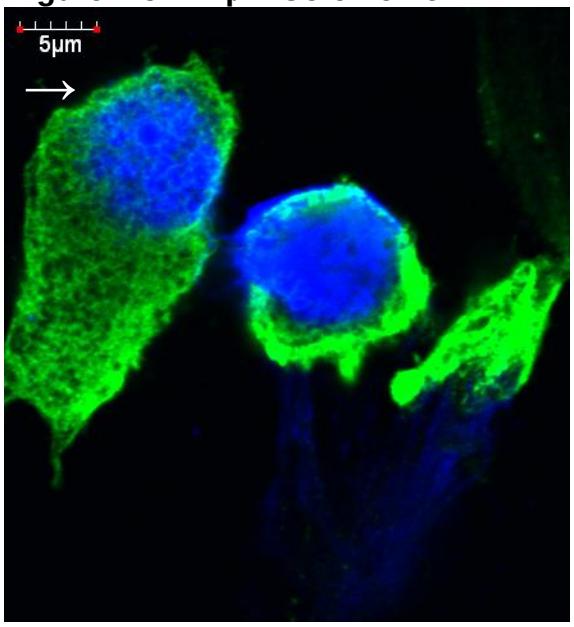

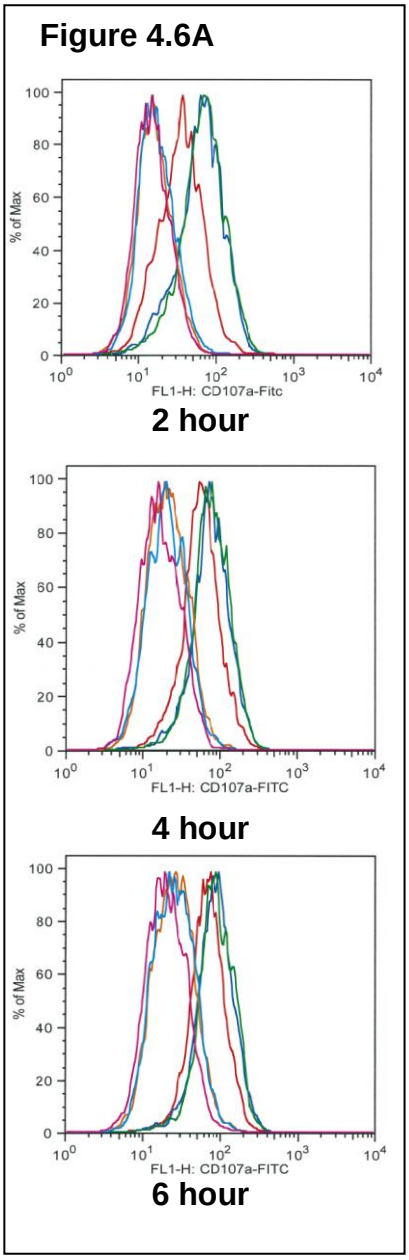

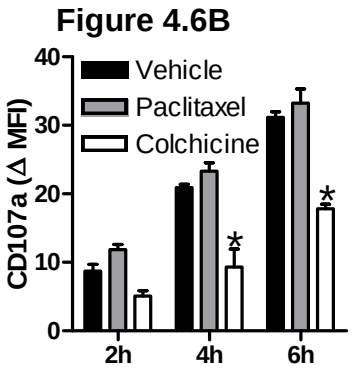

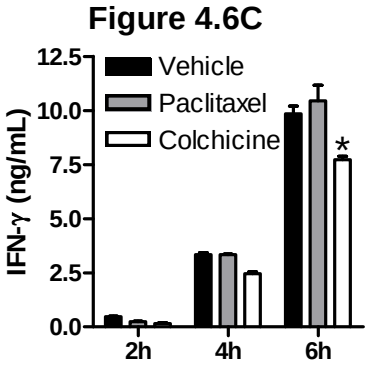

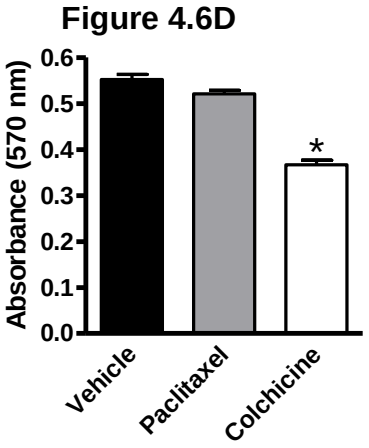

10 µM paclitaxel does not affect CTL exocytosis *in vitro*. CTL ($1x10^5$/well) were pre-treated for 4 hours with 10 µM paclitaxel, 10 µM colchicine or vehicle (1% ethanol) and assessed for lytic granule release by the degranulation assay (**A,B**), IFN-γ production by ELISA (**C**), and survival by the MTT assay (**D**). (**A**) Histograms show CTL CD107a expression 2, 4 and 6 hours after pre-treatment with vehicle (pink), paclitaxel (light blue) or colchicine (orange) without SIINFEKL peptide, or on exposure to SIINFEKL after pretreatment with vehicle (green), paclitaxel (dark blue) or colchicine (red). Paclitaxel did not inhibit degranulation (**A,B**), IFN-γ production (**C**), and had no effect on metabolism (**D**), while colchicine caused reductions in all three. (**B,C**) *p<0.001; Two-Way ANOVA with Bonferroni correction vs. vehicle. (**D**) *p<0.001 One-Way ANOVA with Bonferroni Correction vs. vehicle. (**A**) histograms are representative of duplicate wells from one of two experiments. (**B-D**) Bars show mean+SEM of two to four replicates from one of two similar experiments.

4.3 Discussion

The majority of work into MSD activity has focussed on their anti-mitotic properties and only more recently have the effects of these compounds on interphase cells been investigated. While the effects of paclitaxel on immune cells have been investigated to some extent, the immunological effects of peloruside are largely unknown. Currently, peloruside is known to kill proliferating splenocytes and to inhibit the LPS-induced production of TNF-α and NO, but not IL-12p40 (Crume et al., 2007; Miller et al., 1996). Additionally, Crume et al. showed that peloruside does not stimulate TLR-4 like paclitaxel (Crume et al., 2007). This thesis is the first study to look at the effects of peloruside on interphase CTL processes.

Previously it has been shown that killing by murine CTL at high ratios of CTL:TC is unaffected by paclitaxel treatment, even at concentrations that induce bundling (Knox et al., 1993). In contrast, paclitaxel inhibits killing by human CTL (Chuang, 1994; Chuang et al., 1994; Markasz et al., 2008). Because the study by Knox et al. utilized very high ratios of CTL:TC (50:1) and paclitaxel inhibited cytolysis by human CTL *in vitro*, we hypothesised that a more contact-limited system (lower CTL:TC ratio) may bring to light any subtle effects of paclitaxel on killing by murine CTL. Furthermore, we were interested to determine if effects of peloruside on CTL function were distinct from paclitaxel.

When we examined killing in the presence of paclitaxel we saw no effect at high or low ratios of CTL:TC. Moreover, pre-treating CTL with paclitaxel or peloruside to induce microtubule bundling did not have any evident effects on killing, degranulation or IFN-γ production. Colchicine, as shown previously, inhibited degranulation, IFN-γ production and reduced cell metabolic activity (Betts et al., 2003; Goldfinger et al., 1965; Ito et al., 1976). Given that DSD inhibit normal

MTOC relocalisation in CTL (Kupfer and Dennert, 1984), it is not surprising that degranulation and IFN-γ production, like killing (Wolberg et al., 1984), were inhibited by colchicine.

It is surprising, however, that CTL, even in the presence of high concentrations of MSD, were able to degranulate and kill TC effectively. The lack of inhibition argues that microtubule dynamicity is not essential in the killing process. Our confocal images show bundled microtubules in MSD-treated cells, but also demonstrate that microtubules still radiate out from the MTOC; this has previously been observed in CTL treated with paclitaxel (Knox et al., 1993). Furthermore, the MTOC can relocalise in CTL treated with paclitaxel, but not DSD, suggesting that this process is independent of microtubule dynamicity (Knox et al., 1993; Kupfer and Dennert, 1984). Lytic granules are associated with the peripheral microtubule network in unstimulated CTL (Stinchcombe et al., 2001b) and it is thought that delivery in stimulated CTL at least partially occurs in a dynein-mediated fashion (Kuhn and Poenie, 2002; Poenie et al., 2004; Stinchcombe et al., 2006). Thus, it appears that bundled microtubules operate as a sufficient scaffold for the transport of lytic granules. Because the concentrations of paclitaxel we used are well in excess (10-100 fold) of those required to inhibit dynamic instability in interphase cells (Jordan et al., 1993), our results and others (Knox et al., 1993), indicate that lytic granule delivery by murine CTL occurs sufficiently in the absence of a dynamic microtubule network.

During killing the CTL MTOC becomes a particularly dynamic entity. As well as relocalising to the IS, when at the interface the MTOC often shows oscillatory movements both towards and across the IS (Kuhn and Poenie, 2002). In single CTL:TC conjugates, these oscillations occur exclusively at the IS; in CTL

conjugated to multiple TC large-scale migration of the MTOC is observed between the two (Kuhn and Poenie, 2002). The importance of MTOC motility with regard to lytic granule delivery is unknown. It has been suggested that dynein proteins are the driving forces that pull the MTOC through to the IS, and as such are important not only for lytic granule delivery, but also controlling these dynamic movements across the IS (Poenie et al., 2004). Based on our results it seems that if these oscillatory movements are involved in the killing process they occur even in CTL treated with MSD. Alternatively, these migrations may not be causatively involved in killing. Examining the microtubule network of MSD-treated CTL during killing in greater detail may elucidate the importance of these oscillations and how they are modified in the cell.

The interactions at the IS leading to lytic granule exocytosis and stimulation of proinflammatory signalling pathways (i.e., production of IFN-γ) are differentially regulated in CTL. Lower TCR activation thresholds are required to elicit killing than cytokine production (Faroudi et al., 2003), and lytic granule delivery occurs more rapidly than large-scale TCR aggregation (Wiedemann et al., 2006). Colchicine inhibits recycling endosome activity in the human Jurkat T cell line resulting in lower TCR expression at the IS (Das et al., 2004), while, paclitaxel and vinblastine inhibit similar transport processes in MØ (Blocker et al., 1998). Thus it was possible that MSD could depress TCR expression and inhibit cytokine production by CTL without affecting degranulation. However, our results which measured degranulation and IFN-γ production simultaneously indicated that neither paclitaxel nor peloruside altered either process in activated CTL. Nevertheless, because at any given time only a small number of TCR are bound to ligand at the IS (Monks et al., 1998), it is possible that MSD do reduce CTL TCR recycling but such reductions were not sufficient to alter CTL activity.

Studies into the IS using the Jurkat T cell line and anti-CD3-coated coverslips show that microtubules are involved in stabilising the IS, and removal of microtubules with colchicine decreases the time for which an IS is maintained (Bunnell et al., 2001). Conversely, as colchicine decreases IS stability (Bunnell et al., 2001), inducing bundling may increase the duration of CTL:TC conjugation or increase the time it takes for signalling components to segregate appropriately in the IS (Grakoui et al., 1999; Monks et al., 1998). This increased contact time may explain why the overall rate of killing is reduced in human CTL (Chuang, 1994; Chuang et al., 1994; Markasz et al., 2008). However, the lack of effect we and others (Knox et al., 1993) observe in murine CTL suggests MSD affect CTL from mice and humans differently. Examining the real-time interactions of microtubules, lytic granules and IS components in MSD-treated cells may explain how CTL can elicit specific cell death with an altered microtubule network; explain why murine and human CTL are differently susceptible; and uncover effects of MSD on CTL that were not assessed in our experiments.

Our results add to knowledge of the involvement of the microtubule network in CTL function *in vitro* to show that peloruside, like paclitaxel, does not inhibit specific lysis at high or low CTL:TC ratios; that both compounds induce bundling in CTL; and neither compound inhibits peptide-specific degranulation or IFN-γ production. Our results support work by others showing that MSD treatment does not inhibit murine CTL function *in vitro*.

5 Effects of Paclitaxel on CTL function *in vivo*

5.1 Introduction

There is a modest body of literature looking at modulation of the human immune system *in vivo* after systemic taxane therapy, including effects on plasma cytokine concentrations and alterations to cell populations. While general leukopenia occurs following taxane therapy (Tong et al., 2000), $CD8^+$ T cells show a degree of resistance to the cytotoxic effects of MSD, and *ex vivo* responses of the CTL population actually seem to be enhanced after therapy cessation (Westerterp et al., 2008; Zhang et al., 2008). One study showed that $CD8^+$/IFN-γ^+ T cell responses are associated with decreased tumour burden, and these responses are enhanced following combination carboplatin/paclitaxel therapy (Coleman et al., 2005). In another study, both $CD8^+$/IFN-γ^+ and (activated) $CD44^+/CD8^+$ T cells were more numerous in patients after paclitaxel therapy (Zhang et al., 2008). A recent study investigated the effects of Taxol on the CTL response 2 days post therapy, and saw no change in the baseline killing of TC after 16 hours (Vicari et al., 2009). Because Taxol has an *in vivo* half-life of 0.8 hours (Zhang et al., 1997), and therefore may no longer be at an effective concentration 2 days post therapy, we analyzed the immediate *in vivo* effector response of $CD8^+$ T cells following drug administration.

5.2 Overview of the *In vivo* Cytolytic Assay

To induce an antigen-specific CTL response *in vivo*, mice were injected with LPS-matured, SIINFEKL peptide-pulsed BMDC to immunise mice. One week later mice were administered a single intraperitoneal dose of 20 mg/kg Taxol and approximately 2 hours later injected intravenously with $8x10^6$ syngeneic splenocytes as TC. The TC contained an equal mix of carboxyfluorescein succinimidyl ester (CFSE)-labelled $SIINFEKL^+$ (Ag^+) TC and Cell Tracker

Orange® (CTO)-labelled control (Ag^-) TC. After 10 hours, the mice were euthanized, their spleens removed and stained for CD8, and the % specific lysis was calculated by comparing the survival of Ag^+ TC relative to Ag^- TC. For example, if Ag^- specific lysis occurred *in vivo*, fewer Ag^+ TC would be recovered compared to Ag^- TC.

To determine if Ag-specific CTL survival was altered by Taxol treatment, mice received $1x10^6$ congenic OT-I/ptp-rc^a lymph node cells one day prior to immunisation. OT-I/ptp-rc^a T cells express clonal $V\alpha_2/V\beta_{5.1/5.2}$-TCRs specific for the SIINFEKL peptide, and are $CD45.1^+/CD45.2^+$. Because the recipient C57BL/6 mice T cells are exclusively $CD45.2^+$ we can track the OT-I/ptp-rc^a population by examining CD45.1 expression. As the TCR of the adoptively-transferred population is SIINFEKL-specific, these cells should predominate the immune response following immunization, allowing us to closely monitor the effector CTL *in vivo*. Following euthanasia splenocytes were examined for CD8 and CD45.1 expression alongside Ag^+/Ag^- TC survival.

5.3 Results

5.3.1 Taxol Inhibits Immediate Cytolysis in Mice

Because *in vitro* assays are highly optimized and tightly controlled, it was possible that in the more limiting and variable *in vivo* setting moderate alterations in CTL function would be more evident. During their proliferative phase, the CTL population expands rapidly, reaching a stage where cells divide on average every 5-9 hours (De Boer et al., 2001; Hwang et al., 2006; Oehen and Brduscha-Riem, 1998). However, maximal numbers of CTL are generated around day 6 after which proliferation slows and becomes minimal by day 7 (De Boer et al., 2001). Our immunisation strategy was set in a window that allowed mice to generate a potent CTL response, while avoiding any anti-mitotic effects of Taxol. To further minimise anti-mitotic effects, we examined cytolysis in a short time period (10 hours) which has previously been shown to be sufficient to detect killing (Hermans et al., 2004).

Immunising mice with BMDC pulsed with 1 µM SIINFEKL peptide generated a strong anti-SIINFEKL response causing specific depletion of the Ag^+ TC population (Figure 5.1A; $p<0.01$ by One-way ANOVA with Bonferroni correction; Immunised vs. Unimmunised within drug treatment). Differences in Ag^+ TC survival in unimmunised groups were minimal ($p=0.100$; Effect of Drug alone by Two-way ANOVA; data not shown); nevertheless, to account for any non-specific effect of Taxol we normalised killing within a drug treatment. In contrast to the *in vitro* results, *in vivo* treatment with 20 mg/kg Taxol caused a reduction in CTL-mediated cytolysis (Figure 5.1A; $p<0.05$; One-way ANOVA with Bonferroni correction, Taxol vs. Vehicle, Immunised Groups). While our system was designed to reduce the anti-mitotic effects of Taxol, a decrease in effector CTL numbers would explain the reduced cytolysis in drug-treated mice. However,

examining $CD8^+$ T cell numbers, of which the effector CTL will form a subset, no difference was observed between any groups ($p>0.05$; One way ANOVA with Bonferroni correction; Figure 5.1B). Thus, our data suggest that Taxol inhibits CTL-mediated cytolysis *in vivo* without significant effects on survival of the $CD8^+$ population.

5.3.2 Taxol does not deplete the effector population *in vivo*

Our initial data suggested that Taxol did not inhibit cytolysis by killing $CD8^+$ splenocytes. However, as effector CTL comprise only a subset of all CD8+ T cells, it was possible that the background CD8+ population was masking a depletion of Ag-specific CTL by Taxol. We redesigned our experiment to include the adoptive transfer (AT) of OT-I/ptp-rc^a lymph node cells prior to immunisation, which should then predominate the SIINFEKL-specific CTL response. As expected, immunisation increased numbers of CD8+/CD45.1+ T cells (Figure 5.2A) and greatly enhanced specific lysis (Figure 5.2B) in immunized mice.

To determine the effects of Taxol on CTL survival *in vivo* we administered mice an intraperitoneal dose of 20 mg/kg Taxol or an equivalent dose of Cremophor EL® and submitted them to a 10 hour VITAL assay. As shown in Figure 5.3A, Taxol treatment did not deplete the CTL population. Further, Taxol caused a small reduction in specific lysis that did not reach significance in this assay (Figure 5.3B), which may relate to low animal numbers in each group. This lack of effect is contrary to the results of Figure 5.1 A. Moreover, mean cytolysis at 10 hours in experiments where control mice received transgenic T cells prior to immunisation was higher than in experiments where they did not (*c.f.* Figure 5.1A & 5.3B; $p<0.05$, Student's *t*-test, shown again in Figure 5.3C). Because mice with transgenic T cells potently eliminated SIINFEKL-specific TC, the kinetics of cytolysis may be more rapid in this system, so earlier timepoints may be more

appropriate when using OT-I/ptp-rc^a T cells. Furthermore, Taxol possesses only a short half-life *in vivo* (0.8 hours) and is rapidly eliminated from tissues, including the spleen (Zhang et al., 1997). We reasoned that a higher bolus dose of Taxol may inhibit CTL responses for longer periods, which would exaggerate inhibition at earlier timepoints. Further, higher drug concentrations would accentuate any residual anti-mitotic effects on the effector population. Thus, we repeated the adoptive transfer experiment and treated mice with 30 mg/kg Taxol (0.75 mg/mouse) and examined killing of Ag^+ TC after 8 hours.

Even with this high drug concentration the CTL population was not depleted in drug-treated mice (Figure 5.4A; p=0.5753; Student-s *t*-test, Taxol vs. Vehicle, Immunised groups). Specific lysis was inhibited by Taxol to a similar level as previous experiments (Figure 5.4B), although this difference did not reach statistical significance (p=0.0988; Student's *t*-test, Taxol vs. Vehicle, Immunised groups), we again believe this is most likely due to the low numbers of animals in each group. In support of this supposition, when we combined mice treated with Taxol at either dose, we still did not observe any effect on CTL survival (Figure 5.4C, p=0.4322), whereas combining the groups did lead to a detectable difference in cytolysis (Figure 5.4D, p=0.0329; Student's *t*-test, Vehicle vs. Taxol, immunised groups). To further clarify if the number of CTL was directly related to the level of killing, we correlated the numbers of OT-I/ptp-rc^a CTL to % specific lysis in all mice from both experiments (Figure 5.5). Although the number of CTL was not related to % specific lysis in vehicle-treated mice (r^2=0.2420), there was a significant relationship between CTL number and % specific lysis in Taxol-treated mice (r^2=0.7049; linear regression analysis). Further, the relationship between CTL number and % specific lysis was significantly different in Taxol-treated and vehicle-treated immunised mice (p<0.05; linear regression F-test for difference in

slope). Thus, these results suggest that under conditions where CTL numbers are limiting, Taxol exerts the greatest inhibition on their function. Together these data support the hypothesis that inhibition of CTL-mediated cytolysis *in vivo* is due to functional inhibition of CTL rather than cytotoxic effects on the effector population.

Figure 5.1A

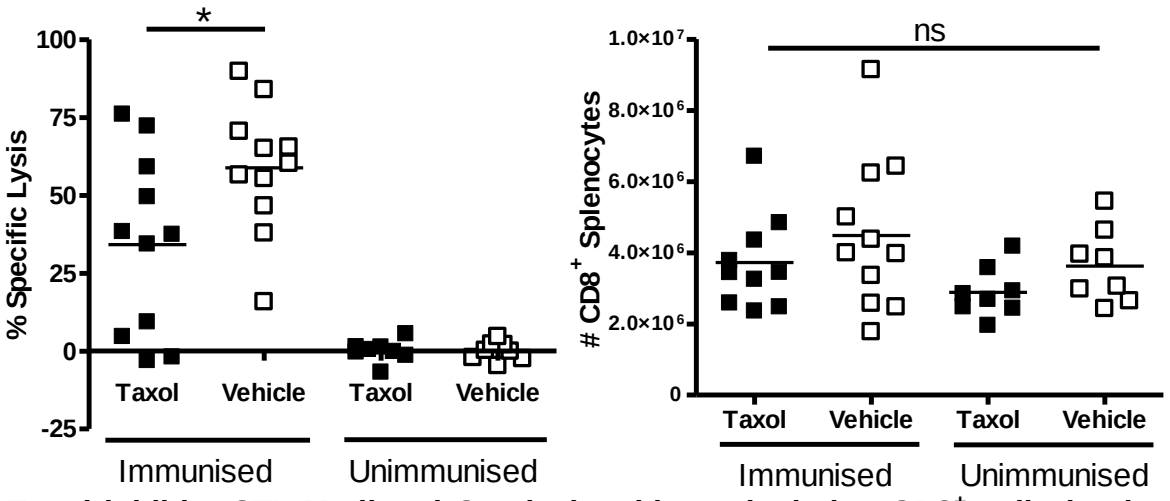

Taxol inhibits CTL-Mediated Cytolysis without depleting CD8$^+$ cells *in vivo*. C57BL/6 mice were immunised as described in general methods. One week later, mice were injected intraperitoneally with 20 mg/kg Taxol or an equivalent vehicle control (Cremophor EL®) and subjected to a 10-hour VITAL assay. Specific lysis (**A**) and numbers of CD8$^+$ splenocytes (**B**) were calculated as described in the general methods section. Data points represent individual mice pooled from three separate experiments; lines represent group means. (**A**) *$p<0.05$; One-way ANOVA with Bonferroni correction, Taxol vs. Vehicle, Immunised Groups. (**B**) No difference in total CD8$^+$ number was detected ($p>0.05$; One-Way ANOVA).

Figure 5.2A

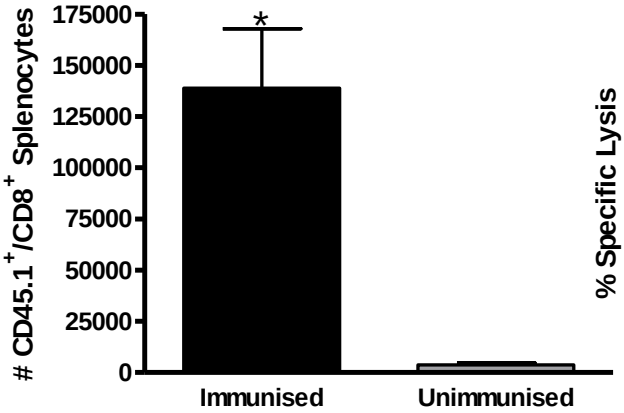

Figure 5.2B

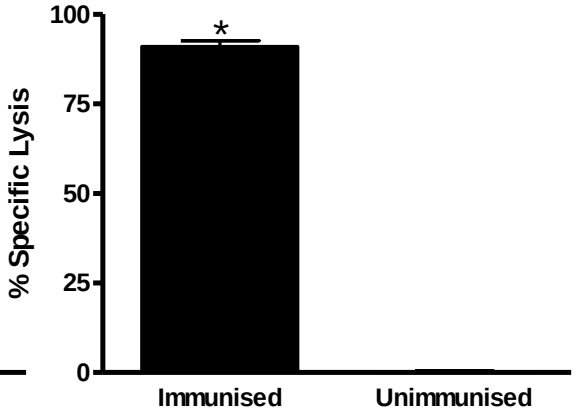

Immunisation Expands the Adoptively-Transferred Population and Permits Specific Lysis. Prior to immunisation mice received $1x10^6$ OT-I/ptp-rc^a lymph node cells. One week later mice were given an intraperitoneal dose of Cremophor EL® or Taxol and subjected to the VITAL assay. (A) Total $CD45.1^+/CD8^+$ numbers (A) and specific lysis (B) were determined as described in general methods. Bars represent mean+SEM from all immunised mice combined from two experiments, shown individually in Figure 5.3A&B and Figure 5.4A&B. *p<0.001, Student's *t*-test Immunised vs. Unimmunised.

Figure 5.3A

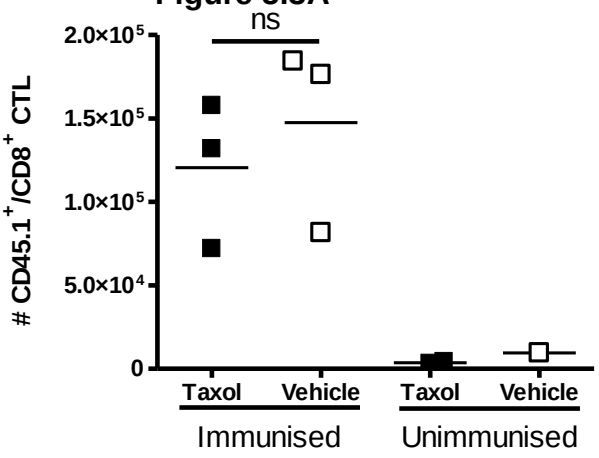

Figure 5.3B

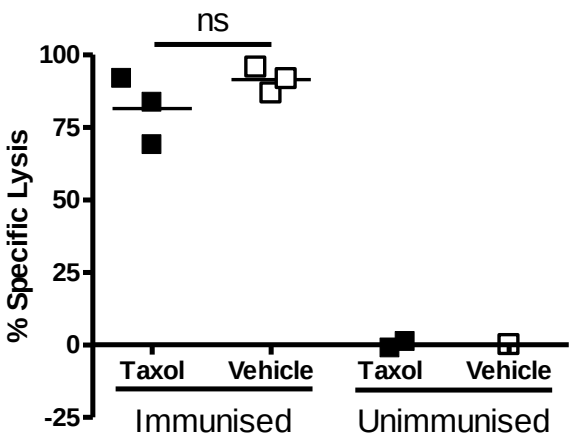

Figure 5.3C

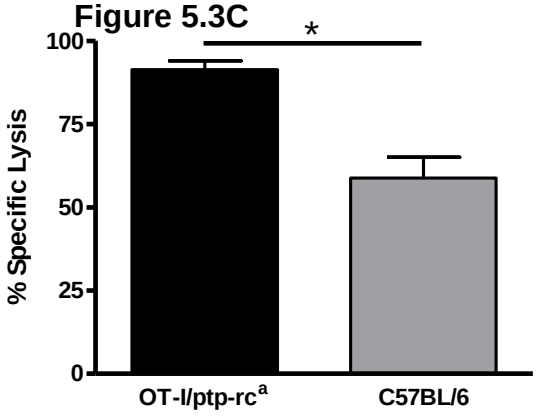

Taxol does not deplete CD45.1$^+$/CD8$^+$ CTL *in vivo*. Prior to immunisation as described in general methods mice received 1x10^6 OT-I/ptp-rc^a lymph node cells. One week later mice were given an intraperitoneal dose of 20 mg/kg Taxol or an equivalent dose of Cremophor EL® as vehicle control. Two hours later mice were subjected to a 10 hour VITAL assay. Total numbers of CD45.1$^+$/CD8$^+$ CTL (**A**) and specific lysis (**B**) were calculated as described in general methods. Data points represent individual mice; lines represent group means. Killing was not significantly inhibited in this assay ($p>0.05$, Student's *t*-test; Immunised groups). (**C**) Killing in vehicle-treated mice that received (OT-I/ptp-rc^a) or did not receive (C57BL/6) transgenic T cells prior to immunisation shown in 5.1A and 5.3B are represented here by bars showing mean+SEM. Mice that received transgenic T cells prior to immunisation eliminated TC to a greater extent than C57BL/6 mice that did not (*$p<0.05$, Student's *t*-test).

Figure 5.4A

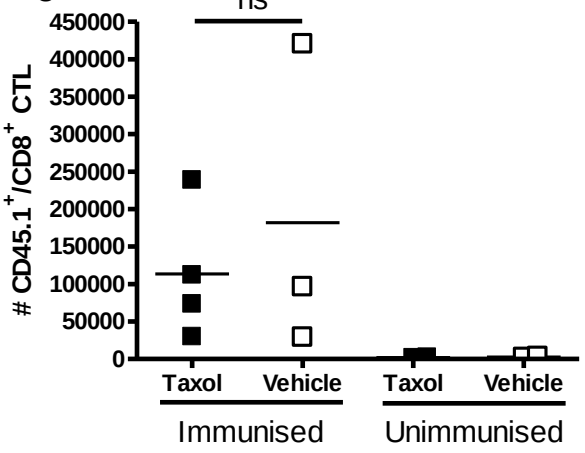

Figure 5.4B

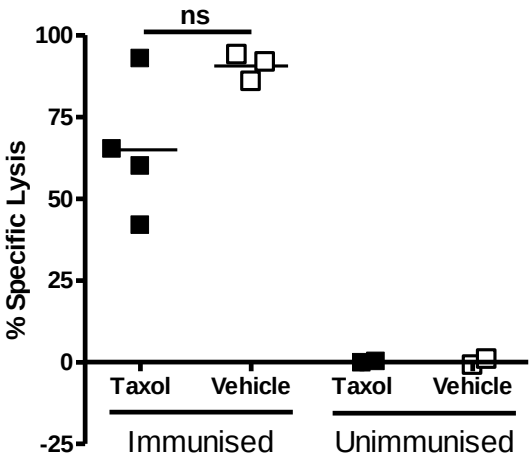

Figure 5.4C

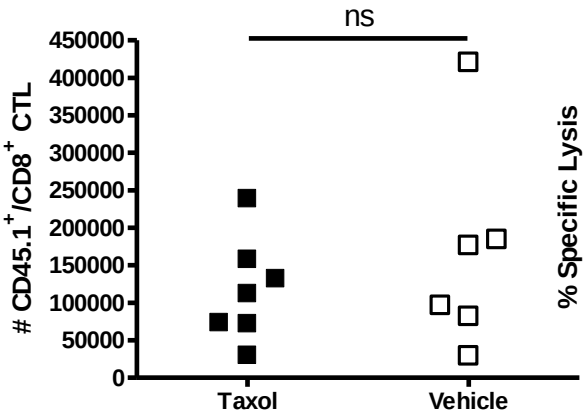

Figure 5.4D

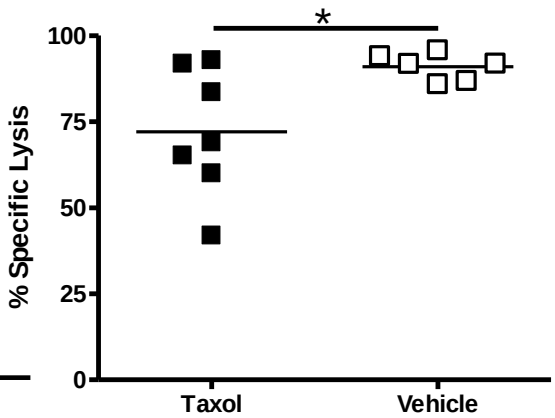

Taxol does not deplete CTL and inhibits CTL-Mediated Cytolysis *in vivo*. Prior to immunisation, mice received $1x10^6$ OT-I/ptp-rc^a lymph node cells. (A,B) One week after immunisation mice were given an intraperitoneal dose of 30 mg/kg Taxol or an equivalent dose of Cremophor EL® as vehicle control. 2 hours later mice were subjected to an 8 hour VITAL assay. Total numbers of $CD45.1^+/CD8^+$ CTL (A) and specific lysis (B) were calculated as described in general methods.(C,D) Immunised mice analysed separately in Figure 5.3A,B and Figure 5.4A,B were combined and analysed together. Data points represent individual mice; lines represent group means. *p<0.05, Student's *t*-test, Taxol vs. Vehicle.

Figure 5.5

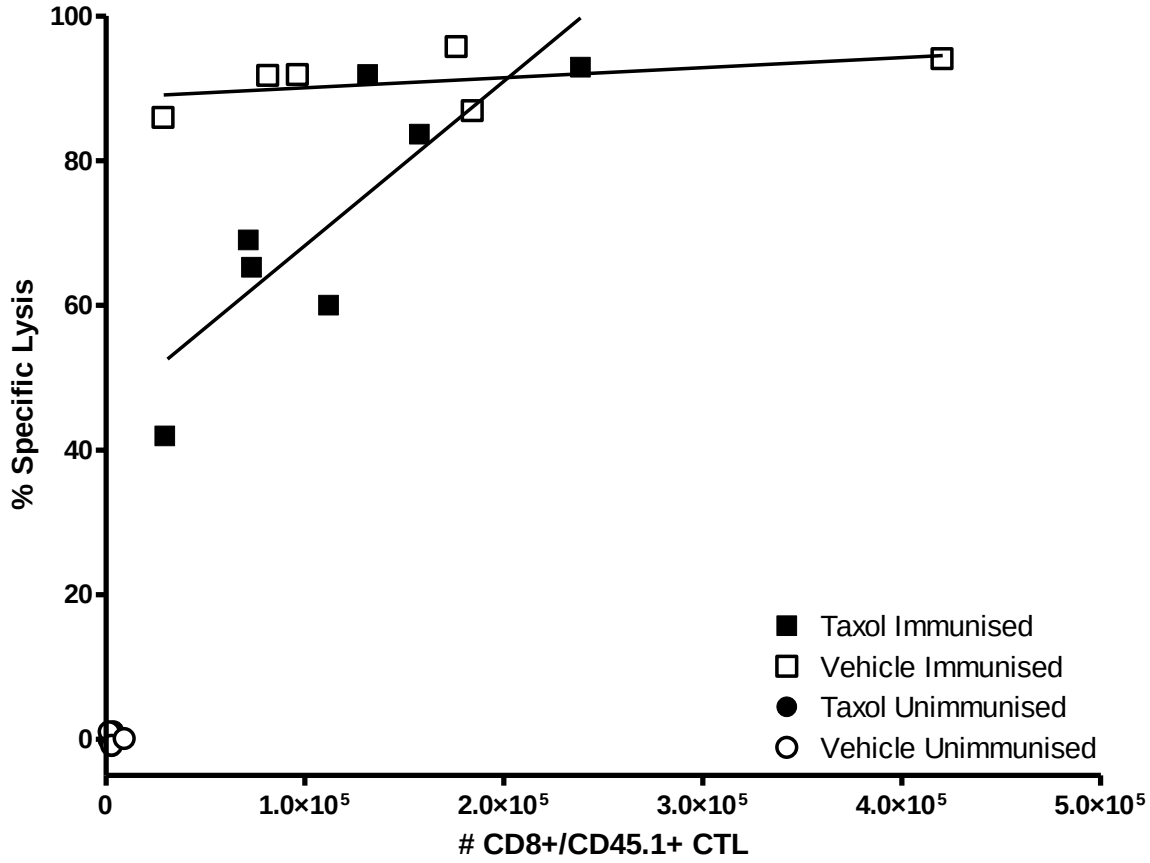

Taxol inhibits CTL-mediated cytolysis in mice with similar numbers of CTL. Numbers of $CD45.1^+/CD8^+$ CTL in mice shown in Figure 5.4C were correlated to specific lysis in Figure 5.4D. Between immunised groups, Taxol-treated mice showed reduced lytic capacity compared to Vehicle-treated mice with similar numbers of $CD45.1^+/CD8^+$ CTL. Dots show individual mice, lines show the group trends, which differ for Taxol- and Vehicle-treated mice ($p<0.01$; Taxol vs. Vehicle, Immunised groups; F-test for difference in slope)

5.4 Discussion

We set up two complementary systems to measure the effects of Taxol on CTL functionality *in vivo*. In the first, we examined the effect of drug on the autologous host response to SIINFEKL peptide. Our results showed that a single 20 mg/kg dose of Taxol inhibited CTL-mediated cytolysis *in vivo*. A second system, the adoptive transfer of OT-I/ptp-rc^{a} lymph node cells into C57BL/6 recipients, allowed us to monitor survival of the effector population and lytic activity simultaneously. In these studies immunisation caused the expansion of CD45.1^{+}/CD8^{+} cells in the spleens of mice and the presence of this population correlated well with cytolysis *in vivo*. Further, similar numbers of CD45.1^{+}/CD8^{+} CTL were detected in mice treated with Cremophor EL® and Taxol. However, control mice appeared better able to eliminate TC than Taxol-treated mice. Taken together our data suggest Taxol inhibits CTL activity *in vivo* and this occurs independently of Taxol's anti-mitotic properties.

In line with our work, Vicari et al. recently reported an inhibitory effect of Taxol on CTL-mediated cytolysis *in vivo*.(Vicari et al., 2009) In a solid-tumor cancer model, this study initially showed paclitaxel enhanced the anti-tumour response in a CD8^{+}-dependent manner.(Vicari et al., 2009) However, when mice were given a TLR-9 agonist and tested for their ability to kill SIINFEKL-pulsed splenocytes (as TC), paclitaxel limited killing to levels of control mice (≈10%). In this experiment both paclitaxel and the immune adjuvant (PF-3512676) were administered 2 days prior to TC transfer, so it may be that paclitaxel depressed the enhancement conferred by the TLR-9 agonist, rather than inhibiting CTL:TC killing. In contrast, our studies aimed to determine the immediate effects of paclitaxel on cytolysis *in vivo*.

In our adoptive transfer (AT) experiments mice given a 30 mg/kg dose of Taxol exhibited impaired killing versus controls at 8 hours. When we assessed the effects of a 20 mg/kg dose at 10 hours, the difference was less pronounced. We resolved that this was likely due to the kinetics of cytolysis. As suggested by others (Hermans et al., 2004), if killing plateaus as TC become sparse, differences will be best detected during the exponential phase of cytolysis in control mice. In experiments assessing the host-generated immune response, 10 hours provided a window in which differences in specific lysis between control and drug treated mice were detected. However, mice that contained OT-I/ptp-rc^{a} CTL appeared to eliminate the target population to a greater extent than C57BL/6 heterologous responders, leading to more pronounced effects of drug at 8 rather than 10 hours.

Kinetically, Taxol may affect killing in two independent but not mutually exclusive ways. Firstly, at early times, high concentrations of drug may ablate killing, but as the drug concentration reduces, killing rates return to those of controls (Figure 5.6). Secondly, following drug exposure, killing may be depressed such that the rate of killing is reduced relative to controls (Figure 5.7). Taxol is eliminated relatively rapidly *in vivo*, with a half-life of approximately 0.8 hours (Zhang et al., 1997), but accumulates in tissues such as the spleen when administered continuously (Klecker et al., 1994). If the effects of Taxol are transient, then differences in specific lysis will best be determined at early times before the effect of drug wears off. Alternatively these effects will be amplified with multiple administrations of drug. Conversely, if Taxol operates by reducing the rate of lysis, inhibition will be most exaggerated at times just prior to plateau in control mice. These two possibilities could be distinguished by maintaining a constant level of drug and by assessing cytolysis at multiple timepoints.

While our results indicate that paclitaxel inhibits CTL function *in vivo*, Taxol does not necessarily affect CTL directly. Because our *in vitro* results indicate that in murine CTL, the process of lytic granule exocytosis is not inhibited by MSD, it is likely that other microtubule-dependent processes are involved in the inhibition of CTL function caused by Taxol *in vivo*. These alternative explanations include altered tissue homing of cells; changes to the surface phenotype of TC; increased CTL:TC conjugation periods; and modification of the signals between CTL and TC.

As CTL-mediated cytolysis is contact dependent, CTL must encounter TC to induce specific lysis. Thus, Taxol may alter the migratory properties of either CTL or TC. Previous studies have shown that systemic Taxol administration inhibits LPS-induced neutrophil extravasation, vascular leakage and protects mice from septic shock (Mirzapoiazova et al., 2007). Further, Taxol ablates the expected leukocyte infiltration into the peritoneum following LPS administration (Mirzapoiazova et al., 2007). Even slight modifications to cell migratory properties could alter the ability of CTL to interact with TC. Depending on the tissue localisation of the targets, paclitaxel may prevent CTL from coming into contact with TC. As we measure lysis and survival in the spleen, it seems unlikely that the populations are prevented from mixing. However, as effector CTL traffic through the periphery is more than naïve T cells (Wherry et al., 2003), and approximately 30% of our *in vivo* TC will be naïve T cells (Garnett et al., 2008), it is possible that paclitaxel alters tissue homing and reduces the rate of encounter of the two cell types prior to final analysis in the spleen.

An alternative explanation is that paclitaxel modifies the target cell, such that the intercellular signals that lead to target cell death are hindered. In order to induce lysis, protein signalling between CTL and TC must be strong enough to form a stable immunological synapse (IS), activate the TCR and polarise the CTL to kill the TC. If the ability of CTL to recognise TC is compromised then the formation of the synapse will be inhibited. In support of this, pre-treatment of murine cell lines with paclitaxel reduces surface expression of CD11a and CD54 (Zhao et al., 2003), both of which are involved in stabilisation of the IS (Monks et al., 1998; Stinchcombe et al., 2001b; Stinchcombe and Griffiths, 2003; Stinchcombe et al., 2006). This decreased expression directly correlates with reduced lysis of the cells by CD3-activated lymphocytes (Zhao et al., 2003). If such modifications have an effect *in vivo,* cytolysis will be inhibited.

Also concerning the interaction between CTL and TC, the ability of CTL to kill multiple targets *in vivo* may be impeded. In human CTL *in vitro* it has been shown that while CTL readily conjugate and elicit cell death in individual TC, their ability to recycle and kill multiple targets is greatly limited by paclitaxel (Chuang, 1994; Chuang et al., 1994). Similar to the *in vitro* setting, CTL *in vivo* are likely to kill multiple TC either serially or simultaneously (Breart et al., 2008), so inhibition of the rate of cytolysis may explain the decreases in killing we observe in mice *in vivo*.

As well as modulation of intercellular adhesion, the stimulatory signals leading to formation of the IS may be depressed by Taxol. For example, paclitaxel has been shown to inhibit DC stimulation of T cell proliferation *in vitro* by effects on the DC, even though the DC have elevated MHC-II expression (Joo, 2003). The ability to form and stabilise an IS is heavily dependent on the strength of interaction

between TCR and MHC-peptide complexes (Grakoui et al., 1999), rather than the number of bound TCR (Monks et al., 1998). If Taxol inhibits the interaction of TCR-MHC-peptide, the drug may have some effect on the ability of CTL to induce death of TC. Transient interactions such as these could be more important for interactions of CTL and TC *in vivo* than *in vitro*.

Our study contrasts a number of reports in humans and mice suggesting enhanced $CD8^+$ T cell function following paclitaxel treatment. In humans, reports suggest that IFN-γ-secreting $CD8^+$ T cells are more numerous after therapy; activated ($CD44^{High}$) $CD8^+$ T cells are more frequent and T_{REG} are specifically inhibited by Taxol (Zhang et al., 2008). This depletion is important because T_{REG} directly suppress CTL activity *in vitro* and *in vivo;* in the absence of T_{REG}, CTL activity is increased (Mempel et al., 2006; Vicari et al., 2009). Moreover, the $CD8^+$ subpopulation of lymphocytes is enriched in cancer sufferers and has been reported to either recover rapidly following or be minimally depleted by paclitaxel treatment (Tong et al., 2000; Westerterp et al., 2008). However, in contrast to our experiments, these reports generally measure cell function following cessation of therapy, so these effects may relate to leukopenia caused by Taxol.

Murine studies demonstrate that as immune adjuvants, paclitaxel and docetaxel enhance anti-tumour responses. Using either DC therapies or GM-CSF-based vaccinations, $CD8^+$ T cell function and $CD8^+$-IFN-γ production are enhanced by paclitaxel (Chu et al., 2006; Garnett et al., 2008; Yu et al., 2003); $CD4^+$ and $CD8^+$ T cell tumour infiltration increase (Zhong et al., 2007); and epitope spreading is induced (Garnett et al., 2008). Most importantly, however, in combination with immunotherapies, taxanes inhibit tumour growth and increase progression-free survival (Chu et al., 2006; Emens et al., 2001; Garnett et al., 2008; Machiels et al.,

2001; Vicari et al., 2009; Yu et al., 2003; Zhong et al., 2007). Reactivation of the tumour-specific immune response with chemotherapeutics seems a promising avenue for effective cancer treatment, particularly considering the positive results of such studies. However, our results show that immediate effector function is inhibited by Taxol prior to the observation of any anti-mitotic effects.

Our system was not designed to measure the anti-tumor response, but rather the immediate cytolytic response to infection of $CD8^+$ T cells. CTL-mediated cytolysis is drastically modified by the tumor micro-environment, and the interactions of CTL with tumor cells differ from those with individual TC (Breart et al., 2008; Mempel et al., 2006; Radoja et al., 2001; Vicari et al., 2009). We suggest that any enhancing effects of paclitaxel on the $CD8^+$ T cell population will not be immediate, and before complete leukocyte recovery, the host immune system will be impaired in its ability to fight infection and elicit specific cell death *in vivo*.

Figure 5.6

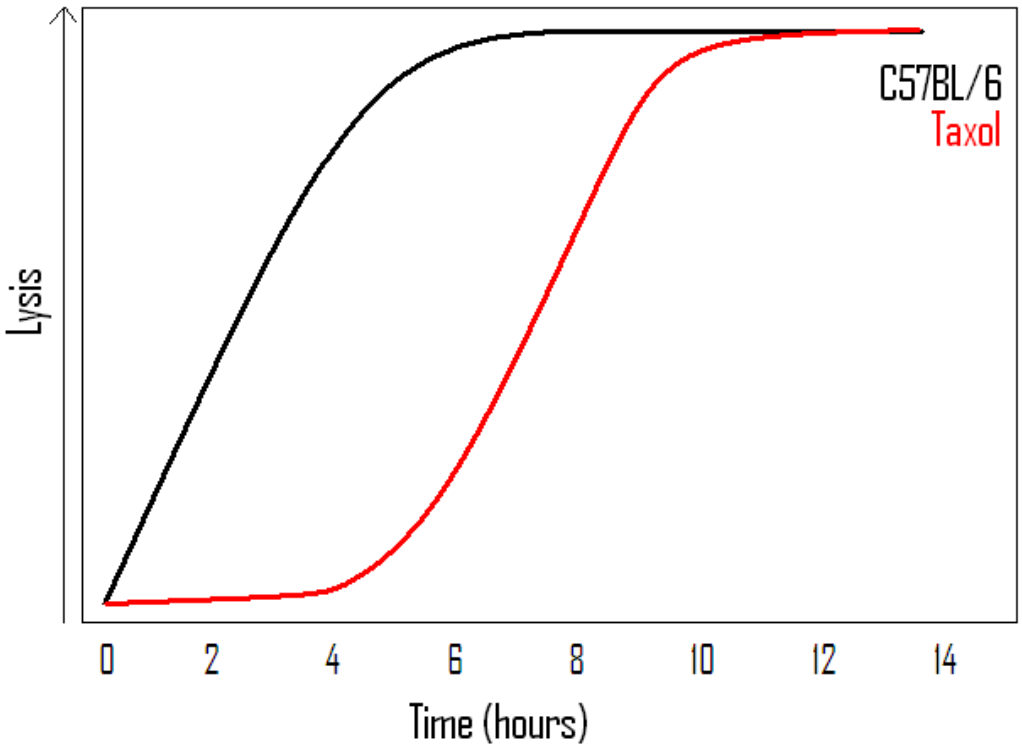

Theory pertaining to *in vivo* inhibition by Taxol 1: Killing is blocked while Taxol is present at significant levels, but killing returns to normal rates after drug is removed from the host. By 8 hours, control mice (in adoptive transfer experiments) have removed the majority of the TC population and killing reaches a plateau. Drug-treated mice at 8 hours are killing TC at a higher rate than controls, so the difference between the two reduces as time continues.

Figure 5.7

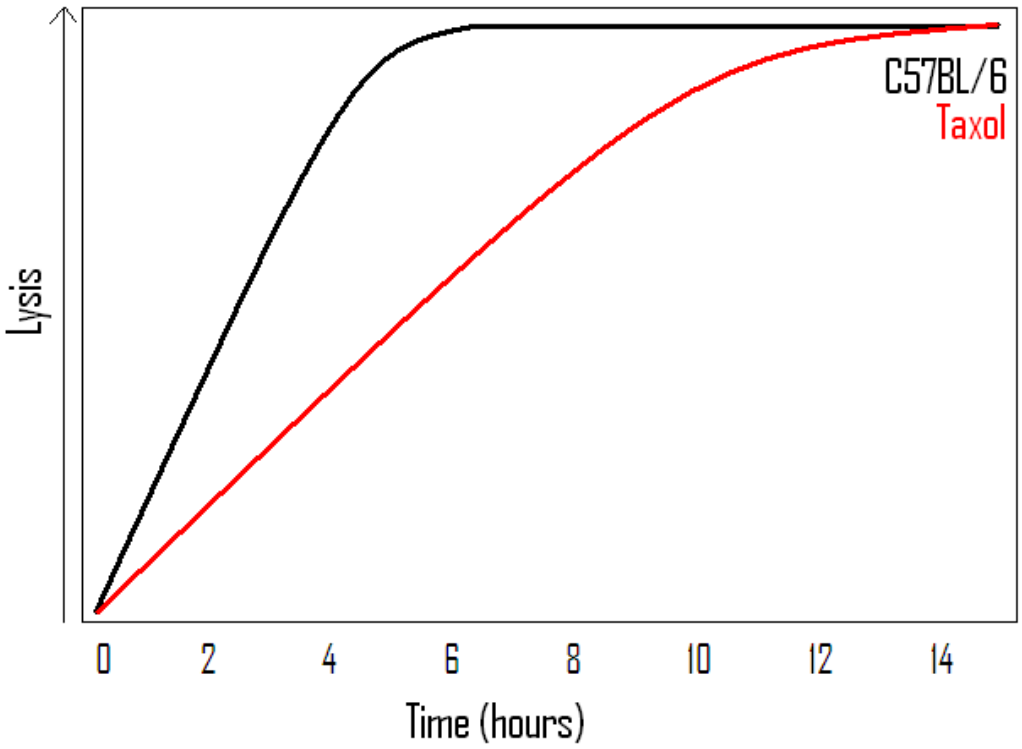

Theory pertaining to *in vivo* inhibition by Taxol 2: Killing is functionally inhibited in drug treated mice. Killing occurs at a consistent but reduced rate compared with control mice and does not recover with drug washout. Killing will reach a plateau phase, but at delayed times in the presence of drug.

6 General Discussion

6.1 General Summary of Work

This thesis set out to determine the functional immunological effects of MSD. It specifically investigated effects of MSD on exocytic function in immune cells. BMMØ are a terminally differentiated cell type and thus are not susceptible to the anti-mitotic effects of MSD (Crume et al., 2007). Degranulation is an interphase CTL process that heavily involves the microtubule network (Mempel et al., 2006; Stinchcombe et al., 2001b; Stinchcombe et al., 2006) and could be examined while avoiding the anti-mitotic effects of MSD.

The current study continued work in our lab showing that BMMØ production of TNF-α and NO are inhibited by MSD (Crume et al., 2007). It investigated the involvement of IFN-γ stimulation in the inhibition; assessed the kinetics of TNF-α production in the presence of paclitaxel; and addressed why the stimulating dose of LPS affects paclitaxel's inhibitory effect on TNF-α production. Furthermore, our research expanded knowledge of how TLR-4 activation alters cellular metabolic activity. The results of the current study implicate functional inhibition and largely exclude kinetic alteration as the mechanism behing MSD-mediated supression of BMMØ inflammatory responses.

Of particular note we observed different LPS-dose responses for BMMØ production of TNF-α and NO, which led to different inhibitory relationships with paclitaxel. With increased concentrations of LPS, NO production plateaued, whereas TNF-α reduced to a basal level. Similar LPS dose-response curves for TNF-α and NO have been observed previously (Kastenbauer and Ziegler-

Heitbrock, 1999; Shnyra et al., 1998; Stuehr and Marletta, 1985; Stuehr and Marletta, 1987; Takasuka et al., 1991). This refractiveness for TNF-α appears to be important in BMMØ responses to LPS and helps explain why paclitaxel does not inhibit TNF-α production above 20 ng/mL as seen in the work by Crume et al. (Crume et al., 2007).

Similar to MØ responses to LPS, CTL-mediated cytolysis occurs after cell division and thus provided an alternative system in which to investigate the functional effects of MSD on immune processes. Furthermore, MØ and CTL are both key components of the cell-mediated immune response, which makes examining CTL and MØ together beneficial to the understanding of the wider immunological implications of MSD therapy.

In this thesis, the results from *in vitro* work using CTL supported work by others (Knox et al., 1993) showing that concentrations of paclitaxel that induce microtubule bundling do not inhibit killing by murine CTL *in vitro.* The current study extended these findings to show that neither degranulation nor IFN-γ production by CTL were inhibited by paclitaxel treatment. Furthermore, this was the first study to assess the effects of peloruside on interphase CTL processes. Like paclitaxel, peloruside showed no inhibitory effect on CTL killing, degranulation or IFN-γ production *in vitro* and also induced microtubule bundling in CTL, albeit to a lesser extent than paclitaxel.

Perhaps the most significant result of this thesis was attained in a murine model of CTL-mediated cytolysis. Investigating CTL-mediated TC death *in vivo* revealed an inhibitory effect of paclitaxel that was not apparent *in vitro*. Importantly, this occurred in the absence of anti-mitotic effects on the CTL population. This is the

first study (to the knowledge of the author) to assess the immediate effects of paclitaxel on CTL-mediated cytolysis *in vivo*. We believe it provides new information relevant to patients undergoing taxane therapy, and illustrates the importance of using *in vivo* models in the search for less invasive and increasingly effective treatments for cancer.

It is important to consider that the interactions of CTL and TC in the tumor micro-environment differ to those in lymphoid tissue (Breart et al., 2008; Mempel et al., 2006), so the data may not apply directly to anti-tumour responses, but rather be more relevant to CTL-dependent control of infection during MSD treatment. Increased risk of infection following MSD therapy is generally associated with the anti-mitotic effect of the drugs (Iura et al., 2009; Souglakos et al., 2002). The current study supports work by others (Chuang et al., 1994; Crume et al., 2007; Markasz et al., 2008) demonstrating functional inhibition of both CTL and MØ responses by paclitaxel. Collectively these results suggest that the increased risk of infection during paclitaxel therapy may occur in part due to functional effects, and not solely anti-mitotic effects of the compound.

Knowledge of how the immune system is modified by chemotherapeutics is becoming more important, particularly with increasing investigation into co-immuno-chemotherapies. Numerous recent studies identify enhancement of the anti-cancer immune response by taxanes both clinically and in murine models (Garnett et al., 2008; Machiels et al., 2001; Vicari et al., 2009; Westerterp et al., 2008; Yu et al., 2003; Zhang et al., 2008; Zhong et al., 2007). These studies generally assess immune responses following cessation of therapy, whereas the current study looked at immune responses during MSD treatment. The results of the current thesis suggest that immediate functional repression of CTL can occur

during MSD treatment *in vivo*. Hopefully a better understanding of the immediate and long-term benefits and risks of MSD treatment will allow for improved quality of life and longer progression-free survival for cancer patients.

As we understand more about the immunological implications of MSD treatment, we are not only better able to limit and control undesirable side effects, but can also find other clinical applications for the drugs. Repressing the immune system can be desirable in settings outside of cancer. The anti-mitotic properties of MSD have already been exploited in a murine model of multiple sclerosis (Cao et al., 2000), and utilised clinically to limit in-stent restenosis (occlusion of a stent by tissue regrowth) (Tanabe et al., 2003). Furthermore, paclitaxel has been shown to block cell extravasation and vascular leakage during murine LPS-induced sepsis (Mirzapoiazova et al., 2007), suggesting MSD have the potential to prevent cytotoxicities involving aberrant cell trafficking. It is important, however, to consider the currently unavoidable toxic effects of high doses of MSD (Tong et al., 2000; Westerterp et al., 2008). As such we are not advocating that treatments with tolerable side effects be replaced with MSD, but rather aim to illustrate the potential use and development of MSD for contexts distinct from cancer therapy. Better understanding of the functional modifications caused by MSD *in vivo* may enable appropriate application to other diseases in the future.

6.2 Future directions

The current study provides some evidence that the immune system is functionally altered by MSD therapy and paves the way for continuing investigations in both BMMØ and CTL. Some, but not all, of the possible interactions leading to depressed cytokine production in BMMØ by paclitaxel were assessed in the current study. Future research examining the signalling molecules, transcription

factors and mRNA transcript levels in LPS stimulated, paclitaxel-treated BMMØ may help determine the functional cellular level at which cytokine production is blocked by MSD. Further, visualising cytokine transport and release from BMMØ treated with MSD or DSD could identify how microtubule-dependent transport mechanisms are involved in cytokine production.

Numerous questions regarding the effects of MSD on CTL function *in vitro* and *in vivo* provide potential avenues of future research. Firstly, while murine CTL function is not inhibited in CTL treated with MSD (this thesis & Knox et al., 1993), exactly how lytic granules can traffick to the IS in CTL with an aberrant microtubule network remains unclear. Modified polarisation microscopy has been used to visualise the interaction of lytic granules with microtubules in live cells (Poenie et al., 2004), and this technology may be useful in determining how CTL can deliver lytic granules to TC when treated with MSD *in vitro*. Secondly, it would be of great interest to extend the *in vivo* component of this project and determine if peloruside or other MSD inhibit CTL-mediated cytolysis *in vivo* to the same extent as Taxol. Lastly, the question of how CTL-mediated cytolysis *in vivo* was altered by Taxol warrants further investigation. Flow cytometric assessment of CTL and TC surface phenotype and tissue distribution may provide basic information about how the cells can interact following MSD administration. Further, using visualisation techniques such as multiphoton intravital microscopy as used by Mempel et al. (Mempel et al., 2006) could allow for clear observation of how CTL and TC interact *in vivo* in mice treated with MSD.

6.3 Final Conclusions

This project aimed to understand the immunological implications of MSD therapy with specific regard to immune-mediated exocytosis. The results of this thesis can

be summarised in two statements. First, LPS-activated BMMØ production of TNF-α and NO is likely to be inhibited at a functional cellular level. Second, paclitaxel and peloruside do not alter CTL-mediated cytolysis, degranulation or IFN-γ production *in vitro;* whereas paclitaxel confers an inhibitory effect on CTL-mediated cytolysis *in vivo.* This project is the first to examine the *in vitro* effects of peloruside on interphase CTL processes. It is also the first to show inhibition of CTL-mediated cytolysis *in vivo* by Taxol. The results of this thesis demonstrate that paclitaxel can functionally repress components of the immune system and suggest that patients undergoing MSD therapy may be unable to fight infection long before the anti-mitotic effects of MSD are apparent.

7 References

Abougergi, M.S., Gidner, S.J., Spady, D.K., Miller, B.C., and Thiele, D.L. (2005). Fas and TNFR1, but not cytolytic granule-dependent mechanisms, mediate clearance of murine liver adenoviral infection. Hepatology *41*, 97-105.

Ahern, M.J., Reid, C., Gordon, T.P., McCredie, M., Brooks, P.M., and Jones, M. (1987). Does Colchicine Work? The Results of the First Controlled Study in Acute Gout. Internal Medicine Journal *17*, 301-304.

Akira, S., Takeda, K., and Kaisho, T. (2001). Toll-like receptors: Critical proteins linking innate and acquired immunity. Nature Immunology *2*, 675-680.

Albert, M.L., Sauter, B., and Bhardwaj, N. (1998). Dendritic cells acquire antigen from apoptotic cells and induce class I- restricted CTLs. Nature *392*, 86-89.

Alderton, W.K., Cooper, C.E., and Knowles, R.G. (2001). Nitric oxide synthases: Structure, function and inhibition. Biochemical Journal *357*, 593-615.

Allen, J.N., Herzyk, D.J., and Wewers, M.D. (1991). Colchicine has opposite effects on interleukin-1beta and tumor necrosis factor-alpha production. American Journal of Physiology - Lung Cellular and Molecular Physiology *261*, L315-L321.

Allen, J.N., Liao, Z., Moore, S.A., and Wewers, M.D. (1997a). Changes in Mononuclear Phagocyte Microtubules after Endotoxin Stimulation: II. Changes in Microtubule Composition. American Journal of Respiratory Cell and Molecular Biology *16*, 127-132.

Allen, J.N., Moore, S.A., Liao, Z., and Wewers, M.D. (1997b). Changes in Mononuclear Phagocyte Microtubules after Endotoxin Stimulation: I. Changes in Microtubule Stability. American Journal of Respiratory Cell and Molecular Biology *16*, 119-126.

Allen, J.N., Moore, S.A., and Wewers, M.D. (1993). Taxol enhances but does not induce interleukin-1-beta and tumor necrosis factor-alpha production. Journal of Laboratory and Clinical Medicine *122*, 374-381.

Auron, P.E., Webb, A.C., and Rosenwasser, L.J. (1984). Nucleotide sequence of human monocyte interleukin 1 precursor cDNA. Proceedings of the National Academy of Sciences of the United States of America *81*, 7907-7911.

Bacallao, R., Antony, C., Dotti, C., Karsenti, E., Stelzer, E.H., and Simons, K. (1989). The subcellular organization of Madin-Darby canine kidney cells during the formation of a polarized epithelium. J. Cell Biol. *109*, 2817-2832.

Bachmann, M.F., McKall-Faienza, K., Schmits, R., Bouchard, D., Beach, J., Speiser, D.E., Mak, T.W., and Ohashi, P.S. (1997). Distinct Roles for LFA-1 and CD28 during Activation of Naive T Cells: Adhesion versus Costimulation. Immunity *7*, 549-557.

Baumgartner, R.A., Deramo, V.A., and Beaven, M.A. (1996). Constitutive and Inducible Mechanisms for Synthesis and Release of Cytokines in Immune Cell Lines. Journal of Immunology *157*, 4087-4093.

Beg, A.A., and Baltimore, D. (1996). An essential role for NF-kappa B in preventing TNF-alpha-induced cell death. Science *274*, 782-784.

Betts, M.R., Brenchley, J.M., Price, D.A., De Rosa, S.C., Douek, D.C., Roederer, M., and Koup, R.A. (2003). Sensitive and viable identification of antigen-specific CD8+ T cells by a flow cytometric assay for degranulation. Journal of Immunological Methods *281*, 65-78.

Beyer, C.F., Zhang, N., Hernandez, R., Vitale, D., Lucas, J., Nguyen, T., Discafani, C., Ayral-Kaloustian, S., and Gibbons, J.J. (2008). TTI-237: A novel microtubule-active compound with in vivo antitumor activity. Cancer Research *68*, 2292-2300.

Blocker, A., Griffiths, G., Olivo, J.C., Hyman, A.A., and Severin, F.F. (1998). A role for microtubule dynamics in phagosome movement. J Cell Sci *111*, 303-312.

Blocker, A., Severin, F.F., Burkhardt, J.K., Bingham, J.B., Yu, H., Olivo, J.C., Schroer, T.A., Hyman, A.A., and Griffiths, G. (1997). Molecular requirements for bi-directional movement of phagosomes along microtubules. Journal of Cell Biology *137*, 113-129.

Blott, E.J., Bossi, G., Clark, R., Zvelebil, M., and Griffiths, G.M. (2001). Fas ligand is targeted to secretory lysosomes via a proline-rich domain in its cytoplasmic tail. Journal of Cell Science *114*, 2405-2416.

Bogdan, C., and Ding, A. (1992). Taxol, a microtubule-stabilizing antineoplastic agent, induces expression of tumor necrosis factor alpha and interleukin-1 in macrophages. J Leukoc Biol *52*, 119-121.

Bohm, K.J., Russwurm, S., Ghaleb, N., Reinhart, K., and Unger, E. (1999). Microtubule formation and kinesin-driven microtubule gliding in vitro in the presence of lipopolysaccharide. Cell Biology International *23*, 431-437.

Boissonnas, A., Combadiere, C., Lavergne, E., Maho, M., Blanc, C., Debre, P., and Combadiere, B. (2004). Antigen distribution drives programmed antitumor CD8 cell migration and determines its efficiency. Journal of Immunology *173*, 222-229.

Bossi, G., and Griffiths, G.M. (1999). Degranulation plays an essential part in regulating cell surface expression of Fas ligand in T cells and natural killer cells. Nature Medicine *5*, 90-96.

Bossi, G., and Griffiths, G.M. (2005). CTL secretory lysosomes: Biogenesis and secretion of a harmful organelle. Seminars in Immunology *17*, 87-94.

Bossi, G., Stinchcombe, J.C., Page, L.J., and Griffiths, G.M. (2000). Sorting out the multiple roles of Fas ligand. European Journal of Cell Biology *79*, 539-543.

Breart, B., Lematre, F., Celli, S., and Bousso, P. (2008). Two-photon imaging of intratumoral CD8+ T cell cytotoxic activity during adoptive T cell therapy in mice. Journal of Clinical Investigation *118*, 1390-1397.

Bredt, D.S., Hwang, P.M., Glatt, C.E., Lowenstein, C., Reed, R.R., and Snyder, S.H. (1991). Cloned and expressed nitric oxide synthase structurally resembles cytochrome P-450 reductase. Nature *351*, 714-718.

Bredt, D.S., and Snyder, S.H. (1989). Nitric oxide mediates glutamate-linked enhancement of cGMP levels in the cerebellum. Proceedings of the National Academy of Sciences of the United States of America *86*, 9030-9033.

Bredt, D.S., and Snyder, S.H. (1990). Isolation of nitric oxide synthetase, a calmodulin-requiring enzyme. Proceedings of the National Academy of Sciences of the United States of America *87*, 682-685.

Brown, D.L., Little, J.E., Chaly, N., Schweitzer, I., and Paulinlevasseur, M. (1985). Effects of Taxol on Microtubule Organization on Mouse Splenic Lymphocytes and on Response to Mitogenic Stimulation. European Journal of Cell Biology *37*, 130-139.

Buey, R.M., Barasoain, I., Jackson, E., Meyer, A., Giannakakou, P., Paterson, I., Mooberry, S., Andreu, J.M., and DiÌ• az, J.F. (2005). Microtubule interactions with chemically diverse stabilizing agents: Thermodynamics of binding to the paclitaxel site predicts cytotoxicity. Chemistry and Biology *12*, 1269-1279.

Bunnell, S.C., Kapoor, V., Trible, R.P., Zhang, W., and Samelson, L.E. (2001). Dynamic Actin Polymerization Drives T Cell Receptor-Induced Spreading: A Role for the Signal Transduction Adaptor LAT. Immunity *14*, 315-329.

Byrd-Leifer C.A., Ellen F Block, Kiyoshi Takeda, Shizuo Akira, and Ding., A. (2001). The role of MyD88 and TLR4 in the LPS-mimetic activity of Taxol. European Journal of Immunology *31*, 2448-2457.

Cao, L., Sun, D., Cruz, T., Moscarello, M.A., Ludwin, S.K., and Whitaker, J.N. (2000). Inhibition of experimental allergic encephalomyelitis in the Lewis rat by paclitaxel. Journal of Neuroimmunology *108*, 103-111.

Carlsson, S.R., and Fukuda, M. (1992). The lysosomal membrane glycoprotein lamp-1 is transported to lysosomes by two alternative pathways. Archives of Biochemistry and Biophysics *296*, 630-639.

Carswell, E.A., Old, L.J., Kassel, R.L., Green, S., Fiore, N., and Williamson, B. (1975). An endotoxin-induced serum factor that causes necrosis of tumors. Proceedings of the National Academy of Sciences of the United States of America *72*, 3666-3670.

Chow, J.C., Young, D.W., Golenbock, D.T., Christ, W.J., and Gusovsky, F. (1999). Toll-like receptor-4 mediates lipopolysaccharide-induced signal transduction. J. Biol. Chem. *274*, 10689-10692.

Chu, Y., Wang, L.X., Yang, G., Ross, H.J., Urba, W.J., Prell, R., Jooss, K., Xiong, S., and Hu, H.M. (2006). Efficacy of GM-CSF-producing tumor vaccine after docetaxel chemotherapy in mice bearing established Lewis lung carcinoma. Journal of Immunotherapy *29*, 367-380.

Chuang, L.T. (1994). Alteration of Lymphocyte Microtubule Assembly, Cytotoxicity, and Activation by the Anticancer Drug Taxol (VOL 54, PG 1286, 1994). Cancer Research *54*, 2523-2524.

Chuang, L.T., Lotzova, E., Heath, J., Cook, K.R., Munkarah, A., Morris, M., and Wharton, J.T. (1994). Alteration of Lymphocyte Microtubule Assembly,

Cytotoxicity, and Activation by the Anticancer Drug Taxol. Cancer Research *54*, 1286-1291.

Chung, I.Y., and Benveniste, E.N. (1990). Tumor necrosis factor-alpha production by astrocytes. Induction by lipopolysaccharide, IFN-gamma, and IL-1 beta. J Immunol *144*, 2999-3007.

Coleman, S., Clayton, A., Mason, M.D., Jasani, B., Adams, M., and Tabi, Z. (2005). Recovery of CD8(+) T-cell function during systemic chemotherapy in advanced ovarian cancer. Cancer Research *65*, 7000-7006.

Collart, M.A., Baeuerle, P., and Vassalli, P. (1990). Regulation of tumor necrosis factor alpha transcription in macrophages: Involvement of four kappa B-like motifs and of constitutive and inducible forms of NF-kappa B. Molecular and Cellular Biology *10*, 1498-1506.

Connelly, E., Markman, M., Kennedy, A., Webster, K., Kulp, B., Peterson, G., and Belinson, J. (1996). Paclitaxel delivered as a 3-hr infusion with cisplatin in patients with gynecologic cancers: Unexpected incidence of neurotoxicity. Gynecologic Oncology *62*, 166-168.

Cottalorda, A., Verschelde, C., Marcais, A., Tomkowiak, M., Musette, P., Uematsu, S., Akira, S., Marvel, J., and Bonnefoy-Berard, N. (2006). TLR2 engagement on CD8 T cells lowers the threshold for optimal antigen-induced T cell activation. European Journal of Immunology *36*, 1684-1693.

Crume, K.P., Miller, J.H., and La Flamme, A.C. (2007). Peloruside A, an antimitotic agent, specifically decreases tumor necrosis factor-alpha production by lipopolysaccharide-stimulated murine macrophages. Experimental Biology and Medicine *232*, 607-613.

da Silva Correia, J., Soldau, K., Christen, U., Tobias, P.S., and Ulevitch, R.J. (2001). Lipopolysaccharide Is in Close Proximity to Each of the Proteins in Its Membrane Receptor Complex. TRANSFER FROM CD14 TO TLR4 AND MD-2. J. Biol. Chem. *276*, 21129-21135.

Das, V., Nal, B., Dujeancourt, A., Thoulouze, M.-I., Galli, T., Roux, P., Dautry-Varsat, A., and Alcover, A. (2004). Activation-Induced Polarized Recycling Targets T Cell Antigen Receptors to the Immunological Synapse: Involvement of SNARE Complexes. Immunity *20*, 577-588.

De Boer, R.J., Oprea, M., Antia, R., Murali-Krishna, K., Ahmed, R., and Perelson, A.S. (2001). Recruitment Times, Proliferation, and Apoptosis Rates during the CD8+ T-Cell Response to Lymphocytic Choriomeningitis Virus. J. Virol. *75*, 10663-10669.

Desai, A., and Mitchison, T.J. (1997). Microtubule polymerization dynamics. In Annual Review of Cell and Developmental Biology, pp. 83-117.

Ding, A., Chen, B., Fuortes, M., and Blum, E. (1996). Association of mitogen-activated protein kinases with microtubules in mouse macrophages. J. Exp. Med. *183*, 1899-1904.

Ding, A., Sanchez, E., Tancinco, M., and Nathan, C. (1992). Interactions of bacterial lipopolysaccharide with microtubule proteins. Journal of Immunology *148*, 2853-2858.

Ding, A.H., Nathan, C.F., and Stuehr, D.J. (1988). Release of reactive nitrogen intermediates and reactive oxygen intermediates from mouse peritoneal macrophages: Comparison of activating cytokines and evidence for independent production. Journal of Immunology *141*, 2407-2412.

Ding, A.H., Porteu, F., Sanchez, E., and Nathan, C.F. (1990a). Downregulation of tumor necrosis factor receptors on macrophages and endothelial cells by microtubule depolymerizing agents. J. Exp. Med. *171*, 715-727.

Ding, A.H., Porteu, F., Sanchez, E., and Nathan, C.F. (1990b). Shared actions of endotoxin and taxol on TNF receptors and TNF release. Science *248*, 370-372.

Drechsel, D.N., Hyman, A.A., Cobb, M.H., and Kirschner, M.W. (1992). Modulation of the dynamic instability of tubulin assembly by the microtubule-associated protein tau. Molecular Biology of the Cell *3*, 1141-1154.

Dvorak, Z., Ulrichova, J., Pichard-Garcia, L., Modriansky, M., and Maurel, P. (2002). Comparative effect of colchicine and colchiceine on cytotoxicity and CYP gene expression in primary human hepatocytes. Toxicology in Vitro *16*, 219-227.

Emens, L.A., Machiels, J.P., Reilly, R.T., and Jaffee, E.M. (2001). Chemotherapy: Friend or foe to cancer vaccines? Current Opinion in Molecular Therapeutics *3*, 77-84.

Ezratty, E.J., Partridge, M.A., and Gundersen, G.G. (2005). Microtubule-induced focal adhesion disassembly is mediated by dynamin and focal adhesion kinase. Nature Cell Biology *7*, 581-590.

Faroudi, M., Utzny, C., Salio, M., Cerundolo, V., Guiraud, M., Muller, S., and Valitutti, S. (2003). Lytic versus stimulatory synapse in cytotoxic T lymphocyte/target cell interaction: Manifestation of a dual activation threshold. Proceedings of the National Academy of Sciences of the United States of America *100*, 14145-14150.

Feng, Y.H., Zou, J.P., and Li, X.Y. (2002). Effects of resveratrol and ethanol on production of pro-inflammatory factors from endotoxin activated murine macrophages. Acta Pharmacologica Sinica *23*, 1002-1006.

Fernandez-Lizarbe, S., Pascual, M., Gascon, M.S., Blanco, A., and Guerri, C. (2008). Lipid rafts regulate ethanol-induced activation of TLR4 signaling in murine macrophages. Molecular Immunology *45*, 2007-2016.

Fiorentino, D.F., Zlotnik, A., Mosmann, T.R., Howard, M., and Ogarra, A. (1991). IL-10 Inhibits Cytokine Production by Activated Macrophages. Journal of Immunology *147*, 3815-3822.

Fujihara, M., Ito, N., Pace, J.L., Watanabe, Y., Russell, S.W., and Suzuki, T. (1994). Role of endogenous interferon-beta in lipopolysaccharide-triggered activation of the inducible nitric-oxide synthase gene in a mouse macrophage cell line, J774. J. Biol. Chem. *269*, 12773-12778.

Gaitanos, T.N., Buey, R.M., Fernando Diaz, J., Northcote, P.T., Teesdale-Spittle, P., Andreu, J.M., and Miller, J.H. (2004). Peloruside A does not bind to the taxoid site on beta-tubulin and retains its activity in multidrug-resistant cell lines. Cancer Research *64*, 5063-5067.

Garnett, C.T., Schlom, J., and Hodge, J.W. (2008). Combination of docetaxel and recombinant vaccine enhances T-cell responses and antitumor activity: Effects of docetaxel on immune enhancement. Clinical Cancer Research *14*, 3536-3544.

Geginat, J., Lanzavecchia, A., and Sallusto, F. (2003). Proliferation and differentiation potential of human CD8+ memory T-cell subsets in response to antigen or homeostatic cytokines. Blood *101*, 4260-4266.

Geiger, B., Rosen, D., and Berke, G. (1982). Spatial relationships of microtubule-organizing centers and the contact area of cytotoxic T lymphocytes and target cells. Journal of Cell Biology *95*, 137-143.

Gelderblom, H., Verweij, J., Nooter, K., and Sparreboom, A. (2001). Cremophor EL: the drawbacks and advantages of vehicle selection for drug formulation. European Journal of Cancer *37*, 1590-1598.

Geller, D.A., Nussler, A.K., Disilvio, M., Lowenstein, C.J., Shapiro, R.A., Wang, S.C., Simmons, R.L., and Billiar, T.R. (1993). Cytokines, Endotoxin, and Glucocorticoids Regulate the Expression of Inducible Nitric-Oxide Synthase in Hepatocytes. Proceedings of the National Academy of Sciences of the United States of America *90*, 522-526.

Gibbons, I.R. (1981). Cilia and flagella of eukaryotes. J. Cell Biol. *91*, 107s-124.

Gifford, G.E., and Lohmann-Matthes, M.L. (1987). Gamma interferon priming of mouse and human macrophages for induction of tumor necrosis factor production by bacterial lipopolysaccharide. Journal of the National Cancer Institute *78*, 121-124.

Goldfinger, S.E., Howell, R.R., and Seegmiller, J.E. (1965). Suppression of metabolic accompaniments of phagocytosis by colchicine. Arthritis & Rheumatism *8*, 1112-1122.

Goldstein, L.J., Galski, H., Fojo, A., Willingham, M., Lai, S.L., Gazdar, A., Pirker, R., Green, A., Crist, W., Brodeur, G.M.*, et al.* (1989). Expression of a multidrug resistance gene in human cancers. Journal of the National Cancer Institute *81*, 116-124.

Grakoui, A., Shannon, K.B., Sumen, C., Davis, M.M., Shaw, A.S., Allen, P.M., and Dustin, M.L. (1999). The Immunological Synapse: A Molecular Machine Controlling T Cell Activation. Science *285*, 221-227.

Hamann, D., Baars, P.A., Rep, M.H.G., Hooibrink, B., Kerkhof-Garde, S.R., Klein, M.R., and vanLier, R.A.W. (1997). Phenotypic and Functional Separation of Memory and Effector Human CD8+ T Cells. J. Exp. Med. *186*, 1407-1418.

Hamel, E., Day, B.W., Miller, J.H., Jung, M.K., Northcote, P.T., Ghosh, A.K., Curran, D.P., Cushman, M., Nicolaou, K.C., Paterson, I., and Sorensen, E.J. (2006). Synergistic effects of peloruside A and laulimalide with taxoid site drugs,

but not with each other, on tubulin assembly. Molecular Pharmacology *70*, 1555-1564.

Havell, E.A. (1989). Evidence that tumor necrosis factor has an important role in antibacterial resistance. Journal of Immunology *143*, 2894-2899.

He, J.-S., and Ostergaard, H.L. (2007). CTLs Contain and Use Intracellular Stores of FasL Distinct from Cytolytic Granules. J Immunol *179*, 2339-2348.

Hermans, I.F., Silk, J.D., Yang, J., Palmowski, M.J., Gileadi, U., McCarthy, C., Salio, M., Ronchese, F., and Cerundolo, V. (2004). The VITAL assay: A versatile fluorometric technique for assessing CTL- and NKT-mediated cytotoxicity against multiple targets in vitro and in vivo. Journal of Immunological Methods *285*, 25-40.

Hirohashi, N., and Morrison, D.C. (1996). Low-dose lipopolysaccharide (LPS) pretreatment of mouse macrophages modulates LPS-dependent interleukin-6 production in vitro. Infect. Immun. *64*, 1011-1015.

Hirokawa, N. (1998). Kinesin and Dynein Superfamily Proteins and the Mechanism of Organelle Transport. Science *279*, 519-526.

Hirschfeld, M., Ma, Y., Weis, J.H., Vogel, S.N., and Weis, J.J. (2000). Cutting edge: Repurification of lipopolysaccharide eliminates signaling through both human and murine toll-like receptor 2. Journal of Immunology *165*, 618-622.

Hogquist, K.A., Jameson, S.C., Heath, W.R., Howard, J.L., Bevan, M.J., and Carbone, F.R. (1994). T cell receptor antagonist peptides induce positive selection. Cell *76*, 17-27.

Hohlbaum, A.M., Moe, S., and Marshak-Rothstein, A. (2000). Opposing Effects of Transmembrane and Soluble Fas Ligand Expression on Inflammation and Tumor Cell Survival. J. Exp. Med. *191*, 1209-1220.

Holmes, F.A., Walters, R.S., Theriault, R.L., Forman, A.D., Newton, L.K., Raber, M.N., Buzdar, A.U., Frye, D.K., and Hortobagyi, G.N. (1991). Phase II trial of taxol, an active drug in the treatment of metastatic breast cancer. Journal of the National Cancer Institute *83*, 1797-1805.

Hood, K.A., Backstrom, B.T., West, L.M., Northcote, P.T., Berridge, M.V., and Miller, J.H. (2001). The novel cytotoxic sponge metabolite peloruside A, structurally similar to bryostatin-1, has unique bioactivity independent of protein kinase C. Anti-Cancer Drug Design *16*, 155-166.

Hood, K.A., West, L.M., Rouwe, B., Northcote, P.T., Berridge, M.V., Wakefield, S.J., and Miller, J.H. (2002). Peloruside A, a novel antimitotic agent with paclitaxel-like microtubule-stabilizing activity. Cancer Research *62*, 3356-3360.

Hoshino, K., Takeuchi, O., Kawai, T., Sanjo, H., Ogawa, T., Takeda, Y., Takeda, K., and Akira, S. (1999). Cutting Edge: Toll-Like Receptor 4 (TLR4)-Deficient Mice Are Hyporesponsive to Lipopolysaccharide: Evidence for TLR4 as the Lps Gene Product. J Immunol *162*, 3749-3752.

Huzil, J.T., Chik, J.K., Slysz, G.W., Freedman, H., Tuszynski, J., Taylor, R.E., Sackett, D.L., and Schriemer, D.C. (2008). A Unique Mode of Microtubule Stabilization Induced by Peloruside A. Journal of Molecular Biology *378*, 1016-1030.

Hwang, L.N., Yu, Z., Palmer, D.C., and Restifo, N.P. (2006). The in vivo expansion rate of properly stimulated transferred CD8 + T cells exceeds that of an aggressively growing mouse tumor. Cancer Research *66*, 1132-1138.

Innocenti, F., Danesi, R., Di Paolo, A., Agen, C., Nardini, D., Bocci, G., and Del Tacca, M. (1995). Plasma and tissue disposition of paclitaxel (taxol) after intraperitoneal administration in mice. Drug Metab Dispos *23*, 713-717.

Isowa, N., Xavier, A.M., Dziak, E., Opas, M., McRitchie, D.I., Slutsky, A.S., Keshavjee, S.H., and Liu, M. (1999). LPS-induced depolymerization of cytoskeleton and its role in TNF-Î± production by rat pneumocytes. American Journal of Physiology - Lung Cellular and Molecular Physiology *277*, L606-L615.

Ito, Y., Nishiyama, Y., and Shimokata, K. (1976). The effects of cytochalasin and colchicine on interferon production. Journal of General Virology *33*, 1-5.

Itoh, N., and Nagata, S. (1993). A novel protein domain required for apoptosis. Mutational analysis of human Fas antigen. J. Biol. Chem. *268*, 10932-10937.

Iura, A., Katsumata, N., Kouno, T., Shimizu, C., Ando, M., and Fujiwara, Y. (2009). Outpatient management of low-risk febrile patients on paclitaxel and carboplatin for ovarian cancer
International Journal of Gynecology & Obstetrics *Article in press*.

Janes, P.W., Ley, S.C., and Magee, A.I. (1999). Aggregation of Lipid Rafts Accompanies Signaling Via the T Cell Antigen Receptor. J. Cell Biol. *147*, 447-461.

Janes, P.W., Ley, S.C., Magee, A.I., and Kabouridis, P.S. (2000). The role of lipid rafts in T cell antigen receptor (TCR) signalling. Seminars in Immunology *12*, 23-34.

Janeway, C.A., Travers, P., Walport, M., and Shlomchik, M. (2001). Immunobiology: The Immune System in Health And Disease, 5 edn (Garland Publishing).

Janssens, S.P., Shimouchi, A., Quertermous, T., Bloch, D.B., and Bloch, K.D. (1992). Cloning and expression of a cDNA encoding human endothelium-derived relaxing factor/nitric oxide synthase. J. Biol. Chem. *267*, 14519-14522.

Joo, H.G. (2003). Altered maturation of dendritic cells by taxol, an anticancer drug. Journal of veterinary science (Suwon-si, Korea) *4*, 229-234.

Jordan, M.A., Toso, R.J., Thrower, D., and Wilson, L. (1993). Mechanism of mitotic block and inhibition of cell proliferation by taxol at low concentrations. Proceedings of the National Academy of Sciences of the United States of America *90*, 9552-9556.

Jordan, M.A., and Wilson, L. (2004). Microtubules as a target for anticancer drugs. Nature Reviews Cancer *4*, 253-265.

Kagi, D., Ledermann, B., Burki, K., Seiler, P., Odermatt, B., Olsen, K.J., Podack, E.R., Zinkernagel, R.M., and Hengartner, H. (1994). Cytotoxicity mediated by T cells and natural killer cells is greatly impaired in perforin-deficient mice. Nature *369*, 31-37.

Kagi, D., Seiler, P., Pavlovic, J., Ledermann, B., Burki, K., Zinkernagel, R.M., and Hengartner, H. (1995). The roles of perforin- and Fas-dependent cytotoxicity in protection against cytopathic and noncytopathic viruses. European Journal of Immunology *25*, 3256-3262.

Kastenbauer, S., and Ziegler-Heitbrock, H.W.L. (1999). NF-kappa B1 (p50) Is Upregulated in Lipopolysaccharide Tolerance and Can Block Tumor Necrosis Factor Gene Expression. Infect. Immun. *67*, 1553-1559.

Kaverina, I., Rottner, K., and Small, J.V. (1998). Targeting, Capture, and Stabilization of Microtubules at Early Focal Adhesions. J. Cell Biol. *142*, 181-190.

Kawai, T., Adachi, O., Ogawa, T., Takeda, K., and Akira, S. (1999). Unresponsiveness of MyD88-deficient mice to endotoxin. Immunity *11*, 115-122.

Kawasaki, K., Akashi, S., Shimazu, R., Yoshida, T., Miyake, K., and Nishijima, M. (2000). Mouse toll-like receptor 4·MD-2 complex mediates lipopolysaccharide-mimetic signal transduction by Taxol. J. Biol. Chem. *275*, 2251-2254.

Kawasaki, K., Gomi, K., and Nishijima, M. (2001). Cutting edge: Gln22 of mouse MD-2 is essential for species-specific lipopolysaccharide mimetic action of Taxol1. Journal of Immunology *166*, 11-14.

Kelly, K., Crowley, J., Bunn P.A, Jr., Presant, C.A., Grevstad, P.K., Moinpour, C.M., Ramsey, S.D., Wozniak, A.J., Weiss, G.R., Moore, D.F.*, et al.* (2001). Randomized phase III trial of paclitaxel plus carboplatin versus vinorelbine plus cisplatin in the treatment of patients with advanced non-small-cell lung cancer: A Southwest Oncology Group trial. Journal of Clinical Oncology *19*, 3210-3218.

Kikkawa, I., Saito, S., Tominaga, K., Hoshino, Y., Ooi, Y., and Nakano, M. (1998). Lipopolysaccharide (LPS) stimulates the production of tumor necrosis factor (TNF)-alpha and expression of inducible nitric oxide synthase (iNOS) by osteoclasts (OCL) in murine bone marrow cell culture. Microbiology and Immunology *42*, 591-598.

Kincy-Cain, T., and Bost, K.L. (1997). Substance P-induced IL-12 production by murine macrophages. J Immunol *158*, 2334-2339.

Kirikae, T., Kirikae, F., Oghiso, Y., and Nakano, M. (1996). Microtubule-disrupting agents inhibit nitric oxide production in murine peritoneal macrophages stimulated with lipopolysaccharide or paclitaxel (Taxol). Infect. Immun. *64*, 3379-3384.

Klecker, R.W., Jamis-Dow, C.A., Egorin, M.J., Erkmen, K., Parker, R.J., Stevens, R., and Collins, J.M. (1994). Effect of cimetidine, probenecid, and ketoconazole on the distribution, biliary secretion, and metabolism of [^{3}H]taxol in the Sprague-Dawley rat. Drug Metabolism and Disposition *22*, 254-258.

Knox, J.D., Mitchel, R.E.J., and Brown, D.L. (1993). Effects of taxol and taxol/hyperthermia treatments on the functional polarization of cytotoxic T lymphocytes. Cell Motility and the Cytoskeleton *24*, 129-138.

Kolls, J.K., Xie, J., Lei, D., Greenberg, S., Summer, W.R., and Nelson, S. (1995). Differential effects of in vivo ethanol on LPS-induced TNF and nitric oxide production in the lung. American Journal of Physiology - Lung Cellular and Molecular Physiology *268*, L991-L998.

Konigsberg, P.J., and Podack, E.R. (1986). DNA Damage of Target-Cells by Cytolytic T-Cell Granules. Journal of Cellular Biochemistry, 85-85.

Kuhn, J.R., and Poenie, M. (2002). Dynamic polarization of the microtubule cytoskeleton during CTL-mediated killing. Immunity *16*, 111-121.

Kuncl, R.W., Bilak, M.M., Craig, S.W., and Adams, R. (2003). Exocytotic "constipation" is a mechanism of tubulin/lysosomal interaction in colchicine myopathy. Experimental Cell Research *285*, 196-207.

Kupfer, A., and Dennert, G. (1984). Reorientation of the microtubule-organizing center and the Golgi apparatus in cloned cytotoxic lymphocytes triggered by binding to lysable target cells. Journal of Immunology *133*, 2762-2766.

Kupfer, A., Dennert, G., and Singer, S.J. (1983). Polarization of the Golgi apparatus and the microtubule-organizing center within cloned natural killer cells bound to their targets. Proceedings of the National Academy of Sciences of the United States of America *80*, 7224-7228.

Kupfer, A., Dennert, G., and Singer, S.J. (1985). The reorientation of the Golgi apparatus and the microtubule-organizing center in the cytotoxic effector cell is a prerequisite in the lysis of bound target cells. Journal of Molecular and Cellular Immunology *2*, 37-49.

Lee, M., and Jeon, Y.J. (2001). Paclitaxel-induced immune suppression is associated with NF-kappa-B activation via conventional PKC isotypes in lipopolysaccharide-stimulated 70Z/3 pre-B lymphocyte tumor cells. Molecular Pharmacology *59*, 248-253.

Lee, M., Yea, S.S., and Jeon, Y.J. (2000). Paclitaxel causes mouse splenic lymphocytes to a state hyporesponsive to lipopolysaccharide stimulation. International Journal of Immunopharmacology *22*, 615-621.

Li, H., DeRosier, D.J., Nicholson, W.V., Nogales, E., and Downing, K.H. (2002). Microtubule Structure at 8 Angstrom Resolution. Structure *10*, 1317-1328.

Li, Z., Davis, G.S., Mohr, C., Nain, M., and Gemsa, D. (1996). Inhibition of LPS-induced tumor necrosis factor-alpha production by colchicine and other microtubule disrupting drugs. Immunobiology *195*, 624-639.

Liu, Z.G., Hsu, H., Goeddel, D.V., and Karin, M. (1996). Dissection of TNF receptor 1 effector functions: JNK activation is not linked to apoptosis while NF-kB activation prevents cell death. Cell *87*, 565-576.

Löwe, J., Li, H., Downing, K.H., and Nogales, E. (2001). Refined structure of [alpha][beta]-tubulin at 3.5 Å resolution. Journal of Molecular Biology *313*, 1045-1057.

Lowenstein, C.J., Glatt, C.S., Bredt, D.S., and Snyder, S.H. (1992). Cloned and expressed macrophage nitric oxide synthase contrasts with the brain enzyme. Proceedings of the National Academy of Sciences of the United States of America *89*, 6711-6715.

Lowin, B., Hahne, M., Mattmann, C., and Tschopp, J. (1994). Cytolytic T-cell cytotoxicity is mediated through perforin and Fas lytic pathways. Nature *370*, 650-652.

Luescher, I.F., Vivier, E., Layer, A., Mahion, J., Godeau, F., Malissen, B., and Romero, P. (1995). CD8 modulation of T-cell antigen receptor-ligand interactions on living cytotoxic T lymphocytes. Nature *373*, 353-356.

Ma, W., Gee, K., Lim, W., Chambers, K., Angel, J.B., Kozlowski, M., and Kumar, A. (2004). Dexamethasone Inhibits IL-12p40 Production in Lipopolysaccharide-Stimulated Human Monocytic Cells by Down-Regulating the Activity of c-Jun N-Terminal Kinase, the Activation Protein-1, and NF-kappa-B Transcription Factors. J Immunol *172*, 318-330.

Ma, X., Chow, J.M., Gri, G., Carra, G., Gerosa, F., Wolf, S.F., Dzialo, R., and Trinchieri, G. (1996). The interleukin 12 p40 gene promoter is primed by interferon gamma in monocytic cells. J. Exp. Med. *183*, 147-157.

Macdermott, R.P., Schmidt, R.E., Caulfield, J.P., Hein, A., Bartley, G.T., Ritz, J., Schlossman, S.F., Austen, K.F., and Stevens, R.L. (1986). Proteoglycans in Cell-Mediated Cytotoxicity - Identification, Localization, and Exocytosis of a Chondroitin Sulfate Proteoglycan From Human Cloned Natural-Killer-Cells During Target-Cell lysis. Journal of Cellular Biochemistry, 88-88.

Machiels, J.P.H., Todd Reilly, R., Emens, L.A., Ercolini, A.M., Lei, R.Y., Weintraub, D., Okoye, F.I., and Jaffee, E.M. (2001). Cyclophosphamide, doxorubicin, and paclitaxel enhance the antitumor immune response of granulocyte/macrophage-colony stimulating factor-secreting whole-cell vaccines in HER-2/neu tolerized mice. Cancer Research *61*, 3689-3697.

MacMicking, J., Xie, Q.W., and Nathan, C. (1997). Nitric oxide and macrophage function. In Annual Review of Immunology, pp. 323-350.

Manderson, A.P., Kay, J.G., Hammond, L.A., Brown, D.L., and Stow, J.L. (2007). Subcompartments of the macrophage recycling endosome direct the differential secretion of IL-6 and TNF-alpha. Journal of Cell Biology *178*, 57-69.

Manthey, C.L., Brandes, M.E., Perera, P.Y., and Vogel, S.N. (1992). Taxol increases steady-state levels of lipopolysaccharide-inducible genes and protein-tyrosine phosphorylation in murine macrophages. Journal of Immunology *149*, 2459-2465.

Manthey, C.L., Perera, P.Y., Salkowski, C.A., and Vogel, S.N. (1994). Taxol provides a second signal for murine macrophage tumoricidal activity. Journal of Immunology *152*, 825-831.

Manthey, C.L., Qureshi, N., Stutz, P.L., and Vogel, S.N. (1993). Lipopolysaccharide antagonists block taxol-induced signaling in murine macrophages. Journal of Experimental Medicine *178*, 695-702.

Marikovsky, M., Ziv, V., Nevo, N., Harris-Cerruti, C., and Mahler, O. (2003). Cu/Zn Superoxide Dismutase Plays Important Role in Immune Response. J Immunol *170*, 2993-3001.

Markasz, L., Skribek, H., Uhlin, M., Otvos, R., Flaberg, E., Eksborg, S., Olah, E., Stuber, G., and Szekely, L. (2008). Effect of frequently used chemotherapeutic drugs on cytotoxic activity of human cytotoxic T-lymphocytes. Journal of Immunotherapy *31*, 283-293.

Markasz, L., Stuber, G., Vanherberghen, B., Flaberg, E., Olah, E., Carbone, E., Eksborg, S., Klein, E., Skribek, H., and Szekely, L. (2007). Effect of frequently used chemotherapeutic drugs on the cytotoxic activity of human natural killer cells. Molecular Cancer Therapeutics *6*, 644-654.

Marsden, P.A., Schappert, K.T., Chen, H.S., Flowers, M., Sundell, C.L., Wilcox, J.N., Lamas, S., and Michel, T. (1992). Molecular cloning and characterization of human endothelial nitric oxide synthase. FEBS Letters *307*, 287-293.

Masopust, D., Vezys, V., Marzo, A.L., and Lefrancois, L. (2001). Preferential localization of effector memory cells in nonlymphoid tissue. Science *291*, 2413-2417.

Matzinger, P. (1991). The JAM test. A simple assay for DNA fragmentation and cell death. Journal of Immunological Methods *145*, 185-192.

Mempel, T.R., Pittet, M.J., Khazaie, K., Weninger, W., Weissleder, R., von Boehmer, H., and von Andrian, U.H. (2006). Regulatory T Cells Reversibly Suppress Cytotoxic T Cell Function Independent of Effector Differentiation. Immunity *25*, 129-141.

Menendez, M., Rivas, G., Diaz, J.F., and Andreu, J.M. (1998). Control of the Structural Stability of the Tubulin Dimer by One High Affinity Bound Magnesium Ion at Nucleotide N-site. J. Biol. Chem. *273*, 167-176.

Miller, A.R., Suttles, J., and Stout, R.D. (1996). Cytokine priming reduces dependence on TNF-R2 for TNF-alpha-mediated induction of macrophage nitric oxide generation. Journal of Interferon and Cytokine Research *16*, 1055-1063.

Miller, J.H., Rouwe, B., Gaitanos, T.N., Hood, K.A., Crume, K.P., Backstrom, B.T., La Flamme, A.C., Berridge, M.V., and Northcote, P.T. (2004). Peloruside A enhances apoptosis in H-ras-transformed cells and is cytotoxic to proliferating T cells. Apoptosis *9*, 785-796.

Ming, W.J., Bersani, L., and Mantovani, A. (1987). Tumor necrosis factor is chemotactic for monocytes and polymorphonuclear leukocytes. J Immunol *138*, 1469-1474.

Mirzapoiazova, T., Kolosova, I.A., Moreno, L., Sammani, S., Garcia, J.G.N., and Verin, A.D. (2007). Suppression of endotoxin-induced inflammation by taxol. European Respiratory Journal *30*, 429-435.

Monks, C.R.F., Freiberg, B.A., Kupfer, H., Sciaky, N., and Kupfer, A. (1998). Three-dimensional segregation of supramolecular activation clusters in T cells. Nature *395*, 82-86.

Mooberry, S.L., Tien, G., Hernandez, A.H., Plubrukarn, A., and Davidson, B.S. (1999). Laulimalide and isolaulimalide, new paclitaxel-like microtubule- stabilizing agents. Cancer Research *59*, 653-660.

Munger, W.E., Reynolds, C.W., and Henkart, P.A. (1986). DNAase Activity in Cytoplasmic Granules of Cytotoxic Lymphocytes (LGL and CTL). Journal of Cellular Biochemistry, 88-88.

Murray, R.Z., Kay, J.G., Sangermani, D.G., and Stow, J.L. (2005). Cell biology: A role for the phagosome in cytokine secretion. Science *310*, 1492-1495.

Nagata, S. (1997). Apoptosis by death factor. Cell *88*, 355-365.

Nagata, S., and Golstein, P. (1995). The Fas death factor. Science *267*, 1449-1456.

Nakano, M., Tominaga, K., Saito, S., Kirikae, F., Lin, S.N., Fumero, C.L., Ojima, I., and Kirikae, T. (1999). Lipopolysaccharide- and paclitaxel (Taxol)-induced tolerance in murine peritoneal macrophages. Journal of Endotoxin Research *5*, 102-106.

Newman, M.J., Rodarte, J.C., Benbatoul, K.D., Romano, S.J., Zhang, C., Krane, S., Moran, E.J., Uyeda, R.T., Dixon, R., Guns, E.S., and Mayer, L.D. (2000). Discovery and Characterization of OC144-093, a Novel Inhibitor of P-Glycoprotein-mediated Multidrug Resistance. Cancer Res *60*, 2964-2972.

Nogales, E., Whittaker, M., Milligan, R.A., and Downing, K.H. (1999). High-resolution model of the microtubule. Cell *96*, 79-88.

Nogales, E., Wolf, S.G., and Downing, K.H. (1998). Structure of the alpha-beta tubulin dimer by electron crystallography. Nature *391*, 199-203.

Nole, F., Crivellari, D., Mattioli, R., Pinotti, G., Foa, P., Verri, E., Fougeray, R., Brandely, M., and Goldhirsch, A. (2009). Phase II study of an all-oral combination of vinorelbine with capecitabine in patients with metastatic breast cancer. Cancer Chemotherapy and Pharmacology, 1-8.

O'Brien Jr, J.M., Wewers, M.D., Moore, S.A., and Allen, J.N. (1995). Taxol and colchicine increase LPS-induced pro-IL-1beta production, but do not increase IL-1beta secretion: A role for microtubules in the regulation of IL-1beta production. Journal of Immunology *154*, 4113-4122.

Oehen, S., and Brduscha-Riem, K. (1998). Differentiation of naive CTL to effector and memory CTL: Correlation of effector function with phenotype and cell division. Journal of Immunology *161*, 5338-5346.

Parekh, H., Wiesen, K., and Simpkins, H. (1997). Acquisition of taxol resistance via P-glycoprotein- and non-P-glycoprotein-mediated mechanisms in human ovarian carcinoma cells. Biochemical Pharmacology *53*, 461-470.

Peachman, K.K., Rao, M., Palmer, D.R., Zidanic, M., Sun, W., Alving, C.R., and Rothwell, S.W. (2004). Functional microtubules are required for antigen processing by macrophages and dendritic cells. Immunology Letters *95*, 13-24.

Penson, R.T., Kronish, K., Duan, Z., Feller, A.J., Stark, P., Cook, S.E., Duska, L.R., Fuller, A.F., Goodman, A.K., Nikrui, N.*, et al.* (2000). Cytokines IL-1β, IL-2, IL-6, IL-8, MCP-1, GM-CSF and TNF-alpha in patients with epithelial ovarian cancer and their relationship to treatment with paclitaxel. International Journal of Gynecological Cancer *10*, 33.

Perera, P.Y., Mayadas, T.N., Takeuchi, S., Akira, O., Zaks-Zilberman, M., Goyert, S.M., and Vogel, S.N. (2001). CD11b/CD18 acts in concert with CD14 and Toll-like receptor (TLR) 4 to elicit full lipopolysaccharide and Taxol-inducible gene expression. Journal of Immunology *166*, 574-581.

Peters, P.J., Borst, J., Oorschot, V., Fukuda, M., Krahenbuhl, O., Tschopp, J., Slot, J.W., and Geuze, H.J. (1991). Cytotoxic T lymphocyte granules are secretory

lysosomes, containing both perforin and granzymes. J. Exp. Med. *173*, 1099-1109.

Piel, M., Meyer, P., Khodjakov, A., Rieder, C.L., and Bornens, M. (2000). The respective contributions of the mother and daughter centrioles to centrosome activity and behavior in vertebrate cells. Journal of Cell Biology *149*, 317-329.

Plaut, M., Lichtenstein, L.M., and Henney, C.S. (1973). Studies on the Mechanism of Lymphocyte-Mediated Cytolysis: III. The Role of Microfilaments and Microtubules. J Immunol *110*, 771-780.

Podack, E.R., and Dennert, G. (1983). Assembly of 2 Types of Tubules with Putative Cytolytic Function by Cloned Natural-Killer Cells. Nature *302*, 442-445.

Podack, E.R., and Konigsberg, P.J. (1984). Cytolytic T cell granules. Isolation, structural, biochemical, and functional characterization. J. Exp. Med. *160*, 695-710.

Poenie, M., Kuhn, J., and Combs, J. (2004). Real-time visualization of the cytoskeleton and effector functions in T cells. Current Opinion in Immunology *16*, 428-438.

Presley, J.F., Cole, N.B., Schroer, T.A., Hirschberg, K., Zaal, K.J.M., and Lippincott-Schwartz, J. (1997). ER-to-Golgi transport visualized in living cells. Nature *389*, 81-85.

Radoja, S., Saio, M., Schaer, D., Koneru, M., Vukmanovic, S., and Frey, A.B. (2001). CD8+ tumor-infiltrating T cells are deficient in perforin-mediated cytolytic activity due to defective microtubule-organizing center mobilization and lytic granule exocytosis. Journal of Immunology *167*, 5042-5051.

Rammes, A., Roth, J., Goebeler, M., Klempt, M., Hartmann, M., and Sorg, C. (1997). Myeloid-related Protein (MRP) 8 and MRP14, Calcium-binding Proteins of the S100 Family, Are Secreted by Activated Monocytes via a Novel, Tubulin-dependent Pathway. J. Biol. Chem. *272*, 9496-9502.

Rao, P., Falk, L.A., Dougherty, S.F., Sawada, T., and Pluznik, D.H. (1997). Colchicine Down-Regulates Lipopolysaccharide-Induced Granulocyte-Macrophage Colony-Stimulating Factor Production in Murine Macrophages. Journal of Immunology *159*, 3531-3539.

Resman, N., Gradisar, H., Vasl, J., Keber, M.M., Pristovsek, P., and Jerala, R. (2008). Taxanes inhibit human TLR4 signaling by binding to MD-2. FEBS Letters *582*, 3929-3934.

Rothe, J., Lesslauer, W., Lotscher, H., Lang, Y., Koebel, P., Kontgen, F., Althage, A., Zinkernagel, R., Steinmetz, M., and Bluethmann, H. (1993). Mice lacking the tumour necrosis factor receptor 1 are resistant to TNF-mediated toxicity but highly susceptible to infection by Listeria monocytogenes. Nature *364*, 798-802.

Rothe, M., Wong, S.C., Henzel, W.J., and Goeddel, D.V. (1994). A novel family of putative signal transducers associated with the cytoplasmic domain of the 75 kDa tumor necrosis factor receptor. Cell *78*, 681-692.

Rousseau, S., Papoutsopoulou, M., Symons, A., Cook, D., Lucocq, J.M., Prescott, A.R., O'Garra, A., Ley, S.C., and Cohen, P. (2008). TPL2-mediated activation of

ERK1 and ERK2 regulates the processing of pre-TNF-alpha in LPS-stimulated macrophages. J Cell Sci *121*, 149-154.

Roy, C., Chaly, N., and Brown, D.L. (1988). Taxol-induced reorganization of the microtubule system in murine splenic lymphocytes inhibits response to allogeneic cells but not to concanavalin A. Biochemistry and Cell Biology *66*, 389-395.

Sander, B., Andersson, J., and Andersson, U. (1991). Assessment of Cytokines by Immunofluorescence and the Paraformaldehyde-Saponin Procedure. Immunological Reviews *119*, 65-93.

Santos, J.L., Andrade, A.A., Dias, A.A.M., Bonjardim, C.A., Reis, L.F.L., Teixeira, S.M.R., and Horta, M.F. (2006). Differential sensitivity of C57BL/6 (M-1) and BALB/c (M-2) macrophages to the stimuli of IFN-gamma/LPS for the production of NO: Correlation with iNOS mRNA and protein expression. Journal of Interferon and Cytokine Research *26*, 682-688.

Schartner, J.M., Hagar, A.R., Van Handel, M., Zhang, L., Nadkarni, N., and Badie, B. (2005). Impaired capacity for upregulation of MHC class II in tumor-associated microglia. GLIA *51*, 279-285.

Schiff, P.B., Fant, J., and Horwitz, S.B. (1979). Promotion of microtubule assembly in vitro by taxol. Nature *277*, 665-667.

Seino, K.I., Iwabuchi, K., Kayagaki, N., Miyata, R., Nagaoka, I., Matsuzawa, A., Fukao, K., Yagita, H., and Okumura, K. (1998). Cutting edge: Chemotactic activity of soluble Fas ligand against phagocytes. Journal of Immunology *161*, 4484-4488.

Shi, L., Kishore, R., McMullen, M.R., and Nagy, L.E. (2002). Chronic ethanol increases lipopolysaccharide-stimulated Egr-1 expression in RAW 264.7 macrophages. Contribution to enhanced tumor necrosis factor alpha production. J. Biol. Chem. *277*, 14777-14785.

Shimizu, J., Yamazaki, S., and Sakaguchi, S. (1999). Induction of Tumor Immunity by Removing CD25+CD4+ T Cells: A Common Basis Between Tumor Immunity and Autoimmunity. J Immunol *163*, 5211-5218.

Shnyra, A., Brewington, R., Alipio, A., Amura, C., and Morrison, D.C. (1998). Reprogramming of lipopolysaccharide-primed macrophages is controlled by a counterbalanced production of IL-10 and IL-12. Journal of Immunology *160*, 3729-3736.

Souglakos, J., Kotsakis, A., Kouroussis, C., Kakolyris, S., Mavroudis, D., Kalbakis, K., Agelaki, S., Vlachonikolis, J., Georgoulias, V., and Samonis, G. (2002). Nonneutropenic febrile episodes associated with docetaxel-based chemotherapy in patients with solid tumors. Cancer *95*, 1326-1333.

Stenger, S., Donhauser, N., Thuring, H., Rollinghoff, M., and Bogdan, C. (1996). Reactivation of latent leishmaniasis by inhibition of inducible nitric oxide synthase. Journal of Experimental Medicine *183*, 1501-1514.

Stevenson, F.T., Torrano, F., Locksley, R.M., and Lovett, D.H. (1992). Interleukin 1: The patterns of translation and intracellular distribution support alternative secretory mechanisms. Journal of Cellular Physiology *152*, 223-231.

Stinchcombe, J.C., Barral, D.C., Mules, E.H., Booth, S., Hume, A.N., Machesky, L.M., Seabra, M.C., and Griffiths, G.M. (2001a). Rab27a is required for regulated secretion in cytotoxic T lymphocytes. Journal of Cell Biology *152*, 825-833.

Stinchcombe, J.C., Bossi, G., Booth, S., and Griffiths, G.M. (2001b). The immunological synapse of CTL contains a secretory domain and membrane bridges. Immunity *15*, 751-761.

Stinchcombe, J.C., and Griffiths, G.M. (2003). The role of the secretory immunological synapse in killing by CD8 + CTL. Seminars in Immunology *15*, 301-305.

Stinchcombe, J.C., Majorovits, E., Bossi, G., Fuller, S., and Griffiths, G.M. (2006). Centrosome polarization delivers secretory granules to the immunological synapse. Nature *443*, 462-465.

Stoltz, D.A., Nelson, S., Kolls, J.K., Zhang, P., Bohm Jr, R.P., Murphey-Corb, M., and Bagby, G.J. (2000). In vitro ethanol suppresses alveolar macrophage TNF-alpha during Simian immunodeficiency virus infection. American Journal of Respiratory and Critical Care Medicine *161*, 135-140.

Stuehr, D.J., and Marletta, M.A. (1985). Mammalian Nitrate Biosynthesis: Mouse Macrophages Produce Nitrite and Nitrate in Response to Escherichia coli Lipopolysaccharide. Proceedings of the National Academy of Sciences of the United States of America *82*, 7738-7742.

Stuehr, D.J., and Marletta, M.A. (1987). Induction of nitrite/nitrate synthesis in murine macrophages by BCG infection, lymphokines, or interferon-gamma. J Immunol *139*, 518-525.

Takasuka, N., Matsuura, K., Yamamoto, S., and Akagawa, K.S. (1995). Suppression of TNF-alpha mRNA expression in LPS-primed macrophages occurs at the level of nuclear factor-kappa B activation, but not at the level of protein kinase C or CD14 expression. J Immunol *154*, 4803-4812.

Takasuka, N., Tokunaga, T., and Akagawa, K.S. (1991). Preexposure of macrophages to low doses of lipopolysaccharide inhibits the expression of tumor necrosis factor-alpha mRNA but not of IL-1 beta mRNA. J Immunol *146*, 3824-3830.

Tamandl, D., Bahrami, M., Wessner, B., Weigel, G., Ploder, M., Furst, W., Roth, E., Boltz-Nitulescu, G., and Spittler, A. (2003). Modulation of toll-like receptor 4 expression on human monocytes by tumor necrosis factor and interleukin-6: Tumor necrosis factor evokes lipopolysaccharide hyporesponsiveness, whereas interleukin-6 enhances lipopolysaccharide activity. Shock *20*, 224-229.

Tanabe, K., Serruys, P.W., Grube, E., Smits, P.C., Selbach, G., van der Giessen, W.J., Staberock, M., de Feyter, P., Muller, R., Regar, E.*, et al.* (2003). TAXUS III Trial: In-Stent Restenosis Treated With Stent-Based Delivery of Paclitaxel Incorporated in a Slow-Release Polymer Formulation. Circulation *107*, 559-564.

Tanaka, M., Suda, T., Takahashi, T., and Nagata, S. (1995). Expression of the functional soluble form of human Fas ligand in activated lymphocytes. EMBO Journal *14*, 1129-1135.

Tanchot, C., Lemonnier, F.A., Perarnau, B., Freitas, A.A., and Rocha, B. (1997). Differential requirements for survival and proliferation of CD8 naive or memory T cells. Science *276*, 2057-2062.

Tartaglia, L.A., Ayres, T.M., Wong, G.H.W., and Goeddel, D.V. (1993). A novel domain within the 55 kd TNF receptor signals cell death. Cell *74*, 845-853.

Tobias, P.S., Soldau, K., Kline, L., Lee, J.D., Kato, K., Martin, T.P., and Ulevitch, R.J. (1993). Cross-linking of lipopolysaccharide (LPS) to CD14 on THP-1 cells mediated by LPS-binding protein. J Immunol *150*, 3011-3021.

Tominaga, K., Saito, S., Matsuura, M., and Nakano, M. (1999). Lipopolysaccharide tolerance in murine peritoneal macrophages induces downregulation of the lipopolysaccharide signal transduction pathway through mitogen-activated protein kinase and nuclear factor-kappa-B cascades, but not lipopolysaccharide-incorporation steps. Biochimica et Biophysica Acta - Molecular Cell Research *1450*, 130-144.

Tong, A.W., Seamour, B., Lawson, J.M., Ordonez, G., Vukelja, S., Hyman, W., Richards, D., Stein, L., Maples, P.B., and Nemunaitis, J. (2000). Cellular immune profile of patients with advanced cancer before and after taxane treatment. American Journal of Clinical Oncology: Cancer Clinical Trials *23*, 463-472.

Townsend, A.R.M., Rothbard, J., Gotch, F.M., Bahadur, G., Wraith, D., and McMichael, A.J. (1986). The epitopes of influenza nucleoprotein recognized by cytotoxic T lymphocytes can be defined with short synthetic peptides. Cell *44*, 959-968.

Trinchieri, G. (1995). Interleukin-12: A proinflammatory cytokine with immunoregulatory functions that bridge innate resistance and antigen-specific adaptive immunity. Annual Review of Immunology *13*, 251-276.

Tsavaris, N., Kosmas, C., Vadiaka, M., Kanelopoulos, P., and Boulamatsis, D. (2002). Immune changes in patients with advanced breast cancer undergoing chemotherapy with taxanes. Br J Cancer *87*, 21-27.

Usharauli, D., Perez-Diez, A., and Matzinger, P. (2006). The JAM Test and its daughter P-JAM: Simple tests of DNA fragmentation to measure cell death and stasis. Nature Protocols *1*, 672-682.

Vale, R.D., Reese, T.S., and Sheetz, M.P. (1985). Identification of a novel force-generating protein, kinesin, involved in microtubule-based motility. Cell *42*, 39-50.

Vandenabeele, P., Declercq, W., Beyaert, R., and Fiers, W. (1995a). Two tumour necrosis factor receptors: structure and function. Trends in Cell Biology *5*, 392-399.

Vandenabeele, P., Declercq, W., Vanhaesebroeck, B., Grooten, J., and Fiers, W. (1995b). Both TNF receptors are required for TNF-mediated induction of apoptosis in PC60 cells. J Immunol *154*, 2904-2913.

Vasiliev, J.M., Gelfand, I.M., Domnina, L.V., Ivanova, O.Y., Komm, S.G., and Olshevskaja, L.V. (1970). Effect of colcemid on the locomotory behaviour of fibroblasts. J Embryol Exp Morphol *24*, 625-640.

Vicari, A.P., Luu, R., Zhang, N., Patel, S., Makinen, S.R., Hanson, D.C., Weeratna, R.D., and Krieg, A.M. (2009). Paclitaxel reduces regulatory T cell numbers and inhibitory function and enhances the anti-tumor effects of the TLR9 agonist PF-3512676 in the mouse. Cancer Immunology, Immunotherapy *58*, 615-628.

Vignaux, F., Vivier, E., Malissen, B., Depraetere, V., Nagata, S., and Golstein, P. (1995). TCR/CD3 coupling to Fas-based cytotoxicity. J. Exp. Med. *181*, 781-786.

Vila-del Sol, V., Diaz-Munoz, M.D., and Fresno, M. (2006). Requirement of tumor necrosis factor-alpha and nuclear factor-kappa-B in the induction by IFN-gamma of inducible nitric oxide synthase (iNOS) in macrophages. J Leukoc Biol, jlb.0905529.

Virca, G.D., Kim, S.Y., Glaser, K.B., and Ulevitch, R.J. (1989). Lipopolysaccharide Induces Hyporesponsiveness to its Own Action in Raw 264.7 Cells. J. Biol. Chem. *264*, 21951-21956.

Walker, R.A., Inoue, S., and Salmon, E.D. (1989). Asymmetric behavior of severed microtubule ends after ultraviolet- microbeam irradiation of individual microtubules in vitro. J. Cell Biol. *108*, 931-937.

Wang, C.Y., Mayo, M.W., Korneluk, R.G., Goeddel, D.V., and Baldwin Jr, A.S. (1998). NF-kB antiapoptosis: Induction of TRAF1 and TRAF2 and c-IAP1 and c-IAP2 to suppress caspase-8 activation. Science *281*, 1680-1683.

Wani, M.C., Taylor, H.L., Wall, M.E., Coggon, P., and McPhail, A.T. (1971). Plant antitumor agents. VI. The isolation and structure of taxol, a novel antileukemic and antitumor agent from Taxus brevifolia. Journal of the American Chemical Society *93*, 2325-2327.

West, L.M., Northcote, P.T., and Battershill, C.N. (2000). Peloruside A: A potent cytotoxic macrolide isolated from the New Zealand marine sponge Mycale sp. Journal of Organic Chemistry *65*, 445-449.

Westerterp, M., Boermeester, M.A., Omloo, J.M.T., Hulshof, M., Vervenne, W.L., Lutter, R., Out, T.A., and van Lanschot, J.J.B. (2008). Differential responses of cellular immunity in patients undergoing neoadjuvant therapy followed by surgery for carcinoma of the oesophagus. Cancer Immunology Immunotherapy *57*, 1837-1847.

Wherry, E.J., Teichgraber, V., Becker, T.C., Masopust, D., Kaech, S.M., Antia, R., von Andrian, U.H., and Ahmed, R. (2003). Lineage relationship and protective immunity of memory CD8T cell subsets. Nature Immunology *4*, 225-234.

Wiedemann, A., Depoil, D., Faroudi, M., and Valitutti, S. (2006). Cytotoxic T lymphocytes kill multiple targets simultaneously via spatiotemporal uncoupling of lytic and stimulatory synapses. Proceedings of the National Academy of Sciences of the United States of America *103*, 10985-10990.

Wilmes, A., Bargh, K., Kelly, C., Northcote, P.T., and Miller, J.H. (2007). Peloruside A synergizes with other microtubule stabilizing agents in cultured cancer cell lines. Molecular Pharmaceutics *4*, 269-280.

Wolberg, G., Stopford, C.R., and Zimmerman, T.P. (1984). Antagonism by taxol of effects of microtubule-disrupting agents on lymphocyte cAMP metabolism and cell function. Proceedings of the National Academy of Sciences of the United States of America *81*, 3496-3500.

Wolint, P., Betts, M.R., Koup, R.A., and Oxenius, A. (2004). Immediate Cytotoxicity but Not Degranulation Distinguishes Effector and Memory Subsets of CD8+ T Cells. Journal of Experimental Medicine *199*, 925-936.

Woo, C.-H., Lim, J.-H., and Kim, J.-H. (2004). Lipopolysaccharide Induces Matrix Metalloproteinase-9 Expression via a Mitochondrial Reactive Oxygen Species-p38 Kinase-Activator Protein-1 Pathway in Raw 264.7 Cells. J Immunol *173*, 6973-6980.

Wright, S.D., Ramos, R.A., Tobias, P.S., Ulevitch, R.J., and Mathison, J.C. (1990). CD14, a Receptor for Complexes of Lipopolysaccharide (LPS) and LPS Binding Protein. Science *249*, 1431-1433.

Xie, B., Dong, Z., and Fidler, I.J. (1994). Regulatory mechanisms for the expression of type IV collagenases/gelatinases in murine macrophages. J Immunol *152*, 3637-3644.

Xie, J., Kolls, J., Bagby, G., and Greenberg, S.S. (1995). Independent suppression of nitric oxide and TNF-alpha in the lung of conscious rats by ethanol. FASEB Journal *9*, 253-261.

Xie, Q.-w., Cho, H.J., Calaycay, J., Mumford, R.A., Swiderek, K.M., Lee, T.D., Ding, A., Troso, T., and Nathan, C. (1992). Cloning and Characterization of Inducible Nitric Oxide Synthase from Mouse Macrophages. Science *256*, 225-228.

Yamamoto, Y., He, P., Klein, T.W., and Friedman, H. (1994). Endotoxin induced cytotoxicity of macrophages is due to apoptosis caused by nitric oxide production. Journal of Endotoxin Research *1*, 181-187.

Yang, J., Huck, S.P., McHugh, R.S., Hermans, I.F., and Ronchese, F. (2006). Perforin-dependent elimination of dendritic cells regulates the expansion of antigen-specific CD8+ T cells in vivo. Proceedings of the National Academy of Sciences of the United States of America *103*, 147-152.

Yeh, E., Skibbens, R.V., Cheng, J.W., Salmon, E.D., and Bloom, K. (1995). Spindle dynamics and cell cycle regulation of dynein in the budding yeast, Saccharomyces cerevisiae. J. Cell Biol. *130*, 687-700.

Yisraeli, J.K., Sokol, S., and Melton, D.A. (1990). A 2-Step Model For the Localization of Maternal Messenger-RNA in Xenopus Oocytes - Involvement of Microtubules and Microfilaments in the Translocation and Anchoring of VG1 Messenger-RNA. Development *108*, 289-298.

Yu, B., Kusmartsev, S., Cheng, F.D., Paolini, M., Nefedova, Y., Sotomayor, E., and Gabrilovich, D. (2003). Effective combination of chemotherapy and dendritic cell administration for the treatment of advanced-stage experimental breast cancer. Clinical Cancer Research *9*, 285-294.

Zhang, L., Dermawan, K., Jin, M.L., Liu, R.J., Zheng, H.R., Xu, L., Zhang, Y., Cai, Y.C., Chu, Y.W., and Xiong, S.D. (2008). Differential impairment of regulatory T

cells rather than effector T cells by paclitaxel-based chemotherapy. Clinical Immunology *129*, 219-229.

Zhang, X., Burt, H.M., Mangold, G., Dexter, D., Von Hoff, D., Mayer, L., and Hunter, W.L. (1997). Anti-tumor efficacy and biodistribution of intravenous polymeric micellar paclitaxel. Anti-Cancer Drugs *8*, 696-701.

Zhang, X., and Morrison, D.C. (1993a). Lipopolysaccharide-induced selective priming effects on tumor necrosis factor alpha and nitric oxide production in mouse peritoneal macrophages. J. Exp. Med. *177*, 511-516.

Zhang, X., and Morrison, D.C. (1993b). Lipopolysaccharide structure-function relationship in activation versus reprogramming of mouse peritoneal macrophages. J Leukoc Biol *54*, 444-450.

Zhao, C., Morgan, M., Haeryfar, S.M.M., Blay, J., and Hoskin, D.W. (2003). Exposure to paclitaxel or vinblastine down-regulates CD11a and CD54 expression by P815 mastocytoma cells and renders the tumor cells resistant to killing by nonspecific cytotoxic T lymphocytes induced with anti-CD3 antibody. Cancer Immunology, Immunotherapy *52*, 185-193.

Zhong, H., Han, B., Tourkova, I.L., Lokshin, A., Rosenbloom, A., Shurin, M.R., and Shurin, G.V. (2007). Low-dose paclitaxel prior to intratumoral dendritic cell vaccine modulates intratumoral cytokine network and lung cancer growth. Clinical Cancer Research *13*, 5455-5462.

Appendices

Appendix A: Recipes

Phosphate Buffered Saline (PBS):

Sterile double distilled water with:

Na_2HPO_4 8.7 mM

NaH_2PO_4 1.3 mM

NaCl 145 mM

FACS buffer:

2% FCS

0.1% Sodium Azide

97.9% PBS.

Complete T cell Medium (CTCM) – Medium for MØ work:

85.9% Dulbecco's Modified Eagle Medium (dMEM; Invitrogen)

10% FCS

1%HEPES (1 M) (Sigma)

1%$_L$-Glutamine (200 mM) (Invitrogen)

1% Penicillin-Streptomycin (Penstrep; 100000 U/mL, 10000 μg/mL respectively; Invitrogen)

0.1% β-Mercaptoethanol (1000 x 55 mM; Invitrogen)

1% Non-essential Amino Acids (10 mM 100x;Invitrogen)

Handling medium - For MØ work:

96% dMEM;

3% HEPES;

1% PenStrep.

Complete Iscove's Modified Dulbecco's Medium (cIMDM) – Medium for CTL and BMDC work:

93.9% Iscove's Modified Dulbecco's Medium (IMDM; Invitrogen)

5% FCS

1% Penstrep

0.1% β-Mercaptoethanol

Freezing Medium – For cell storage:

90% DMSO (Sigma)

10% FCS

Greiss Reagents:

A: 1% w.v Sulphanilamide in 2.5% phosphoric Acid

B: 0.1% w/v N-(1-naphthyl) ethylenediamine in 2.5% phosphoric Acid

Appendix B: Antibodies:

Streptavidin-CyC (BD Bioscience)

Anti-I-Ab-PE (BD Bioscience)

Anti-CD11b-Fitc (BD Bioscience)

Anti-CD107a-Fitc (BD Bioscience)

Anti-CD8a-Cyc (BD Bioscience)

Anti-$V\beta_{5.1/5.2}$-PE (BD Bioscience)

Anti-CD44-AP (BD Bioscience)

Anti-CD62L-AP (BD Bioscience)

IgG2-α-Fitc (BD Bioscience)

IgG2-α-PE (BD Bioscience)

IgG2-α-Cyc (BD Bioscience)

Anti-F4/80-biotin (Serotec, Oxford, UK)

Anti-alpha-tubulin-IgG (Abcam)

Alexafluor 488 polyclonal anti-rabbit IgG (Invitrogen)

Anti-$V\alpha_2$-Fitc (eBioscience, San Diego, CA, USA)

Anti-CD45.1-APC (eBioscience)

Anti-mouse-CD16/32 (FcR block) (eBioscience)